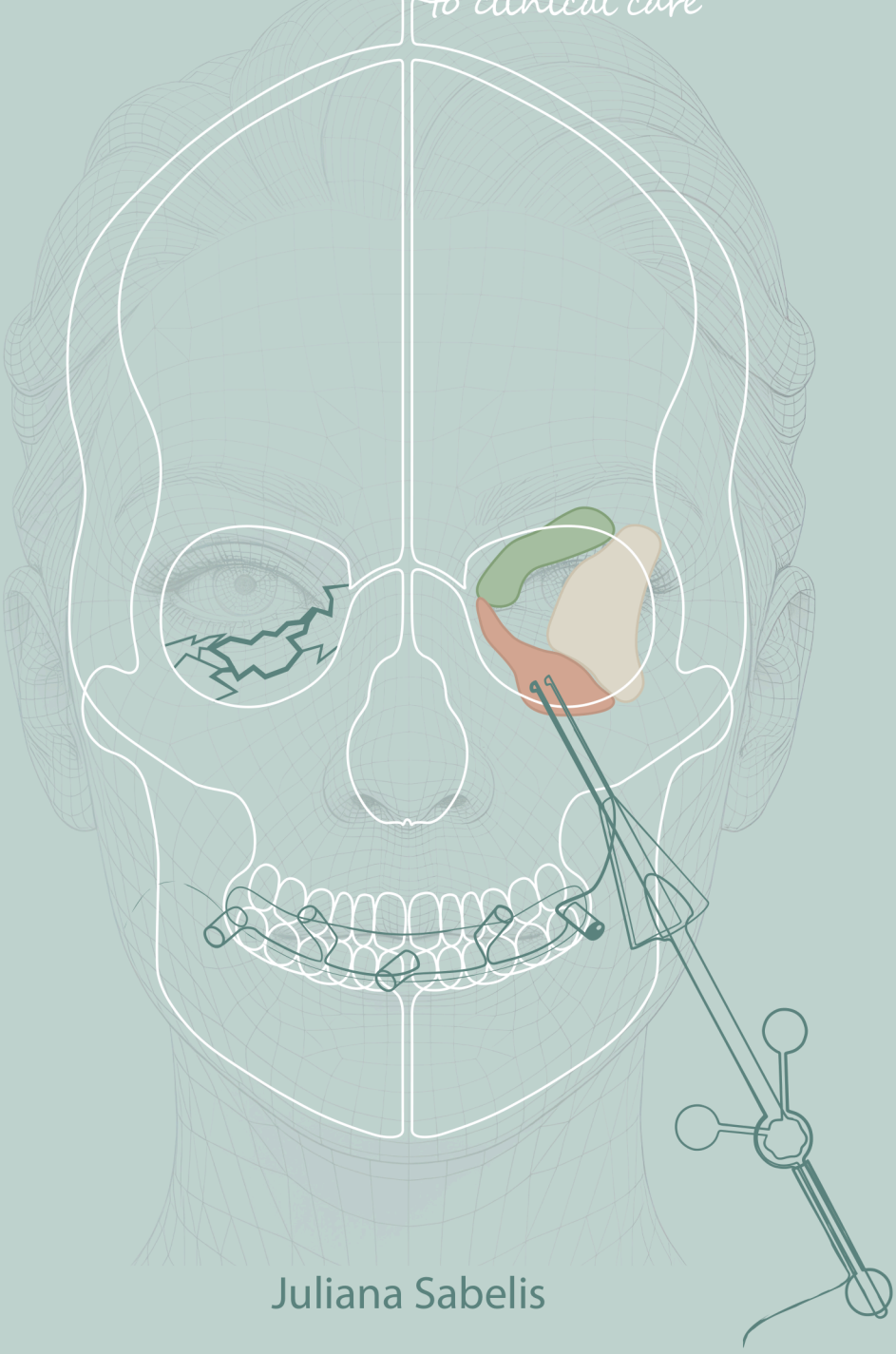
Optimizing computer-assisted orbital reconstruction

From digital design to clinical care



Juliana Sabelis

Optimizing computer-assisted orbital reconstruction

From digital design to clinical care

Juliana Sabelis
2026

Financial support for printing and distribution of this thesis was kindly provided by

KNMT

KLS Martin Nederland

Optimizing computer-assisted orbital reconstruction

From digital design to clinical care

Academic thesis, University of Amsterdam, The Netherlands

ISBN 978-94-6537-912-8

Printing: Ridderprint, www.ridderprint.nl

Copyright © 2026, J.F. Sabelis, Haarlem, The Netherlands

All rights reserved. No part of this publication may be reproduced or transmitted in any form, by any means, electronic or mechanical, including photocopy, recording or any information storage and retrieval system, without written permission of the author.

Optimizing computer-assisted orbital reconstruction

From digital design to clinical care

ACADEMISCH PROEFSCHRIFT

ter verkrijging van de graad van doctor
aan de Universiteit van Amsterdam
op gezag van de Rector Magnificus
ten overstaan van een door het College voor Promoties ingestelde commissie,
in het openbaar te verdedigen in de Aula der Universiteit
op woensdag 18 november 2026, te 14.00 uur

door Juliana Francisca Sabelis
geboren te Haarlem

Promotiecommissie

Promotores:	prof. dr. A.G. Becking	Universiteit van Amsterdam
	prof. dr. T.J.J. Maal	Radboud Universiteit
Copromotores:	prof. dr. L. Dubois	Universiteit van Amsterdam
	prof. dr. R. Schreurs	Vrije Universiteit Amsterdam
Overige leden:	prof. dr. J. de Lange	Universiteit van Amsterdam
	prof. dr. P. Saeed	Universiteit van Amsterdam
	prof. dr. B.J. van Royen	Vrije Universiteit Amsterdam
	prof. dr. S.J. Bergé	Radboud Universiteit
	dr. B. van Minnen	UMCG
	dr. F. Baan	Radboudumc
	dr. R. Helmers	Universiteit van Amsterdam

Faculteit der Tandheelkunde

Funding statement

The research for this doctoral thesis received financial assistance from:

KLS Martin (Tuttlingen, Germany) and Brainlab AG (Munich, Germany).

None of the funding parties had any involvement in the contents or decision to submit the manuscripts.

Table of contents

Introduction

Chapter 1 General introduction 9

Chapter 2 Personalized orbital reconstruction workflow 25

Part I Patient-specific implants

Chapter 3 Multi-wall reconstructions 47

Chapter 4 Patient-specific implant design 63

Part II Surgical navigation

Chapter 5 Clinical validation of virtual splint registration 77

Chapter 6 Visualization of real-time navigation 91

Chapter 7 Preclinical validation of real-time navigation 107

Discussion

Chapter 8 General Discussion 123

Appendices

Summaries 138

Author list 146

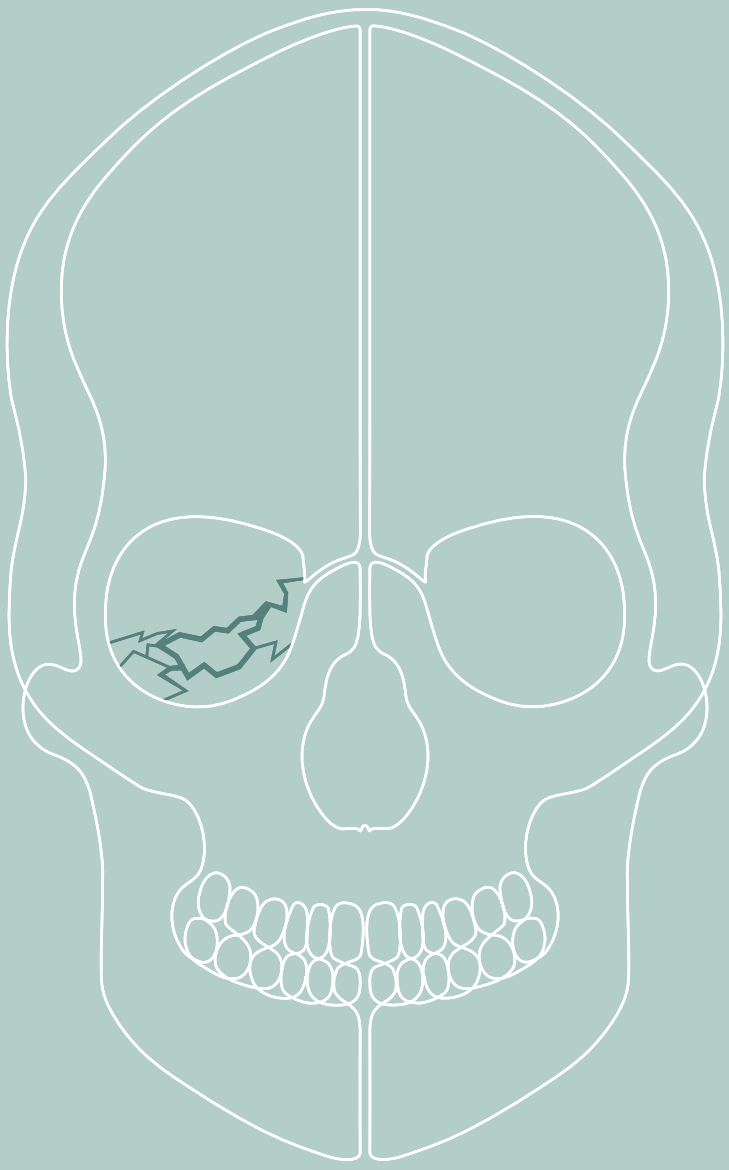
Chapter information 148

List of publications 156

Acknowledgements – Dankwoord 158

About the author 164

Introduction



Chapter 1

General introduction

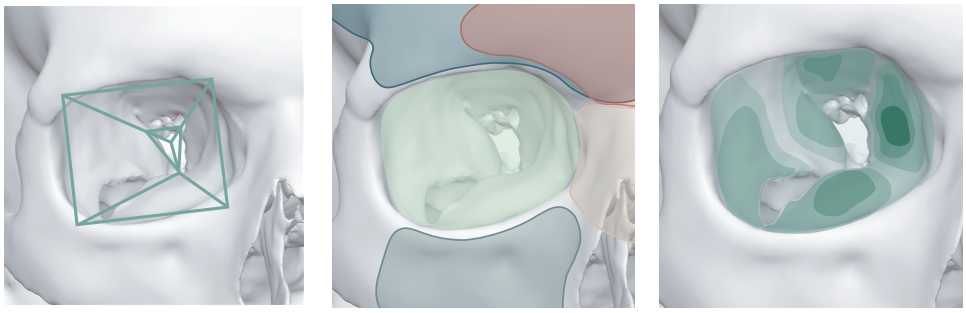
The eyes have long been regarded as the mirror of the soul. In the field of maxillofacial trauma, the eyes may also serve as a mirror of surgical accuracy. The orbit, which houses the globe, is a complex three-dimensional structure and even minor changes caused by trauma or surgery may have significant consequences. Accurate anatomical restoration is therefore essential.

Clinical aspects

Anatomy

Surgical accuracy in orbital trauma reconstruction relies on a thorough understanding of orbital anatomy. Thze orbit is a complex anatomical structure, composed of segments of seven bones: the sphenoid, frontal, ethmoid, lacrimal, palatine, maxillary, and zygomatic bones.[1, 2] Together, these parts form a quadrangular pyramid that tapers posteriorly into a three-sided triangular apex (*Figure 1A*).[3] This cavity contains soft tissues, including neurovascular structures, adipose and connective tissue, extraocular muscles, and the globe itself.[4]

The orbital walls act as barriers, separating the orbit from adjacent anatomical zones: the maxillary sinus inferiorly, the ethmoidal sinus medially, and the frontal sinus and cranial cavity superiorly (*Figure 1B*).[5] Wall thickness varies considerably: the roof consists of relatively thick bone, but the medial wall and orbital floor are paper-thin and more prone to fracturing (*Figure 1C*).[6]



a b c

Figure 1. *Visualization of the orbit. (a) Orbit with a geometric scheme depicting its shape. The base of the quadrangular pyramid forms the frontal border of the orbit. The quadrangular pyramid transitions posteriorly into a three-sided apex. (b) Surrounding anatomical zones of the orbit: maxillary sinus caudally, ethmoidal sinus medially, and cranial cavity cranially. (c) Color map projected on the bone depicting the local bone thickness. The darkest green indicates a thickness of less than one millimeter.*

Pathophysiology

The orbit is highly exposed to physical impact and is involved in up to 40% of maxillofacial trauma cases.[7, 8] The most common causes of orbital fractures include interpersonal violence, sports-related injuries, traffic accidents, and falls.[9] The distribution varies by age and gender: interpersonal violence is more frequent in young adults, sports-related injuries are common in pediatric cohorts and falls are predominant in the elderly.[10] Men are more frequently affected, likely due to greater exposure to high-risk environments and activities.[11-13]

Two biomechanical theories have been proposed to explain fracture development:

buckling and hydraulic theories.[14-17] The hydraulic theory suggests that traumatic energy causes a sudden rise in intraorbital pressure, forcing the thinner orbital floor or medial wall outward, often resulting in large fractures with soft tissue herniation. In contrast, the buckling theory proposes that direct traumatic impact to the orbital rim is transmitted to the thinner posterior portion of the orbital floor, resulting in a fracture. Both mechanisms are likely to contribute to orbital fractures, with their relative influence depending on the nature, direction, and magnitude of the traumatic force.[15, 18]

Symptoms

Orbital fracture patterns are highly variable, producing a spectrum of clinical symptoms affecting function and esthetics. The clinical presentation may evolve over time, with delayed alterations in globe position being a common example. Predicting the effect of the fracture on globe position in the acute (primary) setting can be challenging: the true globe position may be obscured due to orbital swelling. Periorbital edema may create the illusion of posterior displacement (enophthalmos), whereas intraorbital swelling initially causes an anterior displacement of the globe (exophthalmos).[19] As the swelling subsides over days or weeks, the true position of the globe becomes apparent.

Figure 2 illustrates the potential long-term effects of orbital fractures on globe position. Fractures may increase orbital volume and allow soft-tissue displacement into adjacent sinuses. The effect on globe position depends on the location and extent of the defect. An axis running from the lateral orbital rim to the posterior lacrimal crest serves as a reference for describing displacement.[20] Defects along the axis mainly influence the vertical position, leading to an inferior displacement, or hypoglobus.[21] Defects posterior to this axis primarily affect ocular projection, causing a posterior displacement, or enophthalmos.[22] Both forms of displacement may lead to facial asymmetry and esthetic or functional sequelae.

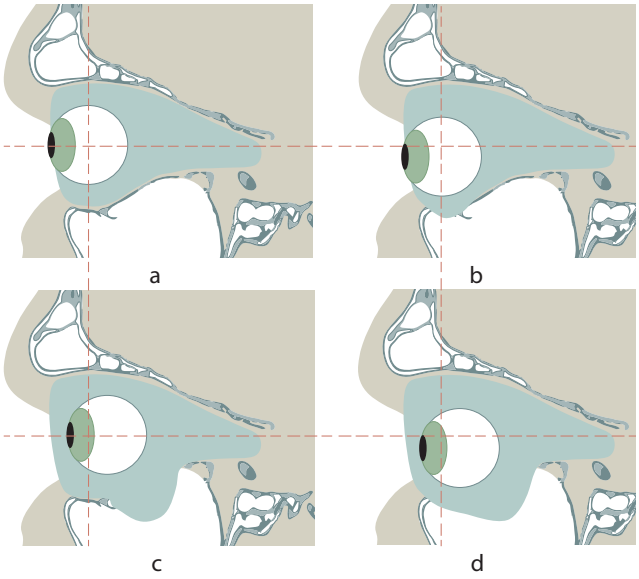


Figure 2. *Illustration of potential globe position alterations. Red lines indicate the axes through the center of the globe in the (a) normal situation. (b) Defect at the location of the vertical axis results in a hypoglobus. (c) Defect behind the vertical axis results in an enophthalmos. (d) Complex defects may result in a combination of both.*

Beyond inducing static changes in globe position, orbital trauma may impair the dynamic coordination required for binocular vision, leading to diplopia. Binocular single vision depends on an intricate system involving precise globe alignment, coordinated muscle function, and intact neural control. Disturbance in any system component may lead to diplopia, the development and persistence of which are therefore difficult to predict. In the acute setting, edema, muscle contusion and altered globe position may temporarily affect muscle function or force vectors, resulting in diplopia.[21] As the acute changes resolve, persistent factors such as muscle entrapment, scarring, adhesion and damage to nerves or connections between the muscles and orbit may remain.[23] Minor deviations in eye motility may lead to serious diplopia and affect quality of life. Orthoptic examination may help identify the cause of diplopia at an early stage and may therefore be helpful to determine the appropriate indication for surgical intervention.[24]

Clinical decision-making

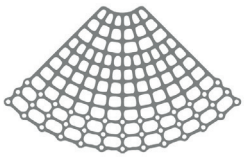
The clinical sequelae of orbital fractures can be significant, and treatment decisions require careful consideration. The main debate concerns the indication and timing of surgery. There is broad consensus regarding indications for immediate surgery (within 24 hours), including pediatric cases and muscle entrapment.[25, 26]. Other cases are considered 'relative' indications and may require time to assess true sequelae before making a decision.[27] In general, small asymptomatic fractures are managed conservatively, whereas larger defects with early symptoms typically warrant surgical reconstruction.[19] For intermediate cases (large defect without early enophthalmos), approaches differ. At Amsterdam UMC, a clinical protocol favoring a wait-and-see strategy is adopted: patients are reassessed after two weeks, once swelling has resolved and spontaneous recovery may have occurred.[25] Reconstruction is indicated if symptoms persist or delayed enophthalmos develops. In contrast, others advocate repair within two weeks to improve the chances of restoring both form and function, arguing that postponing surgery increases the risk of fibrosis and persistent diplopia.[13, 28, 29]

Surgical intervention

The goal of surgical treatment is to restore the pre-traumatized anatomy, re-establish structural support for the orbital contents, and recover ocular function.[30, 31] Since the orbital floor and medial wall fragments can be less than one millimeter thick and may be comminuted, repositioning and fixation is infeasible and reconstruction with an implant is required. The ideal implant must be biocompatible, radiopaque, and stable. It should restore the anatomy, facilitate fluid drainage, and be readily available at reasonable costs.[19, 30] Among the available materials, titanium implants meet most of these criteria and are therefore commonly used.[31]

Titanium implants for orbital reconstruction can be categorized into three main types: pre-bent, preformed implants, and Patient-Specific Implants (PSIs) (*Table 1*). Pre-bent implants are flat meshes that are manually shaped by the surgeon, either freehand or using a 3D printed model of a generic or patient's orbit.[32-34] Preformed implants are based on an average orbital anatomy, available off the shelf, and can be virtually assessed for fit before surgery.[35, 36] In contrast, PSIs are virtually designed to fit the patient's anatomy and defect.[37, 38] While PSIs offer the highest degree of anatomical conformity and predictability, their higher costs and production lead time may restrict their use in acute trauma care.[39-41] At the Amsterdam UMC, preformed implants are generally used in primary reconstructions, whereas PSIs are reserved for secondary cases and selected complex primary reconstructions in which dorsal support is insufficient or absent.[42]

Table 1. *Types of titanium implants showing the main differences*

	Pre-bent	***Preformed***	***PSI***
			
Shape	-	+	++
Readily available	+	+	-
Affordability	++	+	-

The recommended surgical approach for orbital reconstruction is a transconjunctival incision in the inferior fornix.[43] This approach minimizes visible scarring but provides only limited visualization of the orbital cavity. Through this keyhole incision, the surgeon exposes the orbital floor, lower lateral orbit, and medial wall, and mobilizes the soft tissues. The fracture edges are identified to delineate the defect. A key anatomical landmark is the orbital process of the palatine bone, also called the posterior ledge. This consists of relatively solid bone and often remains intact, providing potential posterior support for the implant.[44]

Several factors make accurate implant positioning particularly challenging, including restricted access through a small incision, and presence of delicate soft tissues and vital structures within the confined orbital volume.[45] These factors limit direct visualization of the implant and contribute to the technical complexity of orbital reconstruction. When the medial orbital wall is involved, the risk of implant misplacement in terms of roll or yaw increases. The complexity is further increased in secondary reconstructions. Over time, healing processes lead to bone remodeling, altering the native anatomy and compromising the reliability of standard anatomical references.[42, 46] The principal challenge arises from scarring and adhesions, which distort tissue planes, restrict implant placement, and make both positioning and clinical outcomes less predictable.

Computer-Assisted Surgery Workflow

Computer-assisted surgery (CAS) has been increasingly integrated into clinical practice to improve reconstruction accuracy reconstruction. CAS is an umbrella term encompassing a broad range of technologies and techniques designed to support the planning, guidance, and evaluation of surgical interventions. These technologies have evolved over the past century, building on early principles such as stereotactic systems introduced by Horsley and Clarke to target brain lesions,[47, 48] which laid the foundation for modern image-guided surgical approaches. CAS has since expanded across multiple specialties, including orthopedics, oncology, spine surgery, and craniomaxillofacial surgery.

Over the past decades, the portfolio of CAS tools for craniomaxillofacial surgery has grown. As the number and complexity of these tools increase, establishing an efficient and well-integrated surgical workflow has become essential to ensure that procedures are performed consistently, efficiently and with minimal error. The CAS workflow can be conceptualized in four distinct phases: Advanced diagnostics, virtual surgical planning,

surgical transfer, and evaluation (*Figure 3*). Within each phase, multiple techniques are available, forming a modular toolbox that can be selected and combined to meet the specific requirements of each case. The Advanced Concepts of Orbital Reconstruction (ACOR) research program at the Amsterdam UMC has systematically evaluated several of these techniques in preclinical models, generating data on their impact on implant positioning accuracy and reconstruction time.[49] By analyzing individual components, ACOR has provided a foundation for evidence-based selection of CAS tools, helping to identify which elements are essential for predictable results. The following paragraphs provide an overview of the individual phases and available tools for orbital reconstruction.

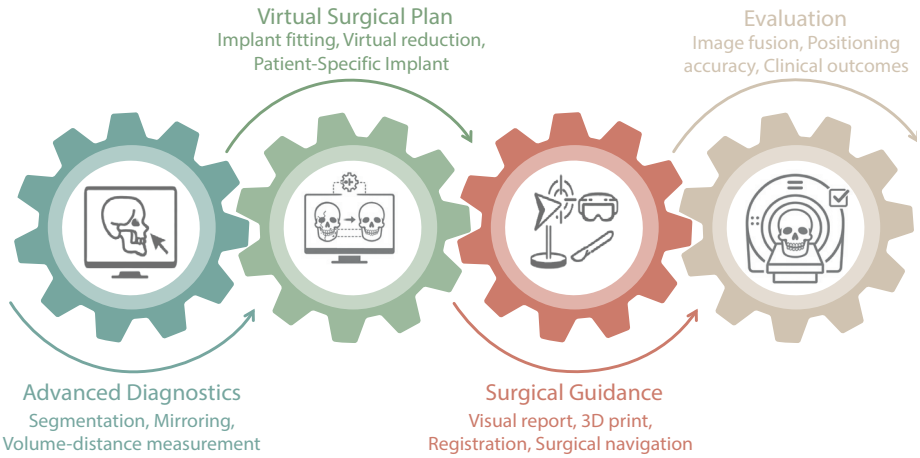


Figure 3. *Computer-assisted surgery modular toolbox visualized per phase.*

Advanced Diagnostics

The first phase in the orbital reconstruction workflow is Advanced Diagnostics. This phase aims to extract the maximum clinically relevant information from the available imaging data. Computed Tomography (CT) scans form the foundation for this process. Specialized software enables the segmentation of key anatomical structures, such as the orbit, orbital cavity, and surrounding bony framework. In unilateral trauma, the unaffected healthy orbit can be mirrored to simulate the patient's original anatomy.[50-52] By creating this virtual mirror model, clinicians can objectively assess the extent of the fracture, visualize anatomical asymmetries, and quantify changes in orbital volume. Integration of quantitative diagnostic information with clinical findings enables an informed decision about the optimal treatment strategy.

Virtual Surgical Planning

Once surgical reconstruction is indicated, the next phase is Virtual Surgical Planning (VSP). This phase enables simulation of the surgical procedure in a virtual environment, allowing the surgeon or clinical engineer to plan the reconstruction with increased accuracy and predictability. It also supports anticipation of intraoperative challenges and selection of the optimal surgical strategy.

For a primary reconstruction, a virtual replica of a preformed implant can be imported into the planning software. The implant fit, orientation and position relative to the mirrored orbital anatomy can be assessed.[52] This process helps identify the most suita-

ble implant type, size, position and any potential adjustments to optimize positioning. Preoperative information derived from the VSP can significantly improve implant positioning accuracy.[53] If no implant is available that can be positioned to meet these parameters, it may be concluded that a preformed implant will not suffice.

Patient-Specific Implant

If a preformed implant does not provide an adequate fit, or if secondary reconstruction is required, a PSI may be indicated. A PSI is custom-made to replicate the patient's unique orbital anatomy and address the specific deformity or defect.[54, 55] The design process is typically carried out by a clinical engineer, either in-house or in collaboration with the implant manufacturer, and is refined in consultation with the surgeon. During this process, both anatomical and functional considerations are integrated. Specific design characteristics can be incorporated to address clinical needs, such as an intentional volume overcorrection to compensate for altered globe position or anticipated postoperative fibrosis.[38, 42, 46, 56] Once the design is finalized and approved by the surgeon, the PSI is manufactured using additive manufacturing techniques, such as selective laser melting.

PSIs provide a personalized approach and enable a high level of anatomical accuracy. Studies have reported mean positioning errors below 1 mm, along with improved orbital symmetry, restoration of globe position and higher rates of functional recovery when compared to conventional implants.[41, 57-59] PSIs are particularly advantageous in complex or secondary reconstructions, as their patient-specific design enables accurate reconstruction despite anatomical distortion and scarring.

Surgical Guidance

Preoperative planning provides the surgeon with detailed anatomical insights and a clear strategy for implant form and placement. These insights must be effectively transferred to the intraoperative setting to guide the reconstruction. Static surgical guidance may include a visual report of the VSP[53] or a 3D-printed model of the mirrored orbit to enable personalized bending of the implant.[32-34]

Dynamic guidance on implant positioning can be obtained using surgical navigation. Surgical navigation requires a tracking system to track the objects of interest in space. In oral and maxillofacial surgery, optical tracking is typically used because it is highly accurate and less susceptible to interference from metallic instruments.[60, 61] An infrared camera monitors reflective markers, firmly attached to the patient and to the surgical instruments (*Figure 4*). This optical approach requires an unobstructed line of sight between the camera and the tracked markers, which may limit freedom of instrument movement.

Before the navigation can be utilized, the patient must be aligned with the preoperative virtual reference frame through a registration process. Various registration techniques are available that vary in invasiveness, radiation exposure, and workflow efficiency. The accuracy of this registration is critical, as any misalignment directly compromises the accuracy of the navigation guidance. Once registration is completed, the surgeon can use surgical navigation to reproduce the planned reconstruction.

The surgeon uses a tracked instrument, such as a pointer, to assess the implant's position. The location of the pointer's tip is continuously visualized on the navigation monitor. The screen typically displays a 3D model of the patient's anatomy combined with

three orthogonal multiplanar CT slices (*Figure 5*). As the pointer is moved over the implant surface, the navigation screen updates in real time. By implementing navigation markers or vectors, the technique becomes object-oriented. These markers and vectors transform the visual feedback into quantitative measurements, providing objective information on implant position.[62]

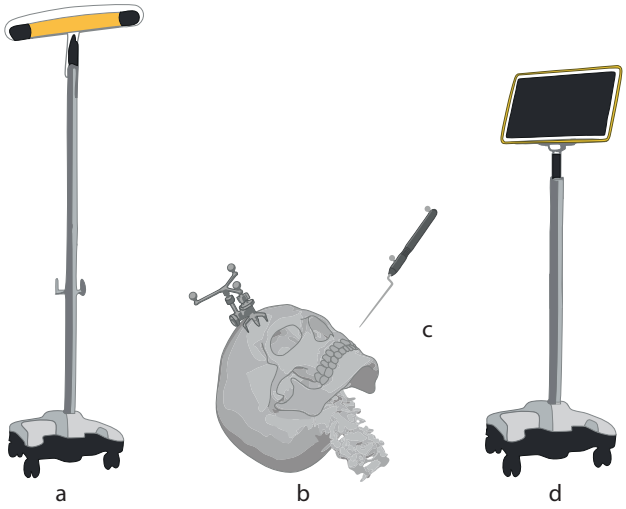


Figure 4. *Components of a surgical navigation system. (a) Infrared camera for optical tracking, (b) skull model with rigid reference array for patient tracking, (c) tracked pointer, and (d) navigation screen.*

Surgical navigation has become an established technique in orbital reconstruction, providing valuable intraoperative orientation and supporting accurate implant positioning. Several studies have demonstrated that navigation-assisted reconstruction can improve implant positioning, restoration of orbital volume, and symmetry.[63, 64] Nonetheless, further improvements in feedback quality are possible. A key limitation is the inability to track the implant continuously during positioning. Surgeons must instead use a tracked pointer to intermittently verify implant alignment with the virtual plan, which may disrupt the operative flow.[65] Moreover, the surgeon needs to interpret the feedback on a 2D screen to assess a 3D spatial situation. This requires spatial insight, which increases complexity and cognitive load for the surgeon.

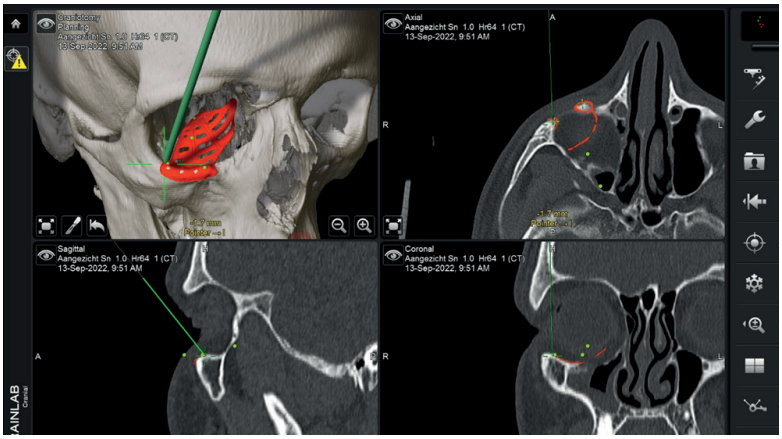


Figure 5. *Example of the object-oriented navigation feedback. Upper left corner displays the 3D model of the patient with navigation pointer. Other three views are multiplanar views indicating the tip of the navigation pointer. Quantitative feedback on the navigation markers is displayed in yellow text.*

Evaluation

The last phase in the orbital reconstruction workflow is evaluation, which is essential for assessing the accuracy of implant positioning. While navigation provides real-time guidance, definitive verification of the implant position requires imaging. Ideally, an intraoperative CT scan is performed immediately after implant positioning, allowing for immediate intraoperative adjustments if necessary.[66] Alternatively, a postoperative CT scan can be used to evaluate implant position, but that raises the threshold for additional interventions.[67]

The intraoperative or postoperative imaging can be fused with the VSP, enabling direct comparison between the planned and realized implant positions. Modern techniques allow for quantitative assessment of translational and rotational deviations, providing objective feedback on surgical accuracy.[68] Evaluation also incorporates clinical outcomes, such as globe position, orbital volume restoration, and resolution of functional deficits including diplopia, to determine whether the planning approach resulted in the intended anatomical and functional correction. Taken together, this evaluation enables a critical appraisal of the preoperative planning by identifying where and why deviations or suboptimal outcomes occur. This process is essential for validating the effectiveness of the reconstruction workflow and supports case-based learning and pooled scientific evaluations, guiding iterative improvements in future planning and reconstruction strategies.

Despite advances in computer-assisted orbital reconstruction, several challenges remain that limit the efficiency, accuracy, and widespread clinical adoption. First, the optimal integration of these tools into a personalized and efficient clinical workflow has not yet been clearly established. Second, variability in PSI design and limitations of current navigation strategies reduce the predictability and usability of these technologies in daily practice. Consequently, further work is needed to optimize the workflow for clinical implementation, thereby improving surgical accuracy and efficiency, and ultimately, enhancing patient-relevant outcomes.

Aims and outline of this thesis

The overall aim of this thesis is to optimize and clinically translate a personalized computer-assisted workflow for orbital reconstruction. To achieve this, the thesis consists of two subgoals. The first subgoal is to evaluate and refine key components of the workflow for orbital reconstruction. This involves analyzing the modular workflow, describing the individual techniques including the use and evaluation of PSIs, and identifying areas where efficiency, accuracy, or predictability can be further improved. The second subgoal is to advance the clinical translation of orbital reconstruction technologies by developing and (pre)clinically validating novel surgical navigation techniques that improve clinical usability and workflow efficiency.

Achieving these aims requires a clear understanding of the personalized workflow, which is presented in **Chapter 2**. This chapter provides the foundation for this thesis by presenting an overview of the personalized workflow for post-traumatic orbital reconstruction. It details each phase, including Diagnostics, Advanced Diagnostics, Virtual Surgical Planning, Patient-Specific Implant Design, Intraoperative Feedback, and Evaluation, with special emphasis on the design of PSIs. Building on this foundation, the thesis is organized into two main parts: Part I focuses on PSI design, whereas Part II focuses on surgical navigation.

Part I Patient-Specific Implants

In **Chapter 3**, the possibilities of implant design are expanded, demonstrating a technical framework for reconstructing complex cases involving more than two orbital walls. Design strategies tailored to address the challenges in these cases are described, including support areas, volume overcorrection, and puzzle connections. A proof-of-principle reconstruction of all four orbital walls illustrates the feasibility of these strategies.

The wide range of PSI design options also presents a challenge: no standardized guidelines for design (options) currently exist. This may lead to variability not only based on patient anatomy, but also on the preferences of designers and surgeons. In **Chapter 4** this issue is highlighted by quantifying differences in PSI design unrelated to patient factors. In a virtual study, PSI designs created by teams from two different hospitals for the same patient cases are compared.

Part II Surgical navigation

In **Chapter 5**, a virtual splint registration technique is introduced and validated in clinical practice, eliminating the need for repeat CT scanning and invasive markers. A novel method for measuring registration accuracy in vivo is developed and applied in a cohort of 10 patients to evaluate the feasibility and accuracy of this workflow.

To solve the limitations of object-oriented navigation, the research in **Chapter 6** is directed towards the development of a real-time navigation technique. A dedicated instrument was developed to rigidly attach to the implant, enabling direct tracking of the implant position. Multiple surgeons evaluated different visualization methods in an in-vitro setting to identify the most intuitive interface for real-time navigation feedback.

Chapter 7 utilizes these findings and validates the optimized real-time navigation technique in a preclinical setting. A cadaveric setup was used to compare the real-time navigation workflow with the current clinical workflow. In addition to positioning ac-

curacy and reconstruction time, this study also evaluates the practical feasibility and usability. Surgeon gaze behavior, measured as the frequency of focus shifts and duration of screen fixation, is analyzed to assess cognitive load and interface intuitiveness. The results provide insights into both the technical performance and the user-centered aspects of the workflow, informing further refinement for clinical translation.

Discussion and summary

In **Chapter 8**, the findings of this thesis are integrated into a general discussion that critically reflects on the strengths and limitations and considers future avenues for innovation and translation toward clinical care in orbital reconstruction.

References

1. Martins C, Costa e Silva IE, Campero A, Yasuda A, Aguiar LR, Tatagiba M, et al. Microsurgical anatomy of the orbit: the rule of seven. Anatomy research international. 2011;2011(1):468727.
2. Scangas GA, Gudis DA, Kennedy DW. The natural history and clinical characteristics of paranasal sinus mucoceles: a clinical review. Int Forum Allergy Rhinol. 2013;3(9):712–7.
3. Cornelius C-P, Gooris PJ. Anatomy of the orbit: overall skeletal and topographical configuration. Surgery in and around the Orbit: Springer; 2023. p. 7–58.
4. Cornelius CP, Probst F, Metzger MC, Gooris PJJ. Anatomy of the Orbits: Skeletal Features and Some Notes on the Periorbital Lining. Atlas Oral Maxillofac Surg Clin North Am. 2021;29(1):1–18.
5. Chastain JB, Sindwani R. Anatomy of the orbit, lacrimal apparatus, and lateral nasal wall. Otolaryngol Clin North Am. 2006;39(5):855–64, v–vi.
6. Hassan BA, Sylvester AD, Wescott DJ, Cunningham DL, Elegbede A, Manson PN, et al. An Introduction to the Orbital Buttresses. Plast Reconstr Surg. 2025;155(4):780e–3e.
7. Khojastepour L, Moannaei M, Eftekharian HR, Khaghaninejad MS, Mahjoori-Ghasrodashti M, Tavanafar S. Prevalence and severity of orbital blowout fractures. British Journal of Oral and Maxillofacial Surgery. 2020;58(9):e93–e7.
8. Hoffmann J, Cornelius CP, Groten M, Pröbster L, Pfannenberg C, Schwenzer N. Orbital reconstruction with individually copy-milled ceramic implants. Plast Reconstr Surg. 1998;101(3):604–12.
9. Bartoli D, Fadda MT, Battisti A, Cassoni A, Pagnoni M, Riccardi E, et al. Retrospective analysis of 301 patients with orbital floor fracture. J Craniomaxillofac Surg. 2015;43(2):244–7.
10. Arslan ED, Solakoglu AG, Komut E, Kavalci C, Yilmaz F, Karakilic E, et al. Assessment of maxillofacial trauma in emergency department. World J Emerg Surg. 2014;9(1):13.
11. Priore P, Di Giorgio D, Marchese G, Della Monaca M, Terenzi V, Battisti A, et al. Orbital bone fractures: 10 years' experience at the Rome trauma centre: retrospective analysis of 543 patients. British Journal of Oral and Maxillofacial Surgery. 2022;60(10):1368–72.
12. Gaddipati R, Ramisetti S, Vura N, Reddy KR, Nalamolu B. Analysis of 1545 Fractures of Facial Region—A Retrospective Study. Craniomaxillofacial Trauma & Reconstruction. 2015;8(4):307–14.
13. Hughes D, McQuillan J, Holmes S. Quantitative analysis of diplopia following orbital fracture repair. Br J Oral Maxillofac Surg. 2023;61(3):202–8.
14. Ahmad F, Kirkpatrick NA, Lyne J, Urdang M, Waterhouse N. Buckling and hydraulic mechanisms in orbital blowout fractures: fact or fiction? J Craniofac Surg. 2006;17(3):438–41.
15. Foletti JM, Martinez V, Haen P, Godio-Raboutet Y, Guyot L, Thollon L. Finite element analysis of the human orbit. Behavior of titanium mesh for orbital floor reconstruction in case of trauma recurrence. J Stomatol Oral Maxillofac Surg. 2019;120(2):91–4.
16. Patel S, Andrecovich C, Silverman M, Zhang L, Shkoukani M. Biomechanic Factors Associated With Orbital Floor Fractures. JAMA Facial Plastic Surgery. 2017;19(4):298–302.
17. Le FOrt R. Etude experimentale sur les fractures de la machoire superieure. Revue Chirurgio. 1901;23:208.
18. Waterhouse N, Lyne J, Urdang M, Garey L. An investigation into the mechanism of orbital blowout fractures. Br J Plast Surg. 1999;52(8):607–12.
19. Jansen J, Maal TJJ, Sabelis JF, Schreurs R, Dubois L. Diagnosis and Clinical Presentation, Workup and Decision-Making of Orbital Fractures. In: Gooris PJJ, Mourits MP, Bergsma JE, editors. Surgery in and around the Orbit: CrossRoads. Cham: Springer International Publishing; 2023. p. 199–213.
20. Pearl RM. Treatment of enophthalmos. Clin Plast Surg. 1992;19(1):99–111.
21. DeSerres JJ, Budning A, Antonyshyn OM. Current Management of Late Posttraumatic Enophthalmos. Plast Reconstr Surg. 2022;150(4):888e–902e.

22. He Y, Zhang Y, An JG. Correlation of types of orbital fracture and occurrence of enophthalmos. J Craniofac Surg. 2012;23(4):1050–3.
23. Braaksma-Besselink Y, Jellema HM. Orthoptic Evaluation and Treatment in Orbital Fractures. Atlas Oral Maxillofac Surg Clin North Am. 2021;29(1):41–50.
24. Braaksma-Besselink Y, Jellema HM. Diplopia. Surgery in and around the Orbit: CrossRoads: Springer; 2023. p. 149–68.
25. Jansen J, Dubois L, Maal TJJ, Mourits MP, Jellema HM, Neomagus P, et al. A nonsurgical approach with repeated orthoptic evaluation is justified for most blow-out fractures. J Craniomaxillofac Surg. 2020;48(6):560–8.
26. Burnstine MA. Clinical recommendations for repair of isolated orbital floor fractures: an evidence-based analysis. Ophthalmology. 2002;109(7):1207–10; discussion 10–1; quiz 12–3.
27. Holmes S. Primary Orbital Fracture Repair. Atlas Oral Maxillofac Surg Clin North Am. 2021;29(1):51–77.
28. Damgaard OE, Larsen CG, Felding UA, Toft PB, von Buchwald C. Surgical Timing of the Orbital "Blowout" Fracture. Otolaryngology–Head and Neck Surgery. 2016;155(3):387–90.
29. Jazayeri HE, Khavanin N, Yu JW, Lopez J, Ganjawalla KP, Shamliyan T, et al. Does Early Repair of Orbital Fractures Result in Superior Patient Outcomes? A Systematic Review and Meta-Analysis. Journal of Oral and Maxillofacial Surgery. 2020;78(4):568–77.
30. Dubois L, Steenen SA, Gooris PJ, Bos RR, Becking AG. Controversies in orbital reconstruction-III. Biomaterials for orbital reconstruction: a review with clinical recommendations. Int J Oral Maxillofac Surg. 2016;45(1):41–50.
31. Dubois L, Dillon J, Jansen J, Becking AG. Ongoing Debate in Clinical Decision Making in Orbital Fractures: Indications, Timing, and Biomaterials. Atlas Oral Maxillofac Surg Clin North Am. 2021;29(1):29–39.
32. Tarsitano A, Badiali G, Pizzigallo A, Marchetti C. Orbital Reconstruction: Patient-Specific Orbital Floor Reconstruction Using a Mirroring Technique and a Customized Titanium Mesh. J Craniofac Surg. 2016;27(7):1822–5.
33. Sigron GR, Rüedi N, Chammartin F, Meyer S, Msallem B, Kunz C, et al. Three-Dimensional Analysis of Isolated Orbital Floor Fractures Pre- and Post-Reconstruction with Standard Titanium Meshes and "Hybrid" Patient-Specific Implants. Journal of Clinical Medicine. 2020;9(5):1579.
34. Metzger MC, Schön R, Zizelmann C, Weyer N, Gutwald R, Schmelzeisen R. Semiautomatic procedure for individual preforming of titanium meshes for orbital fractures. Plast Reconstr Surg. 2007;119(3):969–76.
35. Strong EB, Fuller SC, Wiley DF, Zumbansen J, Wilson MD, Metzger MC. Preformed vs Intraoperative Bending of Titanium Mesh for Orbital Reconstruction. Otolaryngology–Head and Neck Surgery. 2013;149(1):60–6.
36. Metzger MC, Schön R, Tetzlaf R, Weyer N, Rafii A, Gellrich NC, et al. Topographical CT-data analysis of the human orbital floor. Int J Oral Maxillofac Surg. 2007;36(1):45–53.
37. Kärkkäinen M, Wilkman T, Mesimäki K, Snäll J. Primary reconstruction of orbital fractures using patient-specific titanium milled implants: the Helsinki protocol. Br J Oral Maxillofac Surg. 2018;56(9):791–6.
38. Gander T, Essig H, Metzler P, Lindhorst D, Dubois L, Rücker M, et al. Patient specific implants (PSI) in reconstruction of orbital floor and wall fractures. J Craniomaxillofac Surg. 2015;43(1):126–30.
39. Zhao Z, Guo Z, Hu W, Long J. Assessment of the Correlation Between Types of Orbital Fractures and Ocular Symptoms, and the Effect of Manual Preformed and Patient-Specific Mesh Implants: A Retrospective Study. Journal of Craniofacial Surgery. 2025;36(1):84–8.
40. Maher DI, Hall AJ, Gwini S, Ben Artsi E. Patient-specific Implants for Orbital Fractures: A Systematic Review. Ophthalmic Plast Reconstr Surg. 2021.
41. Joachim MV, Farsio F, Markiewicz MR, Miloro M. Patient-Specific Implants in Post-traumatic

Orbital Reconstruction: A Systematic Review. Journal of Oral and Maxillofacial Surgery. 2026;84(2):197–213.e4.
42. Schreurs R, Klop C, Gooris PJJ, Maal TJJ, Becking AG, Dubois L. Critical appraisal of patient-specific implants for secondary post-traumatic orbital reconstruction. Int J Oral Maxillofac Surg. 2021.
43. Gellrich NC, Dittmann J, Spalthoff S, Jehn P, Tavassol F, Zimmerer R. Current Strategies in Post-traumatic Orbital Reconstruction. J Maxillofac Oral Surg. 2019;18(4):483–9.
44. Gooris PJJ, Muller BS, Dubois L, Bergsma JE, Mensink G, van den Ham MFE, et al. Finding the Ledge: Sagittal Analysis of Bony Landmarks of the Orbit. J Oral Maxillofac Surg. 2017;75(12):2613–27.
45. Dubois L, Sabelis JF, Jansen J, Maal TJJ, Schreurs R. Surgical Treatment of Solitary Orbital Wall Fractures. In: Gooris PJJ, Mourits MP, Bergsma JE, editors. Surgery in and around the Orbit: CrossRoads. Cham: Springer International Publishing; 2023. p. 215–36.
46. Baumann A, Sinko K, Dorner G. Late Reconstruction of the Orbit With Patient-Specific Implants Using Computer-Aided Planning and Navigation. Journal of Oral and Maxillofacial Surgery. 2015;73(12, Supplement):S101–S6.
47. HORSLEY V, CLARKE RH. The Structure and Functions of the Cerebellum Examined by a New Method. Brain. 1908;31(1):45–124.
48. Schreurs R, Wilde F, Schramm A, Gellrich NC. Intraoperative Feedback and Quality Control in Orbital Reconstruction: The Past, the Present, and the Future. Atlas Oral Maxillofac Surg Clin North Am. 2021;29(1):97–108.
49. Schreurs R, Becking AG, Jansen J, Dubois L. Advanced Concepts of Orbital Reconstruction: A Unique Attempt to Scientifically Evaluate Individual Techniques in Reconstruction of Large Orbital Defects. Atlas Oral Maxillofac Surg Clin North Am. 2021;29(1):151–62.
50. Metzger MC, Hohlweg-Majert B, Schön R, Teschner M, Gellrich NC, Schmelzeisen R, et al. Verification of clinical precision after computer-aided reconstruction in craniomaxillofacial surgery. Oral Surg Oral Med Oral Pathol Oral Radiol Endod. 2007;104(4):e1–10.
51. Jansen J, Dubois L, Schreurs R, Gooris PJJ, Maal TJJ, Beenen LF, et al. Should Virtual Mirroring Be Used in the Preoperative Planning of an Orbital Reconstruction? J Oral Maxillofac Surg. 2018;76(2):380–7.
52. Schreurs R, Klop C, Maal TJJ. Advanced Diagnostics and Three-dimensional Virtual Surgical Planning in Orbital Reconstruction. Atlas Oral Maxillofac Surg Clin North Am. 2021;29(1):79–96.
53. Jansen J, Schreurs R, Dubois L, Maal TJJ, Gooris PJJ, Becking AG. The advantages of advanced computer-assisted diagnostics and three-dimensional preoperative planning on implant position in orbital reconstruction. J Craniomaxillofac Surg. 2018;46(4):715–21.
54. Rana M, Chui CHK, Wagner M, Zimmerer R, Rana M, Gellrich N-C. Increasing the Accuracy of Orbital Reconstruction With Selective Laser-Melted Patient-Specific Implants Combined With Intraoperative Navigation. Journal of Oral and Maxillofacial Surgery. 2015;73(6):1113–8.
55. Gellrich NC, Schramm A, Hammer B, Rojas S, Cufi D, Lagrèze W, et al. Computer-assisted secondary reconstruction of unilateral posttraumatic orbital deformity. Plast Reconstr Surg. 2002;110(6):1417–29.
56. Pedemonte Trewhela C, Díaz Reiher M, Muñoz Zavala T, González Mora LE, Vargas Farren I. Correction of Delayed Traumatic Enophthalmos Using Customized Orbital Implants. J Oral Maxillofac Surg. 2018;76(9):1937–45.
57. Kotecha S, Ferro A, Harrison P, Fan K. Orbital reconstruction: a systematic review and meta-analysis evaluating the role of patient-specific implants. Oral Maxillofac Surg. 2023;27(2):213–26.
58. Blumer M, Essig H, Steigmiller K, Wagner ME, Gander T. Surgical Outcomes of Orbital Fracture Reconstruction Using Patient-Specific Implants. J Oral Maxillofac Surg.

2021;79(6):1302–12.
59. Probst FA, Cornelius CP, Otto S, Malenova Y, Probst M, Liokatis P, et al. Accuracy of free-hand positioned patient specific implants (PSI) in primary reconstruction after inferior and/or medial orbital wall fractures. Comput Biol Med. 2021;137:104791.
60. Sorriento A, Porfido MB, Mazzoleni S, Calvosa G, Tenucci M, Ciuti G, et al. Optical and Electromagnetic Tracking Systems for Biomedical Applications: A Critical Review on Potentialities and Limitations. IEEE Rev Biomed Eng. 2020;13:212–32.
61. Kral F, Puschban EJ, Riechelmann H, Freysinger W. Comparison of optical and electromagnetic tracking for navigated lateral skull base surgery. Int J Med Robot. 2013;9(2):247–52.
62. Dubois L, Essig H, Schreurs R, Jansen J, Maal TJ, Gooris PJ, et al. Predictability in orbital reconstruction. A human cadaver study, part III: Implant-oriented navigation for optimized reconstruction. J Craniomaxillofac Surg. 2015;43(10):2050–6.
63. Verbist M, Dubron K, Bila M, Jacobs R, Shaheen E, Willaert R. Accuracy of surgical navigation for patient-specific reconstructions of orbital fractures: A systematic review and meta-analysis. Journal of Stomatology, Oral and Maxillofacial Surgery. 2024;125(3):101683.
64. Azarmehr I, Stokbro K, Bell RB, Thygesen T. Surgical Navigation: A Systematic Review of Indications, Treatments, and Outcomes in Oral and Maxillofacial Surgery. J Oral Maxillofac Surg. 2017;75(9):1987–2005.
65. Schreurs R, Dubois L, Becking AG, Maal TJJ. Implant-oriented navigation in orbital reconstruction. Part 1: technique and accuracy study. Int J Oral Maxillofac Surg. 2018;47(3):395–402.
66. Jansen J, Schreurs R, Dubois L, Maal TJJ, Gooris PJJ, Becking AG. Intraoperative imaging in orbital reconstruction: how does it affect the position of the implant? Br J Oral Maxillofac Surg. 2020;58(7):801–6.
67. Schlittler F, Schmidli A, Wagner F, Michel C, Mottini M, Lieger O. What Is the Incidence of Implant Malpositioning and Revision Surgery After Orbital Repair? J Oral Maxillofac Surg. 2018;76(1):146–53.
68. Schreurs R, Dubois L, Becking AG, Maal TJ. Quantitative Assessment of Orbital Implant Position--A Proof of Concept. PLoS One. 2016;11(3):e0150162.

Chapter 2

Personalized orbital reconstruction workflow

This chapter is based on the following publication:

Sabelis J.F., Schreurs R., Essig H., Becking A.G., Dubois L. Personalized Medicine Workflow in Post-Traumatic Orbital Reconstruction. J Pers Med. 2022 Aug 24;12(9):1366.

Abstract

Surgical management of orbital fractures focuses on restoring the bony contours to support the soft tissue and repositioning the globe to recover ocular function. There are different types of titanium implants available: flat, preformed and patient-specific implants. Restoration of the bony contours can be challenging due to the limited overview. Computer-assisted surgery has been implemented in the workflow to improve the accuracy of the reconstruction. Computer-assisted surgery has enabled personalized treatment of orbital fractures: treatment planning is optimized to fit the patient's needs. The design of a patient-specific implant further tailors treatment to the individual. Its design is based on clinical considerations and used to further increase the feed-back for the intraoperative stage. Additional feedback can be obtained by surgical navigation and/or intraoperative imaging to ensure that the implant is placed in the desired position. Evaluation of the surgical result is necessary for further improvement of the computer-assisted workflow in orbital reconstruction.

Introduction

The orbit is an inward-projecting bony structure in the shape of a cone (or pyramid) at the transition between midface and skull base.[1-3] The base of the orbit, the orbital rim, is composed of thick bone; in contrast, the orbit's inner walls are thin bony structures. The orbit provides the casing for the soft-tissue structures associated with the visual (motor) system: neurovascular structures, connective tissue, ocular muscles, and the globe.[4, 5] With its central position and thin bony walls, the orbit is probably the most vulnerable part of the facial skeleton.[1, 2] Two possible theories of orbital fracture pathogenesis have been suggested. The buckling theory suggests that the energy of a traumatic impact on the orbital rim after blunt-force trauma is propagated to the thin inner walls and leads to a fracture in these weaker structures.[6-8] Hydraulic theory considers increased pressure after impact on the globe and orbital contents as the main reason for orbital wall fractures. The exact nature and specifics of a fracture may be explained by a combination of both mechanisms.[7]

The orbital volume may be increased, and soft tissue may be displaced into the adjacent sinuses due to the impact or the dislocation of supporting bony structures. The globe's position may be displaced after trauma, for instance, with inward displacement (enophthalmos) or inferior displacement (hypoglobus). The orbital soft tissue may be affected by the traumatic impact as well. The structural integrity and functional capacities of connective tissue or extraocular muscles may be disrupted, resulting in a disturbance of ocular motility and double vision (diplopia). The location and type of the impact, in combination with the amount of energy transferred to the orbit's bony structures and orbital soft tissue, are responsible for the heterogeneity in clinical presentation.

There is an ongoing debate on the indication of surgical reconstruction, and systematic reviews have not been able to provide evidence-supported guidelines.[9-11] Some advocate a radical approach to prevent clinical symptoms,[12] while others choose a more conservative approach with a delayed surgery if clinical symptoms develop.[13] Indication for reconstruction remains a subjective decision in most cases, depending on the surgeon and patient characteristics. The surgical management of orbital fractures focuses on the repositioning the orbital contents and the globe and reinstating the structural support to recover ocular function. Restoration of the orbit is the first and most predictable step in the surgical treatment of orbital fractures.[14, 15]

Nowadays, titanium mesh implants have become the preferred biomaterial for the surgical reconstruction of the orbit. Titanium implants can be categorized into flat implants, preformed implants, and patient-specific implants (PSIs). Flat implants are manually shaped and trimmed by the surgeon. A generic or individual model of the (mirrored) orbit may aid in the molding process. Preformed implants have a predefined shape, based on a model of the average orbit.[16] Patient-specific implants (PSIs) are designed on an individual basis for the patient and are subsequently produced through additive manufacturing.

The soft tissue's intricate architecture and the proximity to vital structures pose surgical challenges in orbital reconstruction.[17, 18] Orbital reconstruction is keyhole surgery performed in a confined space. This contributes to limited visualization, which is further enhanced by protruding fat. The margin of error is small: an incorrectly positioned implant may have significant implications for the clinical outcome and the patient's quality of life, and it is considered a ground for revision surgery in the literature.[19, 20] Medical

technology has been incorporated in the clinical workflow of orbital reconstructions to reduce the risk of implant malpositioning.[21]

This technology-supported workflow, called computer-assisted surgery (CAS), has become the standard for complex orbital traumatology in many hospitals.[22] The introduction of CAS has also enabled personalization of the treatment: treatment planning is customized to fit the options and needs of the patient, and intraoperative guidance is adjusted to the anatomical possibilities. The main aim of this article is to provide a complete overview of the (CAS) workflow for orbital reconstruction, with an in-depth description of the techniques embedded in the workflow and with a special focus on treatment personalization through patient-specific implant design.

Post-traumatic Orbital Reconstruction Workflow

The conventional workflow of post-traumatic orbital reconstruction and possible CAS techniques are illustrated in *Figure 1*. The individual phases are explained in detail in the following paragraphs.

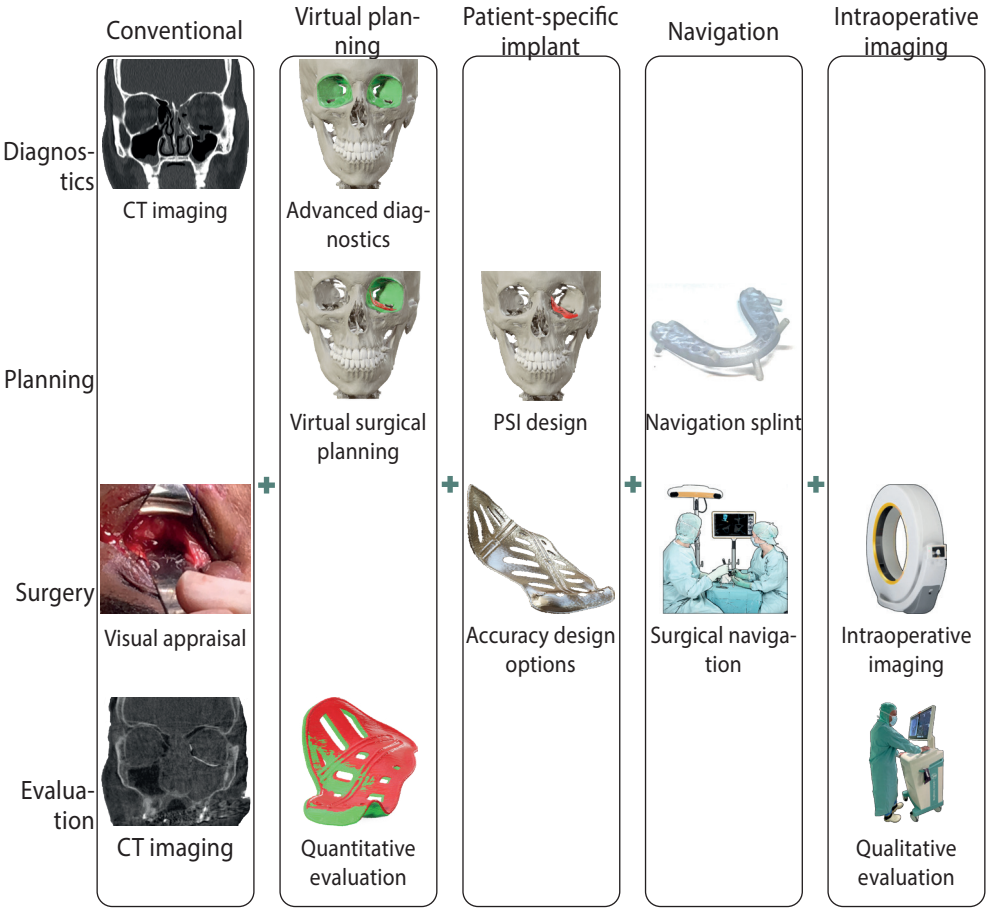


Figure 1. *Schematic overview of the technological possibilities within the orbital reconstruction workflow. Chronologically, a clinical workflow consists of diagnostics, planning, surgery, and evaluation. In the conventional workflow, the surgeon is dependent on clinical assessment and preoperative imaging,*

visual appraisal during surgery and postoperative imaging for evaluation. CAS consists of several techniques that may be combined and affect one or multiple workflow stages. Several CAS technologies may be combined.

Diagnostics

A thorough clinical and radiographic evaluation of the patient is essential to determine the optimal treatment. Clinical evaluation should at least assess the amount of globe displacement and the degree of double vision. The Hertel exophthalmometer is the simplest tool to quantitatively measure the relative ventrodorsal globe position.[23] It is the current gold standard despite the known limitations, such as the asymmetry of lateral orbital rims, the compression of soft tissue, and the lack of a uniform technique.[23, 24] There are no readily available reproducible tools for measuring the relative craniocaudal globe position.[25] It is assessed by the Hirschberg test, which evaluates the light reflex centered on each pupil to reveal vertical asymmetry.[26] Alternative methods have been proposed to quantify globe position differences based on imaging, but these have not been broadly implemented.[23, 27]

One of the difficulties in clinical decision-making is to address the most common complaint in orbital fractures: diplopia. It is challenging to find the actual cause of diplopia; in most cases, it is caused by a restriction of ocular motility. Ocular motility can be disturbed by impingement or the entrapment of the ocular muscles and surrounding soft tissue, but also by muscle edema, muscle injury, hemorrhage, emphysema, or motor nerve palsy. In a trauma setting, orthoptic measurements may be challenging to perform due to logistics, limited mobility of the patient, or considerable periorbital swelling. Absolute restrictions, as seen in trapdoor fractures, need to be treated shortly after the trauma. Ocular motility deficits with different etiology may improve or resolve over time, and surgery might not be indicated. In these cases, it is advisable to perform several orthoptic assessments over time to monitor spontaneous improvement. Moreover, the orthoptist may be able to differentiate between possible causes of double vision through repeated measurements.[9, 28]

Computed tomography (CT) is the modality of choice for radiographic evaluation because of the superior visualization of bony structures. The size and extent of the fracture may be estimated or measured in the coronal, sagittal, or axial plane. Considering that the bone is paper-thin in certain areas, a maximum slice thickness of 1.0 mm is essential for evaluation. In individual cases, the evaluation of soft-tissue changes may become important. Shape alterations of the inferior rectus muscle have been reported to affect delayed or postoperative enophthalmos[29-31] and may affect treatment decisions.[10] In addition, herniation of the orbital soft tissue might be an indication for surgical reconstruction. Magnetic resonance imaging (MRI) provides superior soft-tissue contrast compared to CT and is more sensitive for identifying extraocular muscle or periorbital fat entrapment.[32, 33] Nevertheless, the acquisition of an MRI is not part of the standard imaging protocol for orbital trauma.[13] This may change in the future, considering that all subsequent treatment steps benefit from optimizing the information collection in the diagnostics phase.

Advanced Diagnostics

Advanced diagnostics aim to maximize the information extracted from the available image data. For this purpose, the CT scan is imported into the virtual surgical planning software. The CT scan is subdivided into voxels (3D pixels), each with a grayscale

value corresponding to the X-ray absorption within that volume. These voxels may be segmented (grouped) based on the tissue type or anatomical structure they belong to. Anatomical structures of interest in orbital trauma are the orbit, orbital cavity, and possibly surrounding bony structures such as the zygomatic complex. The segmentation is visualized as an overlay in the multi-planar view and as a 3D model. Additional information may be collected through quantification (e.g., volume measurement), or manipulation (e.g., mirroring) of the segmented anatomy (illustrated in *Figure 2*). The unaffected contralateral orbit and orbital cavity can provide a reference for the affected orbit in unilateral fractures, which provides insight into the extent of the fracture and displacement of orbital walls or surrounding bony structures. The volume of the affected orbit can be compared to the unaffected healthy side to determine the relative volume change, since it has been proven that the orbits are highly symmetrical.[33] These volumetric changes can be incorporated into the treatment plan.[34] Information may also be extracted from multiple image sets. Image fusion allows aligning multiple datasets of the same modality over time or image sets from different modalities. The image sets can be simultaneously visualized and evaluated after image fusion. The segmentation process can also be based on information from multiple fused modalities.

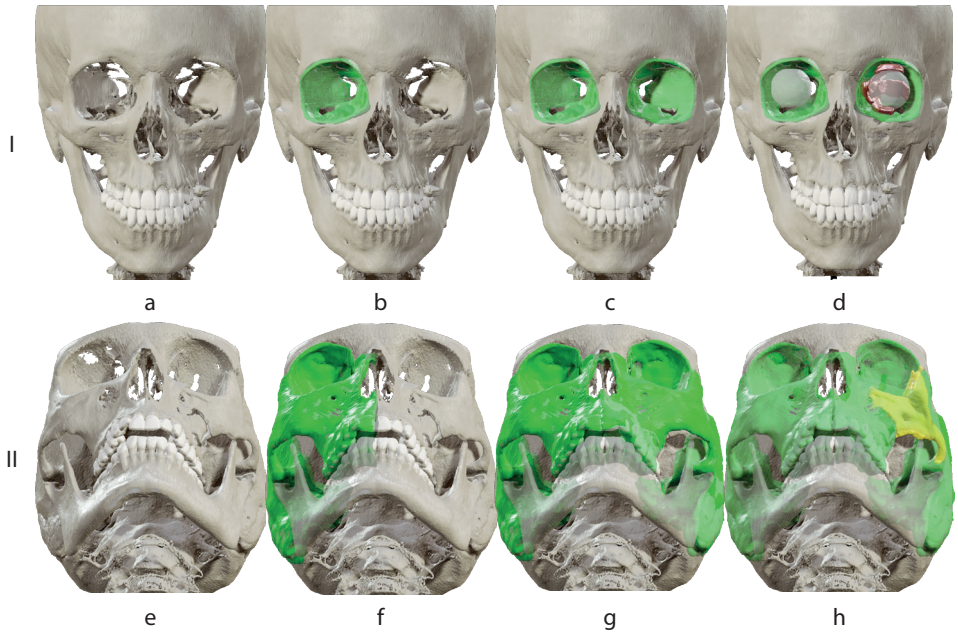


Figure 2. *Advanced diagnostics for two cases. I: Solitary orbital reconstruction (a-d). (a) Visualization of the 3D bone surface model. (b) Segmentation of the unaffected orbit. (c) Mirroring of the segmented orbit to the affected, contralateral side. (d) Visualization of additional structures, such as the globe and eye muscles. II: Zygomatic complex fracture (e-h). (e) Visualization of the 3D bone surface model. (f) Segmentation of the unaffected side. (g) Mirroring of the segmentation to the affected, contralateral side. (h) Visualization of the zygomatic complex displacement.*

Virtual Surgical Planning

Virtual surgical planning (VSP) is a simulation of the actual surgery on the imaging data.[35] It is based on information gathered in the previous treatment stages. The exact content of the virtual surgical planning depends on the type of implant. If a flat mesh plate is used, the virtual models of the mirrored orbit and affected orbit can be exported and 3D printed to serve as individual bending template(s) for molding the flat mesh.

In the preformed implant setting, the stereolithographic model (STL) of a preformed implant is imported into the planning environment to perform a virtual reconstruction of the affected orbit. The implant's fitting potential is evaluated and its optimal position for an accurate reconstruction of the pretraumatized anatomy is simulated. The potential of VSP in the preformed implant setting is thus highly dependent on the willingness of the implant manufacturers to provide STLs of their preformed implants. In modern planning software, the implant may be automatically aligned to another virtual model, for instance, the mirrored orbit. Manual adjustments could be necessary to prevent interferences with the bone and ensure the orbital defect is covered, with adequate implant support on the dorsal ledge and fixation possibility on the infraorbital rim.

The implant may be virtually trimmed to simulate the cutting of medial or posterior parts of the implant. The surgery can be simulated multiple times in the virtual surgical planning, with different implant types and sizes (*Figure 3*). This enables comparison between preformed implant options and substantiated decision making before surgery. The number of try-ins in virtual planning is limitless without consequences for the patient, in contrast to try-ins during actual surgery. Establishing the optimal position in virtual planning provides the surgeon with intraoperative feedback, which could reduce the operating time and extent of manipulation inside the orbit during surgery.[36]

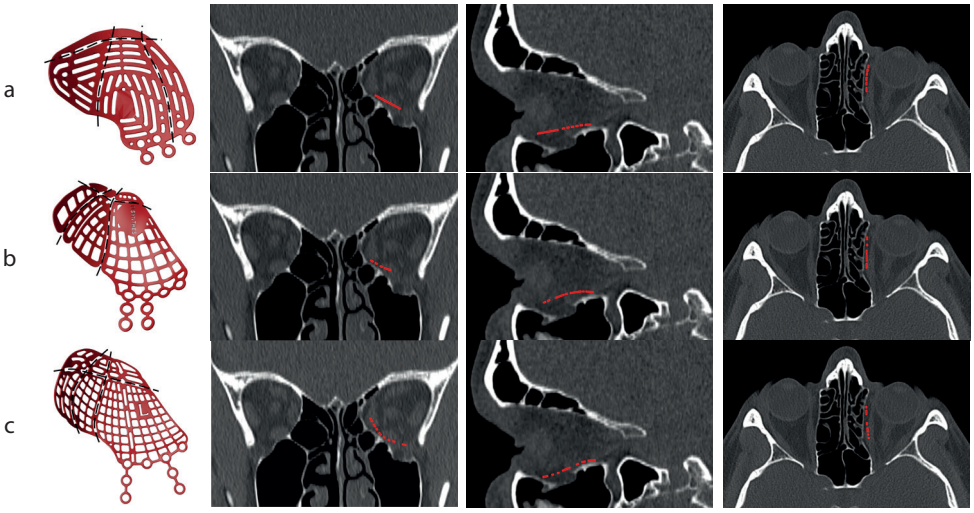


Figure 3. *Virtual fitting of different preformed implants in a solitary orbital fracture. Three-dimensional models of the preformed implants of KLS Martin (a), Synthes (b) and Stryker (c) are visualized with potential cutting lines (black lines) in the first column. The implants are virtually positioned (red contour) and the fit is evaluated in the coronal, sagittal, and axial slices. Important considerations are adequate support (on the posterior ledge, on the medial wall and on the infraorbital rim) and a lack of interference with bone.*

Patient-Specific Implant Design

Reconstructing the orbit with a PSI is the ultimate step of individualization for orbital reconstruction. A PSI is virtually modelled from scratch, using information from the (advanced) diagnostics phase and exported virtual models. In dedicated design software, a prototype implant is generated. The prototype is imported into the virtual surgical planning and its fit is evaluated. The position of the prototype is not adjusted in the virtual surgical planning to improve the fit, but the design of the prototype is adjusted and the novel prototype is reimported. Even though the design of a PSI is not set in stone by protocols, various design considerations have been described in the literature. An overview of options is summarized in *Table 1*. This overview is not comprehensive, and novel design options are regularly introduced in the literature.

Table 1. *List of different design considerations as reported in the literature.*

Design consideration	***Effect on***	***Options***	***References***	***Notes***
Thickness	Positioning, stability	0.3 mm	[22, 37, 38]	
Atraumatic cord	Positioning, stability	Present	[37, 39, 40]	
		Absent	[38, 41, 42]	
Grid	Clinical symptoms	Horizontal	[22, 37, 40, 43]	
		Squares	[38, 39, 41, 44]	
		Porous	[42, 45, 46]	
Support	Stability, accuracy	Three points	[22]	Infraorbital rim, medial wall, posterior ledge
			[38]	Anteromedial, anterolateral, posterior
		Ledge	[37, 40, 43]	Inverted shovel design
		Lateral posterior wall	[43]	Stabilizer for self-centering implant
Extension	Accuracy	Orbital rim	[22, 42, 44, 46-48]	
		Lateral posterior wall	[43]	
		Specific bone features	[45]	
Anterior elevation	Clinical symptoms		[22]	Rim elevation to correct hypoglobus

Overcorrection	Clinical symptoms	Location	[22]	Posterior to bulbus
			[49]	Orbital floor elevated in sagittal relation
		Amount	[22]	Based on clinical findings, advanced diagnostics
			[38]	Slight overcorrection
			[50]	Same amount in cubic cm as mm enophthalmos
		Intraoperatively	[51]	Spacers
Navigation	Accuracy	Markers	[22, 37-39, 52]	Eminence lacrimal foramen[38]
		Vectors	[37, 40, 43]	
Fixation	Stability	Present	[22, 37, 39, 40, 42, 46, 47, 53]	Eccentric screw alters implant position[47]
				Fix implant if form stable[40]
		Absent	[38, 44, 48]	
Fixation re-use	Accuracy	Re-used screw hole	[54]	Only in secondary reconstruction
Multi-piece	Position, stability, accuracy	Lazy-S	[42, 47, 49]	
		Interlocking	[46, 48, 55]	

Design considerations can be categorized based on their intended effect: stability, positioning ease, accuracy of implant positioning or alleviation of clinical symptoms. The size and shape of the implant are dependent on the extent of the defect. The defect should be covered by the implant and its shape should reflect the intended reconstruction of the affected orbital walls. Support on existing bony structures is taken into account to ensure the stability of the reconstruction. Analogous to the preformed implants, support is most often found at three points in the orbit.[22, 38] Fixation is recommended to ensure a stable position of the PSI.[39, 40] Possible screw positions can be assessed in virtual planning, factoring in the patient's anatomy and local bone quality. The thickness of the implant and implementation of an atraumatic cord around the edge are considerations that affect both the stability of the implant and the positioning ease during surgery. Due to additive-manufactured titanium's rigidity, an implant thickness of 0.3 mm in combination with an atraumatic cord results in a good balance between rigidity and positioning ease.

The accuracy of implant positioning can be controlled by extensions over unaffected bony pillars. A compelling fit is created by the extension(s) of the implant over bony structures. An infraorbital rim extension limits rotation and translation in the anteroposterior direction.[47] Additional flanges to the posterior lateral wall may be implemen-

ted to prevent unwanted implant movement.[43] Screw positions from fixation material from a previous reconstruction can be re-used in secondary reconstruction to provide guidance and thus improve the accuracy of the implant positioning.[54] Another design option is to incorporate navigation markers and vectors, which can enhance the interpretation of feedback from the intraoperative navigation system.

The last category, clinical symptoms, deals with the correction of globe displacement. The orbital volume is corrected to alleviate globe displacement, but the volume may be overcorrected to counteract fat atrophy and the anticipated iatrogenic loss of soft tissue.[56] The amount of overcorrection might be subjectively determined during surgery, by inserting additional spacers,[51] or it may be fully integrated into the design of the PSI, posterior to the equator of the bulbus.[22, 38, 50] On the other hand, hypoglobus is the result of caudal displacement of the infra-orbital rim. An anterior elevation corresponding to the amount of downward displacement of the orbital rim may alleviate hypoglobus (*Figure 4*). The grid of the PSI can be designed with different techniques: using a large horizontal pattern to maximize drainage,[37, 40, 43] or a more porous arrangement.[42, 45, 46] The multitude of design options and manual design leads to a wide range of possible PSI shapes (*Figure 5*).

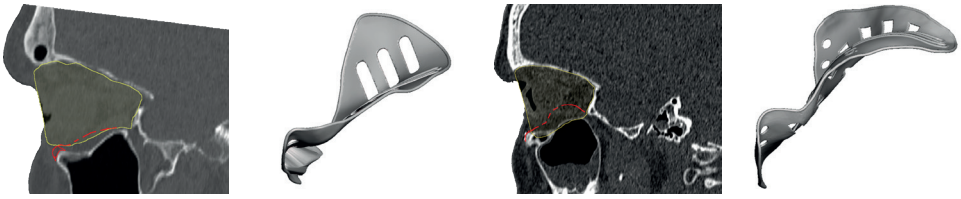


Figure 4. *Examples of two patient-specific implant designs with overcorrection (red contour) of the mirrored orbital volume (yellow contour). The first patient-specific implant is designed with an anterior elevation at the infra-orbital rim to compensate for the asymmetry in globe position (a,b). The second patient-specific implant is designed with a large overcorrection for an anophthalmic socket reconstruction (c,d).*

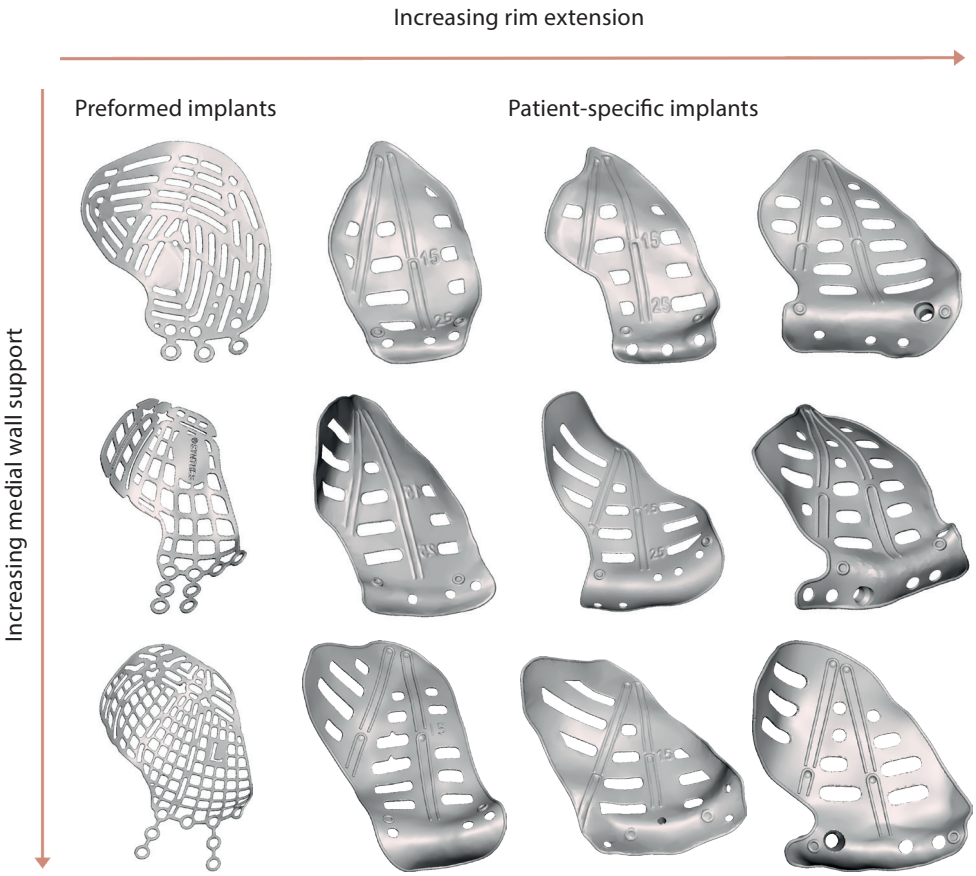


Figure 5. *Different shapes of the available preformed implants and patient-specific implants are illustrated. There is a wide variety in shapes in the patient-specific implants. From left to right the rim extension is increased. From top to bottom the medial wall support is increased.*

The PSI design can be adapted to facilitate the reconstruction of multi-wall defects, for example, through the application of multiple PSIs (*Figure 6*). This enables a reconstruction that covers the entire defect while limiting the size of the PSI and, in turn, the required incision.[46, 55] Depending on the connection used, it also provides the opportunity to create artificial support and relative feedback. A PSI that solely reconstructs the orbit will not suffice in cases with concomitant fractures of the surrounding bony structures. Repositioning the surrounding bone may be required in addition to the orbital reconstruction. Additional design options are available to gain feedback from PSIs on the subsequent reconstruction steps in these more extensive cases. An example of this is embedding the desired position of the zygomatic complex in the PSI design to facilitate correct repositioning.[54]

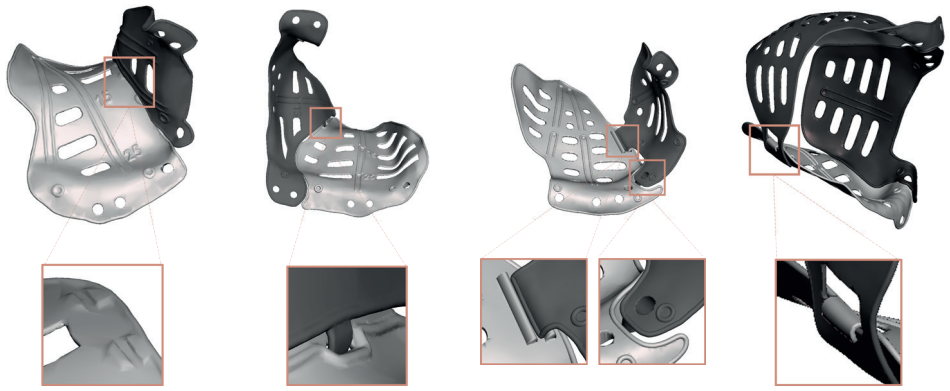


Figure 6. *Patient-specific implant design for multi-wall cases. (a) Ridges on the orbital floor implant provide relative feedback for the positioning of the lateral wall implant. (b) Patrix–matrix connection to connect a medial wall and orbital floor implant. (c) The orbital floor implant with medial wall extension is connected to a lateral wall implant dorsally with ridges and anteriorly with a puzzle connection. (d) Four-wall reconstruction with a hook-and-bar connection for additional support for the orbital floor implant.*

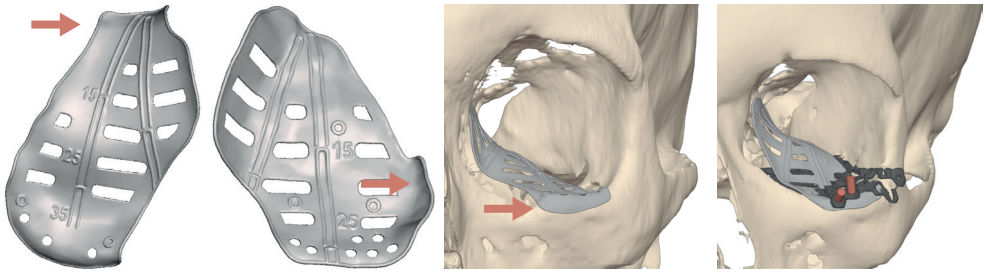
Intraoperative Feedback

During surgery, the surgeon aims to position the implant as closely as possible to the ideal position that was established in the VSP. The availability of the VSP provides intraoperative feedback that improves the result of the reconstruction.[35] Additional types of feedback are available to aid in the accurate positioning of the implant (*Table 2*). The design options relating to implant positioning ensure static feedback through the unique and compelling fit of the PSI (*Figure 7*). In secondary cases, the re-use of screw positions from the primary reconstruction will also help to find the planned position.

During surgery, the surgeon aims to position the implant as closely as possible to the ideal position that was established in the VSP. The availability of the VSP provides intraoperative feedback that improves the result of the reconstruction.[35] Additional types of feedback are available to aid in the accurate positioning of the implant (*Table 2*). The design options relating to implant positioning ensure static feedback through the unique and compelling fit of the PSI (*Figure 7*). In secondary cases, the re-use of screw positions from the primary reconstruction will also help to find the planned position.

Table 2. *Different feedback methods available in the operation room.*

Feedback method	***Static/Dynamic***
Virtual surgical planning	Static
Compelling fit patient-specific implant	Static
Fixation re-use	Static
Navigation	Dynamic
Markers and vectors	Dynamic
Intraoperative imaging	Static



a b c d

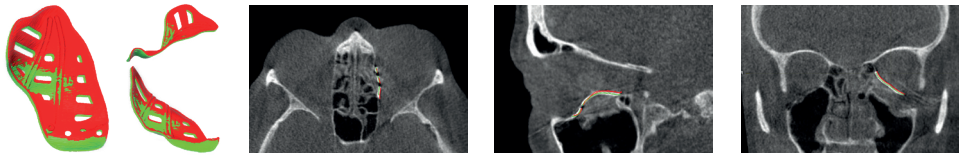
Figure 7. *Illustration of the different feedback methods.). Markers and vectors are visualized in (a) and (b). Compelling fit of the patient-specific implant design is indicated with pink arrows (a–c) Segmentation of screw holes of the previous reconstruction are illustrated in pink (d) and the previous implant in dark grey.*

Surgical navigation may be utilized to provide dynamic feedback on the implant position. During the registration for surgical navigation, the patient's position in the operating room (OR) is linked to the preoperative imaging data in the virtual surgical planning. Several registration methods are available: soft-tissue registration, bone-anchored fiducials, and surgical splints.[57, 58] Splint registration methods used to require repeated radiographic imaging with the fiducial splint in place, but the fusion of intraoral scan data in the advanced diagnostics phase allows the fabrication of a registration splint without additional radiologic imaging.[59] The splint is designed on the individual patient's dentition and carries fiducials that can be indicated virtually in the planning software and physically in the OR.

After registration, the navigation pointer's position in the patient is visualized in the virtual surgical planning on the navigation system's screen. This provides the surgeon with feedback on the position of the pointer, representing the position of the indicated location (a specific spot on the implant's surface). The quality and interpretability of the feedback may be enhanced through navigation markers embedded in the design.[39, 52] The markers are indicated in the VSP as navigation landmarks and used as a reference in the OR. If the surgeon positions the pointer in the navigation marker on the implant, visual and quantitative feedback about the pointer's position compared to the landmark is provided.

Evaluation

Intraoperative imaging of the patient after implant positioning is highly recommended, since the realized implant position can be qualitatively evaluated. If the surgeon is not satisfied with the position, the implant can be repositioned in the same surgical setting, preventing a revision surgery. For a complete quantitative evaluation of the surgical result, the scan can be reconstructed and fused with the VSP. The planned position of the implant can be compared to the achieved position of the implant to enable an objective assessment (*Figure 8*). Differences between planned and realized position can be quantified in three dimensions and expressed as rotations (roll, pitch and yaw) and translations (x, y and z).[60] Additionally, the volumetric difference between the reconstructed and unaffected or planned orbit may be assessed. Postoperative CT-scans are indicated if intraoperative CT is not acquired (or offered incomplete information), or if clinical considerations in the follow-up period necessitate additional imaging.



a b c d

Figure 8. *Illustration of an evaluation. (a) Three-dimensional model of the planned patient-specific implant (red) and the realized patient-specific implant (green) viewed from different perspectives. (b-d) Axial, sagittal, and coronal view of the postoperative computed tomography scan with the planned contour of the patient-specific implant in red.*

An optimally positioned orbital implant is no guarantee for a perfect clinical outcome. Restoration of the globe position can be relatively well achieved with a PSI, even in secondary reconstructions.[22] It is more complex to treat diplopia, as it involves the mechanical mobility of the eye, combined visual perception, and processing in the visual cortex. Visual processing may (partially) adapt over time. At discharge, the patient is informed that double vision will be experienced for the first 10–14 days, possibly longer. Ocular motility can be improved by training the extraocular muscles to prevent scarring and anticipate fibrosis.[61] Instructions are provided to mobilize the eye as much as possible: monocular orthoptic exercises six times per day for 6–12 weeks to prevent adhesions and stimulate a reduction in orbital soft tissue swelling, especially for the extraocular muscles. This protocol positively affects clinical improvement in both primary and secondary cases.[13, 47]

Discussion

Surgical complexity and the fact that an inappropriate reconstruction potentially leads to an adverse outcome have led to the parallel incorporation of computer-assisted surgery and personalized medicine in the orbital reconstruction workflow. Although both concepts aim to optimize treatment outcome, their rationale differs. CAS centralizes medical technology to improve the predictability and accuracy of all treatment stages, but various steps have been standardized and can be considered independent of the patient. CAS has catalyzed the incorporation of personalized medicine in orbital reconstruction: virtual surgical planning technology enables surgical preparation, implant selection, and the simulation of the desired implant position based on the individual's characteristics. The concepts are considerably intertwined in PSI reconstruction, and mutual interactions can be discerned. Personalization of the implant design is directly affected by information gathered in the preoperative CAS stage, and tailoring the implant to the patient's anatomy provides feedback on positioning during the intraoperative stage. Intraoperative CAS technology supports the accurate positioning of the PSI, which is a prerequisite for achieving the intended treatment effect of the personalized implant. In light of this symbiosis, surgical reconstruction with a PSI can be considered the pinnacle of both CAS and personalized medicine in orbital reconstruction.

Several larger comparative studies have demonstrated the beneficial effects of (components of) CAS on the accuracy of volumetric reconstruction,[62] clinical outcome,[36] and need for revision surgery.[63] In practice, a combination of several CAS building stones is often utilized. This yields heterogeneity in surgical approaches, which makes it difficult to compare outcomes between studies. Differences in indication, patient and fractu-

re characteristics, or implant materials used further complicate comparison.[64] Isolating the effect of individual CAS techniques on patient outcome is hampered by an overlap of techniques within study populations. The individual effects of CAS techniques have been assessed in a one-to-one comparison in a cadaver series.[65] Despite limitations associated with the cadaver model and an inability to assess clinical outcome parameters, positive effects of virtual planning, intraoperative imaging, and surgical navigation on reconstruction accuracy were established.

Several indications for PSI in orbital reconstruction have been advocated, relating to defect size, location, or timing of reconstruction.[22, 49, 50, 66-69] The common denominator between extensive defect size, the lack of bone support in the posterior third of the orbit, or secondary reconstruction after inadequate primary reconstruction is that the difficulty of reconstruction has been significantly increased. The possibility to perfectly tailor the shape of the implant to the patient's anatomy makes a PSI better suited for these complex reconstructions compared to implants that lack these options. Other advantages of PSIs are improved ease of use and precise, accurate fit, which leads to accurate implant positioning and a decreased surgery time.[41, 43, 45, 49, 50, 70-72] Iatrogenic soft-tissue damage is prevented as much as possible since the number of try-ins necessary to correctly position the implant is reduced, and no sharp edges are present around the implant's circumference.[37, 71, 73, 74] These factors lead to the high predictability of functional and aesthetic outcomes, fewer complications during or after surgery, and a lower revision rate than other implant types.[37, 45, 54, 62, 67]

The list provided in *Table 1* stipulates an ever-increasing armamentarium of design features to improve (ease of) positioning or alleviate clinical symptoms. The positioning-related characteristics guarantee adequate implant support and a unique, compelling fit for the implant. It is vital to evaluate the surgical accuracy of the PSI reconstruction and the added value of the positioning features.[71] Several studies have used a comparison between unaffected and reconstructed orbital volume or angulation between the floor and medial to measure surgical accuracy.[37, 75-77] These outcome parameters may conceal incorrect implant positioning. In contrast, a direct comparison between planned and acquired implant positions will reveal all surgical errors qualitatively and quantitatively.[60] Assessing individual degrees of freedom is even feasible with this approach. The evaluation phase is an indispensable component of the CAS workflow and should be performed for each orbital reconstruction. A direct comparison between planned and acquired implant positions is advocated to maximize the potential of the evaluation phase.

Incorporating clinical considerations in the design is currently not as clear as the positioning-related features. Since the early introduction of PSI reconstruction, the overcorrection of resulting orbital volume has been suggested several times, and its use has been described (*Table 1*). Still, guidelines to the amount of overcorrection are arbitrary and subjective, and not substantiated by evidence. Information about the location and shape of the overcorrection is lacking. The overcorrection may even be introduced through different pathways: it may be embedded in the PSI design or added afterwards through titanium blocks.[51] While the second option provides some freedom to the surgeon intraoperatively, the judgment is subjective and hampered by the soft-tissue reaction to the surgery (and the trauma in a primary setting). Trial and error positioning leads to the increased manipulation of orbital tissue, and any dislocation of the blocks may warrant a second procedure.[78, 79] Embedding overcorrection in the design is suggested to be the best solution for achieving an optimal result[78] and could be precisely tailored to the individual patient in the future, provided the abovementioned know-

ledge gaps are filled.

Cost, lead time, and logistic demands are drawbacks of using a PSI.[37, 72, 73, 79] Pricing may vary based on geography, but the process usually costs EUR 1500-6000.[56, 72, 80, 81] Manufacturing of the implant takes approximately 3–5 working days; this does not include sterilization, or the time needed for virtual surgical planning and design. Korn et al. described a mean communication time between the surgeon and the PSI company technician during virtual surgical planning of almost nine days for isolated wall fractures and 16 days for multi-wall fractures.[82] An adjustment to the initial design that the technician proposed was necessary in nearly three-quarters of cases, but implants from technicians with previous in-house training required fewer adjustments. Improved communication and mutual understanding are suggested to be the reasons for the efficiency improvement. Complete in-house planning and design by a dedicated, on-site technician may ameliorate planning efficiency, ultimately greatly reducing the lead time (provided the surgeon and technician are experienced and have cooperated on previous cases). In-house design is suggested to reduce costs, since commercial partners are only relied upon for fabrication.[81] These benefits of in-house design may be why surgeons who use in-house planning feel less hindered by the drawbacks of using a PSI.[72]

Although this paper focuses on post-traumatic orbital reconstruction, other PSI applications relating to the orbit have also been described. In zygomatic reconstruction after trauma, ablative surgery, or congenital malformation, PSIs were found to precisely restore the anatomy without the need for additional bone grafts.[83] In secondary post-traumatic reconstruction of the orbit and zygoma, PSIs enable a one-stage surgical procedure in which the surgical order is reversed: by operating the orbit first, the functional result of the orbital reconstruction is independent of repositioning the zygomatic complex.[54] PSIs may also be used to create an artificial orbital rim and floor for globe support after maxillectomy.[84, 85] The most extensive orbital PSI reconstructions have been described after the resection of a spheno-orbital meningioma or neurofibroma.[55, 86] In these cases, the reconstruction of all four orbital walls with multiple PSIs enabled a predictable reconstruction of the internal orbit in the same surgical setting as the resection. The PSI design in the abovementioned cases could differ greatly from the design in the post-traumatic reconstruction of solitary orbital fractures. Still, the rationale behind using a PSI is the same: freedom of design to adapt the PSI to the patient's anatomy and achieve a predictable and accurate final result.

Conclusions

An overview of the CAS workflow for post-traumatic orbital reconstruction has been presented, with an in-depth description of the techniques embedded in the workflow and a special focus on PSI. It has been demonstrated how the conventional workflow can be complemented by both CAS and personalized medicine in order to optimize the clinical outcome of post-traumatic orbital reconstruction. CAS technology has catalyzed the incorporation of personalized medicine in orbital reconstruction. The reconstruction of the orbit with a PSI can be considered the pinnacle of CAS and personalized medicine. There are no strict guidelines for the design of patient-specific implants, but several design considerations can be implemented to improve the positioning or alleviation of clinical symptoms. Because of the high predictability of aesthetic and functional outcomes, the use of PSIs has been advocated especially in difficult reconstructions. Cost, lead time, and logistical demands are known drawbacks, although they may be alleviated by inhouse design.

References

1. Cornelius CP, Probst F, Metzger MC, Gooris PJJ. Anatomy of the Orbits: Skeletal Features and Some Notes on the Periorbital Lining. Atlas Oral Maxillofac Surg Clin North Am. 2021;29(1):1–18.
2. Ellis E, 3rd, el-Attar A, Moos KF. An analysis of 2,067 cases of zygomatico-orbital fracture. J Oral Maxillofac Surg. 1985;43(6):417–28.
3. Hoffmann J, Cornelius CP, Groten M, Pröbster L, Pfannenberg C, Schwenzer N. Orbital reconstruction with individually copy-milled ceramic implants. Plast Reconstr Surg. 1998;101(3):604–12.
4. Koornneef L. Orbital septa: anatomy and function. Ophthalmology. 1979;86(5):876–80.
5. Holmes S. Primary Orbital Fracture Repair. Atlas Oral Maxillofac Surg Clin North Am. 2021;29(1):51–77.
6. Raflo GT. Blow-in and blow-out fractures of the orbit: clinical correlations and proposed mechanisms. Ophthalmic Surg. 1984;15(2):114–9.
7. Grob S, Yonkers M, Tao J. Orbital Fracture Repair. Semin Plast Surg. 2017;31(1):31–9.
8. Foletti JM, Martinez V, Haen P, Godio-Raboutet Y, Guyot L, Thollon L. Finite element analysis of the human orbit. Behavior of titanium mesh for orbital floor reconstruction in case of trauma recurrence. J Stomatol Oral Maxillofac Surg. 2019;120(2):91–4.
9. Dubois L, Dillon J, Jansen J, Becking AG. Ongoing Debate in Clinical Decision Making in Orbital Fractures: Indications, Timing, and Biomaterials. Atlas of the Oral and Maxillofacial Surgery Clinics of North America. 2021;29(1):29–39.
10. Wevers M, Strabbing EM, Engin O, Gardeniers M, Koudstaal MJ. CT parameters in pure orbital wall fractures and their relevance in the choice of treatment and patient outcome: a systematic review. Int J Oral Maxillofac Surg. 2022;51(6):782–9.
11. Choi A, Sisson A, Olson K, Sivam S. Predictors of Delayed Enophthalmos After Orbital Fractures: A Systematic Review. Facial Plast Surg Aesthet Med. 2022.
12. Burnstine MA. Clinical recommendations for repair of isolated orbital floor fractures: an evidence-based analysis. Ophthalmology. 2002;109(7):1207–10; discussion 10–1; quiz 12–3.
13. Jansen J, Dubois L, Maal TJJ, Mourits MP, Jellema HM, Neomagus P, et al. A nonsurgical approach with repeated orthoptic evaluation is justified for most blow-out fractures. J Craniomaxillofac Surg. 2020;48(6):560–8.
14. Dubois L, Steenen SA, Gooris PJ, Mourits MP, Becking AG. Controversies in orbital reconstruction--I. Defect-driven orbital reconstruction: a systematic review. Int J Oral Maxillofac Surg. 2015;44(3):308–15.
15. Dubois L, Steenen SA, Gooris PJ, Bos RR, Becking AG. Controversies in orbital reconstruction-III. Biomaterials for orbital reconstruction: a review with clinical recommendations. Int J Oral Maxillofac Surg. 2016;45(1):41–50.
16. Metzger MC, Schön R, Tetzlaf R, Weyer N, Rafii A, Gellrich NC, et al. Topographical CT-data analysis of the human orbital floor. Int J Oral Maxillofac Surg. 2007;36(1):45–53.
17. Cornelius CP, Mayer P, Ehrenfeld M, Metzger MC. The orbits--anatomical features in view of innovative surgical methods. Facial Plast Surg. 2014;30(5):487–508.
18. Gooris PJJ, Muller BS, Dubois L, Bergsma JE, Mensink G, van den Ham MFE, et al. Finding the Ledge: Sagittal Analysis of Bony Landmarks of the Orbit. J Oral Maxillofac Surg. 2017;75(12):2613–27.
19. Schlittler F, Schmidli A, Wagner F, Michel C, Mottini M, Lieger O. What Is the Incidence of Implant Malpositioning and Revision Surgery After Orbital Repair? J Oral Maxillofac Surg. 2018;76(1):146–53.
20. Chung SY, Langer PD. Pediatric orbital blowout fractures. Curr Opin Ophthalmol. 2017;28(5):470–6.
21. Schreurs R, Wilde F, Schramm A, Gellrich NC. Intraoperative Feedback and Quality Control in Orbital Reconstruction: The Past, the Present, and the Future. Atlas Oral Maxillofac Surg

Clin North Am. 2021;29(1):97–108.
22. Schreurs R, Klop C, Gooris PJJ, Maal TJJ, Becking AG, Dubois L. Critical appraisal of patient-specific implants for secondary post-traumatic orbital reconstruction. Int J Oral Maxillofac Surg. 2021.
23. Nkenke E, Maier T, Benz M, Wiltfang J, Holbach LM, Kramer M, et al. Hertel exophthalmometry versus computed tomography and optical 3D imaging for the determination of the globe position in zygomatic fractures. Int J Oral Maxillofac Surg. 2004;33(2):125–33.
24. Davanger M. Principles and sources of error in exophthalmometry. A new exophthalmometer. Acta Ophthalmol (Copenh). 1970;48(4):625–33.
25. Traber G, Kordic H, Knecht P, Chaloupka K. [Hypoglobus--illusive or real? Etiologies of vertical globe displacement in a tertiary referral centre]. Klin Monbl Augenheilkd. 2013;230(4):376–9.
26. Gart MS, Gosain AK. Evidence-Based Medicine: Orbital Floor Fractures. Plastic and Reconstructive Surgery. 2014;134(6):1345–55.
27. Willaert R, Shaheen E, Deferm J, Vermeersch H, Jacobs R, Mombaerts I. Three-dimensional characterisation of the globe position in the orbit. Graefes Arch Clin Exp Ophthalmol. 2020;258(7):1527–32.
28. Braaksma-Besselink Y, Jellema HM. Orthoptic Evaluation and Treatment in Orbital Fractures. Atlas Oral Maxillofac Surg Clin North Am. 2021;29(1):41–50.
29. Matic DB, Tse R, Banerjee A, Moore CC. Rounding of the inferior rectus muscle as a predictor of enophthalmos in orbital floor fractures. J Craniofac Surg. 2007;18(1):127–32.
30. Banerjee A, Moore CC, Tse R, Matic D. Rounding of the inferior rectus muscle as an indication of orbital floor fracture with periorbital disruption. J Otolaryngol. 2007;36(3):175–80.
31. Kang SJ, Lee KA, Sun H. Swelling of the inferior rectus muscle and enophthalmos in orbital floor fracture. J Craniofac Surg. 2013;24(2):687–8.
32. Freund M, Hähnel S, Sartor K. The value of magnetic resonance imaging in the diagnosis of orbital floor fractures. Eur Radiol. 2002;12(5):1127–33.
33. Jansen J, Dubois L, Schreurs R, Gooris PJJ, Maal TJJ, Beenen LF, et al. Should Virtual Mirroring Be Used in the Preoperative Planning of an Orbital Reconstruction? J Oral Maxillofac Surg. 2018;76(2):380–7.
34. Regensburg NI, Kok PH, Zonneveld FW, Baldeschi L, Saeed P, Wiersinga WM, et al. A new and validated CT-based method for the calculation of orbital soft tissue volumes. Invest Ophthalmol Vis Sci. 2008;49(5):1758–62.
35. Jansen J, Schreurs R, Dubois L, Maal TJJ, Gooris PJJ, Becking AG. The advantages of advanced computer-assisted diagnostics and three-dimensional preoperative planning on implant position in orbital reconstruction. J Craniomaxillofac Surg. 2018;46(4):715–21.
36. Cai EZ, Koh YP, Hing EC, Low JR, Shen JY, Wong HC, et al. Computer-assisted navigational surgery improves outcomes in orbital reconstructive surgery. J Craniofac Surg. 2012;23(5):1567–73.
37. Rana M, Chui CHK, Wagner M, Zimmerer R, Rana M, Gellrich N-C. Increasing the Accuracy of Orbital Reconstruction With Selective Laser-Melted Patient-Specific Implants Combined With Intraoperative Navigation. Journal of Oral and Maxillofacial Surgery. 2015;73(6):1113–8.
38. Kärkkäinen M, Wilkman T, Mesimäki K, Snäll J. Primary reconstruction of orbital fractures using patient-specific titanium milled implants: the Helsinki protocol. Br J Oral Maxillofac Surg. 2018;56(9):791–6.
39. Gander T, Essig H, Metzler P, Lindhorst D, Dubois L, Rücker M, et al. Patient specific implants (PSI) in reconstruction of orbital floor and wall fractures. J Craniomaxillofac Surg. 2015;43(1):126–30.
40. Gellrich NC, Dittmann J, Spalthoff S, Jehn P, Tavassol F, Zimmerer R. Current Strategies in Post-traumatic Orbital Reconstruction. J Maxillofac Oral Surg. 2019;18(4):483–9.

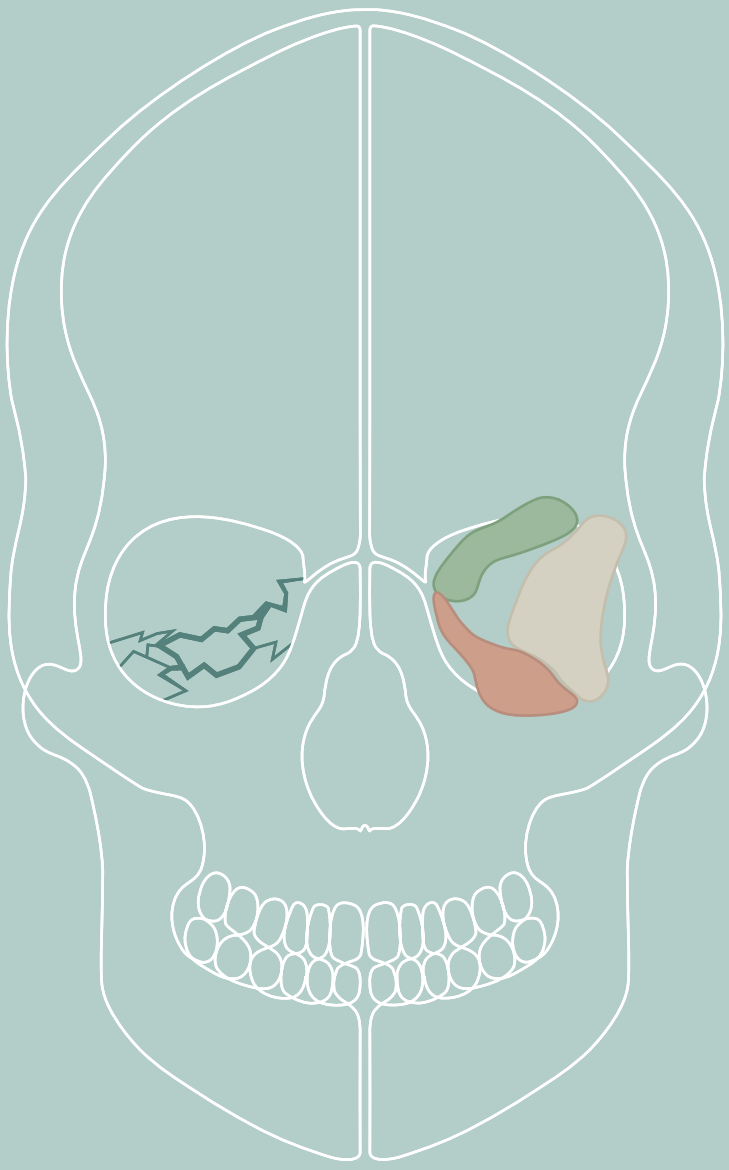
41. Blumer M, Essig H, Steigmiller K, Wagner ME, Gander T. Surgical Outcomes of Orbital Fracture Reconstruction Using Patient-Specific Implants. J Oral Maxillofac Surg. 2021;79(6):1302–12.
42. Hajibandeh J, Be A, Lee C. Custom Interlocking Implants for Primary and Secondary Reconstruction of Large Orbital Floor Defects: Case Series and Description of Workflow. J Oral Maxillofac Surg. 2021;79(12):2539.e1–.e10.
43. Zeller AN, Neuhaus MT, Gessler N, Skade S, Korn P, Jehn P, et al. Self-centering second-generation patient-specific functionalized implants for deep orbital reconstruction. J Stomatol Oral Maxillofac Surg. 2021;122(4):372–80.
44. Kormi E, Männistö V, Lusila N, Naukkarinen H, Suojanen J. Accuracy of Patient-Specific Meshes as a Reconstruction of Orbital Floor Blow-Out Fractures. J Craniofac Surg. 2021;32(2):e116–e9.
45. Bachelet JT, Cordier G, Porcheray M, Bourlet J, Gleizal A, Foletti JM. Orbital Reconstruction by Patient-Specific Implant Printed in Porous Titanium: A Retrospective Case Series of 12 Patients. J Oral Maxillofac Surg. 2018;76(10):2161–7.
46. Mommaerts MY, Büttner M, Vercruysse H, Jr., Wauters L, Beerens M. Orbital Wall Reconstruction with Two-Piece Puzzle 3D Printed Implants: Technical Note. Craniomaxillofac Trauma Reconstr. 2016;9(1):55–61.
47. Holmes S, Schlittler FL. Going beyond the limitations of the non-patient-specific implant in titanium reconstruction of the orbit. Br J Oral Maxillofac Surg. 2021.
48. Tikkanen J, Mesimäki K, Snäll J. Patient-specific two-piece screwless implant for the reconstruction of a large orbital fracture. Br J Oral Maxillofac Surg. 2020;58(1):112–3.
49. Baumann A, Sinko K, Dorner G. Late Reconstruction of the Orbit With Patient-Specific Implants Using Computer-Aided Planning and Navigation. Journal of Oral and Maxillofacial Surgery. 2015;73(12, Supplement):S101–S6.
50. Pedemonte Trewhela C, Díaz Reiher M, Muñoz Zavala T, González Mora LE, Vargas Farren I. Correction of Delayed Traumatic Enophthalmos Using Customized Orbital Implants. J Oral Maxillofac Surg. 2018;76(9):1937–45.
51. Spalthoff S, Dittmann J, Zimmerer R, Jehn P, Tavassol F, Gellrich NC. Intraorbital volume augmentation with patient-specific titanium spacers. J Stomatol Oral Maxillofac Surg. 2020;121(2):133–9.
52. Dubois L, Essig H, Schreurs R, Jansen J, Maal TJ, Gooris PJ, et al. Predictability in orbital reconstruction. A human cadaver study, part III: Implant-oriented navigation for optimized reconstruction. J Craniomaxillofac Surg. 2015;43(10):2050–6.
53. Kittichokechai P, Sirichatchai K, Puncreobutr C, Lohwongwatana B, Saonanon P. A Novel Patient-specific Titanium Mesh Implant Design for Reconstruction of Complex Orbital Fracture. Plast Reconstr Surg Glob Open. 2022;10(1):e4081.
54. Schreurs R, Dubois L, Becking AG, Maal TJJ. The orbit first! A novel surgical treatment protocol for secondary orbitozygomatic reconstruction. J Craniomaxillofac Surg. 2017;45(7):1043–50.
55. Sabelis JF, Youssef S, Hoefnagels FWA, Becking AG, Schreurs R, Dubois L. Technical Note on Three- and Four-Wall Orbital Reconstructions with Patient-Specific Implants. J Craniofac Surg. 2021.
56. Kim JS, Lee BW, Scawn RL, Korn BS, Kikkawa DO. Secondary Orbital Reconstruction in Patients with Prior Orbital Fracture Repair. Ophthalmic Plast Reconstr Surg. 2016;32(6):447–51.
57. 57. Venosta D, Sun Y, Matthews F, Kruse AL, Lanzer M, Gander T, et al. Evaluation of two dental registration-splint techniques for surgical navigation in cranio-maxillofacial surgery. J Craniomaxillofac Surg. 2014;42(5):448–53.
58. Luebbers HT, Messmer P, Obwegeser JA, Zwahlen RA, Kikinis R, Graetz KW, et al. Comparison of different registration methods for surgical navigation in cranio-maxillofacial

surgery. J Craniomaxillofac Surg. 2008;36(2):109–16.
59. Schreurs R, Baan F, Klop C, Dubois L, Beenen LFM, Habets P, et al. Virtual splint registration for electromagnetic and optical navigation in orbital and craniofacial surgery. Sci Rep. 2021;11(1):10406.
60. Schreurs R, Dubois L, Becking AG, Maal TJ. Quantitative Assessment of Orbital Implant Position--A Proof of Concept. PLoS One. 2016;11(3):e0150162.
61. Tokarz-Sawińska E, Lachowicz E. [Conservative management of posttraumatic diplopia]. Klin Oczna. 2015;117(1):14–9.
62. Zimmerer RM, Gellrich NC, von Bülow S, Strong EB, Ellis E, 3rd, Wagner MEH, et al. Is there more to the clinical outcome in posttraumatic reconstruction of the inferior and medial orbital walls than accuracy of implant placement and implant surface contouring? A prospective multicenter study to identify predictors of clinical outcome. J Craniomaxillofac Surg. 2018;46(4):578–87.
63. Nguyen E, Lockyer J, Erasmus J, Lim C. Improved Outcomes of Orbital Reconstruction With Intraoperative Imaging and Rapid Prototyping. J Oral Maxillofac Surg. 2019;77(6):1211–7.
64. Kotecha S, Ferro A, Harrison P, Fan K. Orbital reconstruction: a systematic review and meta-analysis evaluating the role of patient-specific implants. Oral Maxillofac Surg. 2023;27(2):213–26.
65. Schreurs R, Becking AG, Jansen J, Dubois L. Advanced Concepts of Orbital Reconstruction: A Unique Attempt to Scientifically Evaluate Individual Techniques in Reconstruction of Large Orbital Defects. Atlas Oral Maxillofac Surg Clin North Am. 2021;29(1):151–62.
66. Hughes D, McQuillan J, Holmes S. Quantitative analysis of diplopia following orbital fracture repair. Br J Oral Maxillofac Surg. 2023;61(3):202–8.
67. Schlittler F, Vig N, Burkhard JP, Lieger O, Michel C, Holmes S. What are the limitations of the non-patient-specific implant in titanium reconstruction of the orbit? Br J Oral Maxillofac Surg. 2020;58(9):e80–e5.
68. Consorti G, Betti E, Catarzi L. Customized and Navigated Primary Orbital Fracture Reconstruction: Computerized Operation Neuronavigated Surgery Orbital Recent Trauma (CONSORT) Protocol. J Craniofac Surg. 2022.
69. Chen AJ, Chung NN, Liu CY, MacIntosh PW, Korn BS, Kikkawa DO. Precision in Oculofacial Surgery: Made-To-Specification Cast-Molded Implants in Orbital Reconstruction. Ophthalmic Plast Reconstr Surg. 2020;36(3):268–71.
70. Zieliński R, Malińska M, Kozakiewicz M. Classical versus custom orbital wall reconstruction: Selected factors regarding surgery and hospitalization. J Craniomaxillofac Surg. 2017;45(5):710–5.
71. Tarsitano A, Badiali G, Pizzigallo A, Marchetti C. Orbital Reconstruction: Patient-Specific Orbital Floor Reconstruction Using a Mirroring Technique and a Customized Titanium Mesh. J Craniofac Surg. 2016;27(7):1822–5.
72. Goodson AMC, Parmar S, Ganesh S, Zakai D, Shafi A, Wicks C, et al. Printed titanium implants in UK craniomaxillofacial surgery. Part I: access to digital planning and perceived scope for use in common procedures. Br J Oral Maxillofac Surg. 2021;59(3):312–9.
73. Ruiters S, Mombaerts I. Applications of three-dimensional printing in orbital diseases and disorders. Curr Opin Ophthalmol. 2019;30(5):372–9.
74. Falkhausen R, Mitsimponas K, Adler W, Brand M, von Wilmowsky C. Clinical outcome of patients with orbital fractures treated with patient specific CAD/CAM ceramic implants - A retrospective study. J Craniomaxillofac Surg. 2021;49(6):468–79.
75. Timoshchuk MA, Murnan EJ, Chapple AG, Christensen BJ. Do Patient-Specific Implants Decrease Complications and Increase Orbital Volume Reconstruction Accuracy in Primary Orbital Fracture Reconstruction? J Oral Maxillofac Surg. 2022;80(4):669–75.
76. Zimmerer RM, Ellis E, 3rd, Aniceto GS, Schramm A, Wagner ME, Grant MP, et al. A prospective multicenter study to compare the precision of posttraumatic internal orbital recon-

struction with standard preformed and individualized orbital implants. J Craniomaxillofac Surg. 2016;44(9):1485–97.
77. Schönegg D, Wagner M, Schumann P, Essig H, Seifert B, Rücker M, et al. Correlation between increased orbital volume and enophthalmos and diplopia in patients with fractures of the orbital floor or the medial orbital wall. J Craniomaxillofac Surg. 2018;46(9):1544–9.
78. Essig H, Wagner MEH, Blumer M. Secondary Corrections of the Orbit: Solitary Fractures. Atlas Oral Maxillofac Surg Clin North Am. 2021;29(1):129–37.
79. Maher DI, Hall AJ, Gwini S, Ben Artsi E. Patient-specific Implants for Orbital Fractures: A Systematic Review. Ophthalmic Plast Reconstr Surg. 2021.
80. Kang S, Kwon J, Ahn CJ, Esmaeli B, Kim GB, Kim N, et al. Generation of customized orbital implant templates using 3-dimensional printing for orbital wall reconstruction. Eye (Lond). 2018;32(12):1864–70.
81. Goodson AMC, Parmar S, Ganesh S, Zakai D, Shafi A, Wicks C, et al. Printed titanium implants in UK craniomaxillofacial surgery. Part II: perceived performance (outcomes, logistics, and costs). Br J Oral Maxillofac Surg. 2021;59(3):320–8.
82. Korn P, Jehn P, Nejati-Rad N, Winterboer J, Gellrich NC, Spalthoff S. Pitfalls of Surgeon-Engineer Communication and the Effect of In-House Engineer Training During Digital Planning of Patient-Specific Implants for Orbital Reconstruction. J Oral Maxillofac Surg. 2022;80(4):676–81.
83. Chepurnyi Y, Chernogorskyi D, Kopchak A, Petrenko O. Clinical efficacy of peek patient-specific implants in orbital reconstruction. J Oral Biol Craniofac Res. 2020;10(2):49–53.
84. Le Clerc N, Baudouin R, Carlevan M, Khoueir N, Verillaud B, Herman P. 3D titanium implant for orbital reconstruction after maxillectomy. J Plast Reconstr Aesthet Surg. 2020;73(4):732–9.
85. Stoor P, Suomalainen A, Lindqvist C, Mesimäki K, Danielsson D, Westermark A, et al. Rapid prototyped patient specific implants for reconstruction of orbital wall defects. J Craniomaxillofac Surg. 2014;42(8):1644–9.
86. Davidson EH, Khavanin N, Grant M, Kumar AR. Correction of Complex Neurofibromatosis Orbital and Globe Malposition Using the Orbital Box Segmentation Osteotomy With Patient-Specific Internal Orbit Reconstruction. J Craniofac Surg. 2019;30(6):1647–51.

Part I

Patient-specific implants



Chapter 3

Multi-wall reconstructions

This chapter is based on the following publication :

Sabelis J.F., Youssef S.A.L.Y., Hoefnagels F.W.A., Becking A.G., Schreurs R., Dubois L. Technical Note on Three- and Four-Wall Orbital Reconstructions With Patient-Specific Implants. J Craniofac Surg. 2022 Jun 1;33(4):991-996.

Abstract

Orbital reconstruction is one of the most complex procedures in maxillofacial surgery. It becomes even more complex when all references to the original anatomy are lost. The purpose of this article is to provide an overview of techniques for complex three- and four-wall orbital reconstructions. Preoperative virtual surgical planning is essential when considering different reconstruction possibilities. The considerations that may lead to different approaches are described, and the advantages and drawbacks of each technique are evaluated. It is recommended to reconstruct solitary three-wall or four-wall orbital defects with multiple patient-specific implants. Optimizations of this treatment protocol are suggested, and their effects on predictability are demonstrated in a case presentation of a four-wall defect reconstruction with multiple patient-specific implants.

Introduction

The orbit's structural integrity may be affected by trauma, a space-occupying lesion, or infection. In orbital trauma, sequelae like enophthalmos, hypoglobus, and diplopia may be present due to the disruption of hard-tissue or soft-tissue structures. If the orbital floor and the medial orbital wall are affected, the orbital contents may protrude into the adjacent spaces. The primary goal of orbital reconstruction is to relieve clinical symptoms by restoring the lost anatomical dimensions within the orbit. Reconstruction of the bony anatomy creates a solid fundament to support the globe, and it is considered the primary step in restoring form and function.[1] During the reconstruction, the surgeon tries to find support for the implant at the anterior, medial, and posterior boundaries (infraorbital rim, medial wall, and posterior ledge, respectively). Due to the limited overview and protruding orbital fat, orbital reconstruction is considered one of the most challenging maxillofacial procedures. The more extensive the injury is, the more reference points are lost, and the more complex the reconstruction becomes.[2]

Other difficulties in orbital reconstruction are related to the complexity of the defect. Jaquiéry et al developed a complexity driven classification of orbital defects. In general, class I and II defects could be classified as relatively easy cases due to the relatively good implant support. In higher-rated defects (class III, IV, and V), the possibility of positioning the implant suboptimally increases as more anatomical reference is lost. The bony ledge or orbital process of the palatine bone (OPPB) is an important structure for posterior support of the implant. If the OPPB is also lost (class IV defects), the stability of the implant then depends on the support of adjacent walls (lateral wall, orbital roof, or superior strut).[3-7] In class V defects, the orbital roof is also involved.5 If all walls are affected, it can be challenging to find an anatomical reference, which yields a whole new reconstruction complexity level.[1, 4, 8] Different materials are available for orbital reconstructions. There are roughly 2 categories: biologic (autogenous or allogenic materials such as bone and cartilage) and alloplastic (porous ethylene, titanium, etc.) material. Resorbable alloplastic materials should only be used to reconstruct class I defects.[9, 10] For the reconstruction of relatively simple defects (class I/II), various materials can be utilized, from autologous materials[11] to alloplasts.[8, 12, 13] Large, complex defects (class III-V) require more surface area to be covered, implying more stability from the reconstruction material. Because of this large surface area, the reconstruction of the anatomical shape of the orbit also gains importance.[14] Thus, the recommended reconstruction material for these defects is a titanium implant (either preformed or patient-specific).[10]

The literature is sparse in treatment options for the reconstruction of three-wall or four-wall orbital defects. Several publications highly recommend using advanced technologies, such as computer-assisted surgery (CAS), navigation, intraoperative imaging, and patient-specific implants (PSIs) in these complex reconstructions to prevent incorrect implant positioning. During virtual surgical planning(VSP), a reference for reconstruction of the affected anatomy can be created by mirroring the unaffected hard tissue.[15-17] A PSI can be designed to closely reflect the virtual anatomy and unambiguously fit on the remaining bony structures. Theoretically, it would be possible to design a single PSI that covers the entire defect. This would be impractical as the required size would necessitate a larger incision and thus increasing hematoma and edema postoperatively. It is recommended to utilize multiple rigid implants instead of one large implant in three-wall or four-wall defects.[4]

This publication aims to illustrate the treatment options and their rationale in three- and four-wall orbital reconstructions. The dilemmas during the design process and surgery are presented, and possible technological solutions to allow predictable reconstruction are provided. Finally, a technique for the complete reconstruction of the orbit in four-wall defects is illustrated in detail.

Methods

Different pathophysiological mechanisms may introduce the need to reconstruct 3 or more walls of the orbit. An important starting point is evaluating the requirement for the reconstruction of affected facial buttresses surrounding the orbit. These will be affected, for example, in zygomaticomaxillary complex (ZMC) fractures, naso-orbito-ethmoid fractures, and frontal sinus fractures (*Figure 1a*). In clinical practice, the facial buttresses will be reconstructed first. The required reconstruction can provide the opportunity to reduce the complexity of the orbital problem through repositioning the corresponding wall(s).

If the facial buttresses are not affected or still in an anatomically correct position, the necessity for surgical intervention is limited to the inner orbit. Illustrations of cases limited to the inner orbit are provided in *Figure 1b-d*. The redundancy to reconstruct the surrounding facial buttresses entails that it will not be possible to reduce the intraorbital problem before reconstruction. The orbital defect should thus be reconstructed using the other methods. Considering its complexity, patient-specific solutions, either one PSI or multiple PSIs, may be recommended to perform the reconstruction. An overview of reconstruction options for defects similar to *Figure 1a-c* is provided below; a reconstruction option for the defect in *Figure 1d* is detailed in the subsequent case presentation.

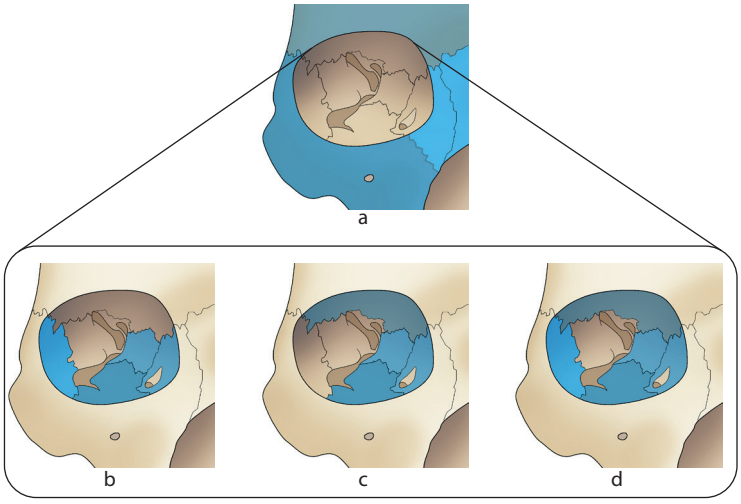


Figure 1. *Anatomical illustration of different orbital defects. (a) Affected facial buttresses in combination with an orbital defect. (b-c) Possible configurations of three-wall orbital defects. In (b), the orbital floor, medial wall, and lateral wall are affected, whereas in (c), the orbital roof, orbital floor, and medial wall are affected. The configuration in (c) is rare. (d) A four-wall orbital defect confined to the inner orbit.*

Reconstruction of the Orbit in Combination with Facial Buttresses (Class a)

Orbital defects in which one or more facial buttresses are affected, are commonly reconstructed in a stepwise fashion, called sequencing.[18] In cases where the ZMC is affected, the first option would be to reposition the ZMC to restore its original position. This reduction might not prevent additional reconstruction of the orbital floor altogether, especially in comminuted fractures. Still, it may relieve the need to reconstruct the orbit's lateral wall and confine the subsequent orbital problem to a two-wall defect. Timing and order of reconstruction may differ according to patient and reconstruction characteristics: in the primary setting, the general order is to reposition the zygomatic complex and reconstruct the orbit afterward, either in the same setting or in a separate surgical intervention. For a secondary reconstruction of a three-wall defect, PSIs may be utilized to reconstruct the orbital floor and medial wall first and subsequently guide the zygoma to the planned position.[19]

In severe midface trauma, both the inner orbit and surrounding facials buttresses are commonly affected. Consequently, little bony support may be left, and the loss of anatomical dimensions may be significant. Staging, or postponing, the last sequence of the reconstruction to a second procedure enables a predictable reconstruction of the inner orbit with a PSI.[20] Staging is essential, as the designing and the production of a PSI require time. Although the first procedure's focus is to reconstruct the facial buttresses, it may provide an opportunity to create temporary support for the globe. The creation of temporary support for the globe and a PSI in the second intervention is illustrated in *Figure 2*.

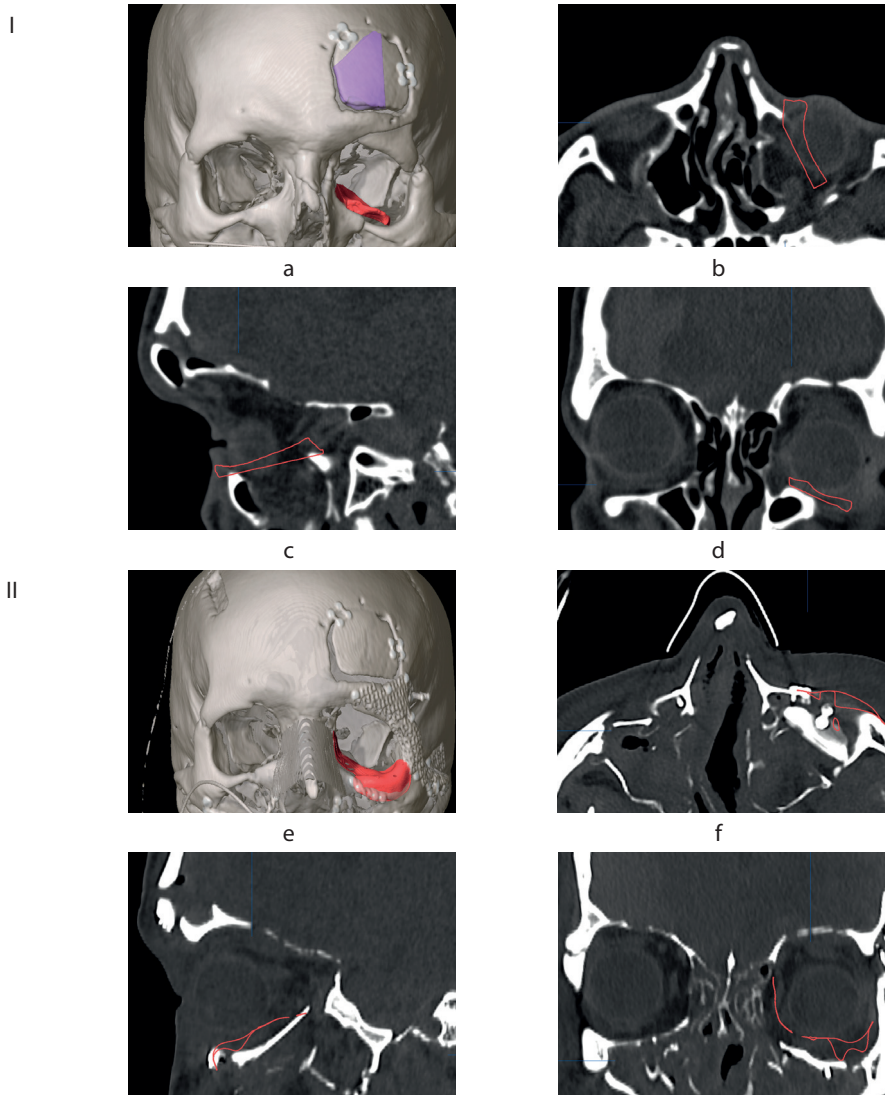


Figure 2. *Secondary reconstruction after conservatively treated panfacial trauma. (a) 3D model view, (b) axial view, (c) sagittal view, and (d) coronal view. (I) VSP of first surgery. The consolidated fractures at the Le Fort I level, the ZMC, and NOE complex were refractured/osteotomized and repositioned. As the orbit was to be reconstructed in a separate surgical session, an autograft was taken from the inner table of the previous craniectomy (purple) for temporary support of the globe. (II) VSP of second surgery. A PSI (red) was designed for positioning on the orbital floor created in the first surgery. An anterior elevation was embedded in the PSI to restore the inferior orbital rim's height. NOE, naso-orbito-ethmoid; PSI, patient-specific implant; VSP, virtual surgical planning; ZMC, zygomaticomaxillary complex.*

Reconstruction of the Solitary Orbit (Class b/c)

Currently available preformed orbital implants cover a maximum of two walls. For the reconstruction of a solitary orbital defect in which three or four walls are affected, mul-

tiple orbital implants are required for a complete orbital reconstruction. Only reconstructions of two-wall defects (floor and medial wall), with two interlocking premolded implants[21] and PSIs,[22] have been reported. The interlocking systems described in the literature were designed to ensure unambiguous positioning and thus provide feedback on the relative positioning of the PSIs. The utilization of multiple PSIs and an interlocking system may be extrapolated to reconstruct three-walled or four-walled defects. If two PSIs are used, one of the implants should cover at least two walls. A connection between the two PSIs can be designed in different ways. An example of a connection, which resembles a patrix-matrix connection, is illustrated in *Figure 3*. Analogous to the connections described in the literature, this connection was designed to provide relative feedback. Due to an affected OPPB, not enough bony support was found and, in combination with gravity, this resulted in an inaccurate implant position. This can be seen in *Figure 3G*. For another case, a less compelling connection between the lateral wall to the orbital floor was designed. The ridges in the orbital floor implant in *Figure 4* will guide the second PSI's positioning.

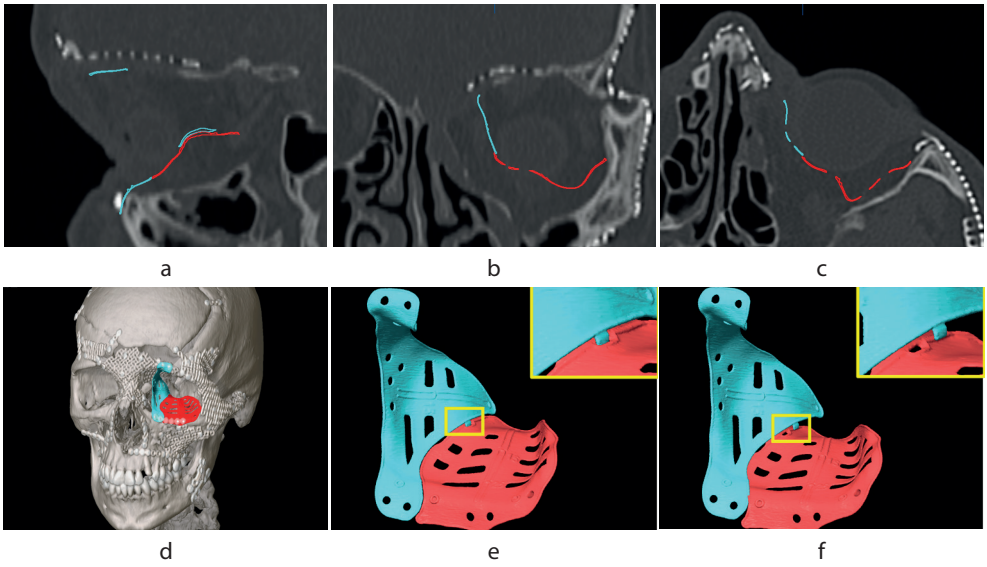


Figure 3. *Reconstruction of a four-wall orbital defect with 2 PSIs. (a-c) Virtual surgical planning in computed tomography data with the planned PSIs; medial wall (blue) and orbital wall with a lateral extension (red). (d-e) 3D models of planned PSI. The connection between the implants is marked with the yellow box in the right image. (f) Resulting 3D models of the implants. In the close-up, it is visible the 2 implants are not connected as planned. PSI, patient-specific implant; 3D, three-dimensional.*

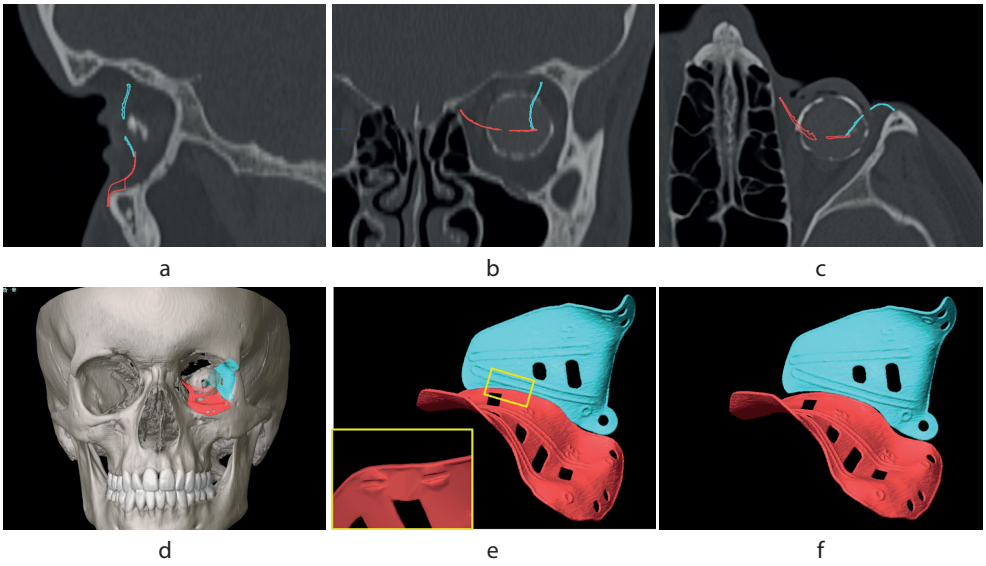
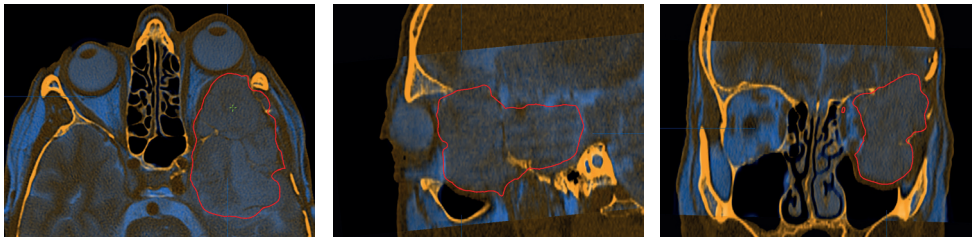


Figure 4. *Reconstruction of an anophthalmic socket with 2 PSIs. Patient previously treated with radiotherapy for a rhabdomyosarcoma. Orbital reconstruction was virtually planned to decrease the orbital volume of the anophthalmic socket to improve the anteroposterior position of the ocular prosthesis. (a-c) Multi-planar reconstruction view of the virtual surgical planning data with the planned PSIs: lateral wall (blue) and orbital floor with a medial extension (red). (d-e) 3D models of planned PSIs. (f) Resulting 3D models of the implants. PSI, patient-specific implant; 3D, three-dimensional.*

Results

Clinical presentation

A 48-year-old male patient presented with a recurring benign left spheno-orbital meningioma. After primary resection and adjuvant radiotherapy in 1996, periodic control with magnetic resonance imaging (MRI) followed to objectify any rest mass growth. In 2017, a second resection was performed without reconstruction of the orbit. During a periodic control in July 2020, a surprising and relatively substantial increase was objectified (68x46x54 mm). *Figure 5* shows the fusion of the computed tomography (CT) images and the magnetic resonance imaging, on which the mass is segmented. Compared to the previous recurrence in 2017, an evidently increased extension into the orbit was objectified with the destruction of all orbital walls. Ocular motility was relatively unharmed, though diplopia occurred in all directions. Loss of vision was objectified in the nasal lower quadrant and became progressive. A subtotal resection with orbital reconstruction was performed to prevent further decrement and restore the function of the eye in November 2020.

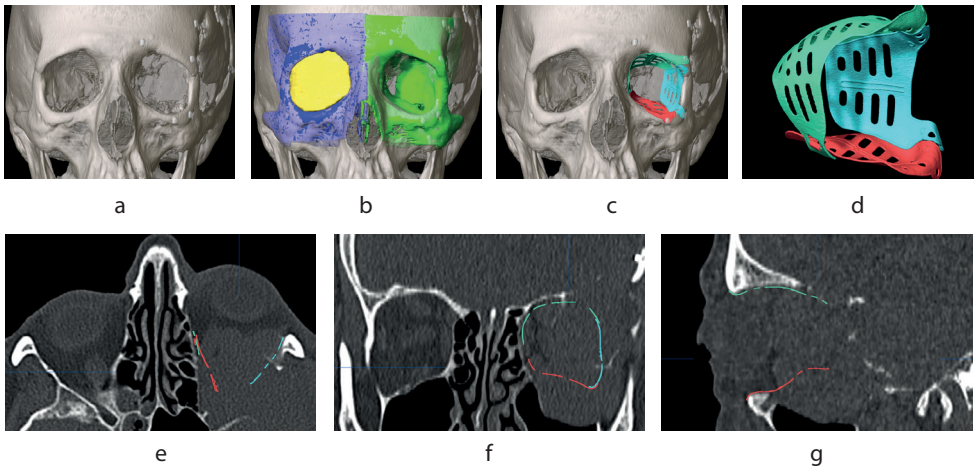


a b c

Figure 5. *Diagnostic evaluation of computed tomography (CT) and magnetic resonance images (MRIs). Tumor segmentation was based on the MRI and outlined in red. Overlay of CT (orange) and MRI (blue) in the (a) axial view, (b) sagittal, and (c) coronal view.*

Preoperative Workup & VSP

The aim was to reconstruct the four-wall defect in a single procedure. A preoperative CT scan was acquired in order to perform the VSP. Preoperatively, 4 screws were inserted around the orbit under local anaesthesia to provide additional reference for positioning the implants (*Figure 6a*). The iPlan software (version 3.0.5, Brainlab AG, Munich, Germany) was used for the VSP. The unaffected orbital cavity, orbit, and surrounding facial buttresses were segmented and mirrored to the affected side, which is illustrated in *Figure 6b*.[23, 24] The mirrored orbital cavity volume was overcorrected with 0.5 cc with the "smart brush" software tool to compensate for the soft-tissue effects.[17, 25]



a b c d

e f g

Figure 6. *Virtual surgical planning of the four-wall reconstruction case. (a) The 4 preoperatively inserted screws are indicated with yellow circles. (b) The segmented unaffected facial buttresses (dark blue) and orbital cavity (yellow) with the mirrored bone (green). (c) The 3 patient-specific implants designed to reconstruct the orbital roof and medial wall (green), the orbital floor (red), and the lateral wall (blue), with incorporation of 3 of the preoperatively inserted screws. (d) Overview of the 3 planned patient-specific implants. (e-g) Virtual surgical planning in computed tomography images with an (e) axial, (f) coronal, and (g) sagittal view.*

The open-source software programs Meshmixer (version 3.5.474, Autodesk Inc., San Rafael, CA) and Blender (version 2.83.3, Blender Foundation, Amsterdam, The Netherlands) were used to design the PSIs on the mirror image. Four walls needed to be recon-

structed and the implant design needed to facilitate positioning in the orbit's confined space. It was decided to design 3 PSIs. This ensured a manageable size of the individual implants. The 3 PSIs are depicted in the VSP in *Figure 6c-f*: one orbital roof implant with medial wall extension (called roof implant), one orbital floor implant (called floor implant), and one lateral wall implant (called lateral implant). The introduction of an additional PSI required a careful consideration of the design of the connections. As described earlier, the connection between the floor and the roof implant need to provide some support compensating for the absent ledge. For this purpose, the hook and bar connection was designed (*Figure 6 and 7*). Ridges were designed for the lateral implant to allow a margin of error for positioning. Three of the four preoperatively inserted screws were incorporated in the design of the PSIs.

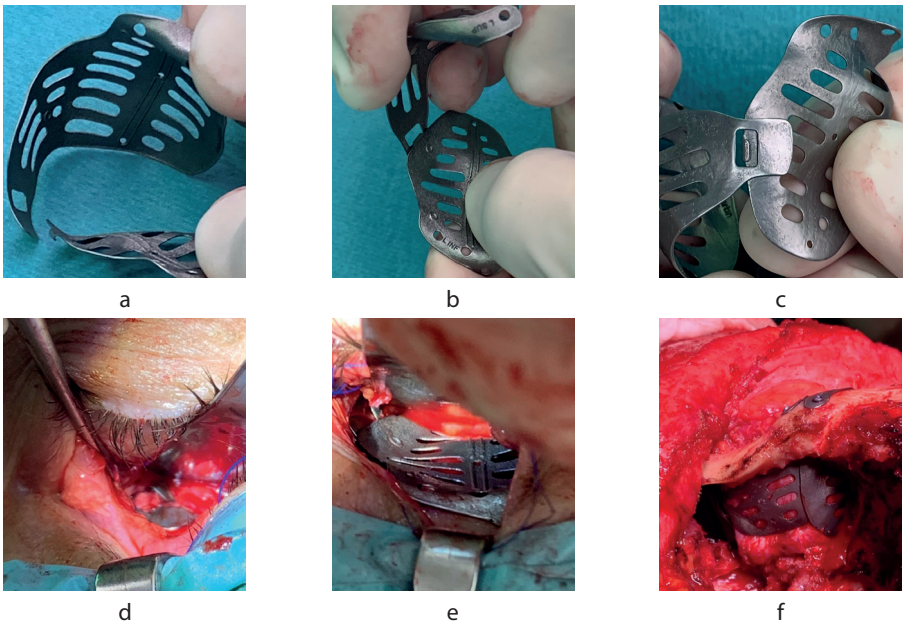


Figure 7. *Titanium 3D-printed orbital implants. (a) Roof and floor implants. (b) Interconnected roof and floor implants. (c) Close-up of hook and bar mechanism. (d) Intraoperative positioning of floor implant. (e) Hook and bar connection in situ. (f) Craniectomy allowed visualization of the implants' positions from a cranial perspective.*

Surgery

The 2 supraorbital and 2 infraorbital screws were used for intraoperative calibration of the navigation system. A transconjunctival approach without lateral canthotomy combined with a coronal approach was used for the reconstruction of the orbit. The coronal approach was primarily used for resection of the meningioma. The orbital roof and medial wall were reconstructed with the roof implant, which was secured to the frontal bone (*Figure 6* in green). The hole of the lateral supraorbital fixation screw was used to fixate the roof implant at the location of the initial fixation screw. Afterward, reconstruction of the orbital floor followed by interlocking the floor implant in the already fixated roof implant along with the hook and bar mechanism (*Figure 7*). Finally, the lateral implant was fixated. The operation proceeded in accordance with the preoperative planning.

Postoperative Recovery

The implant positioning was verified with a postoperative CT scan (*Figure 8*). The total length of hospitalization was 6 weeks after surgery. Postoperatively, the patient was in a deteriorated neurological state and admission to the intensive care was required until 1 week after surgery. As a result of the neurological state, adequate ophthalmic examination, including assessment of diplopia, could not be performed for 2 weeks. Eye muscle exercises to reduce swelling and decrease diplopia were not adequately implemented.

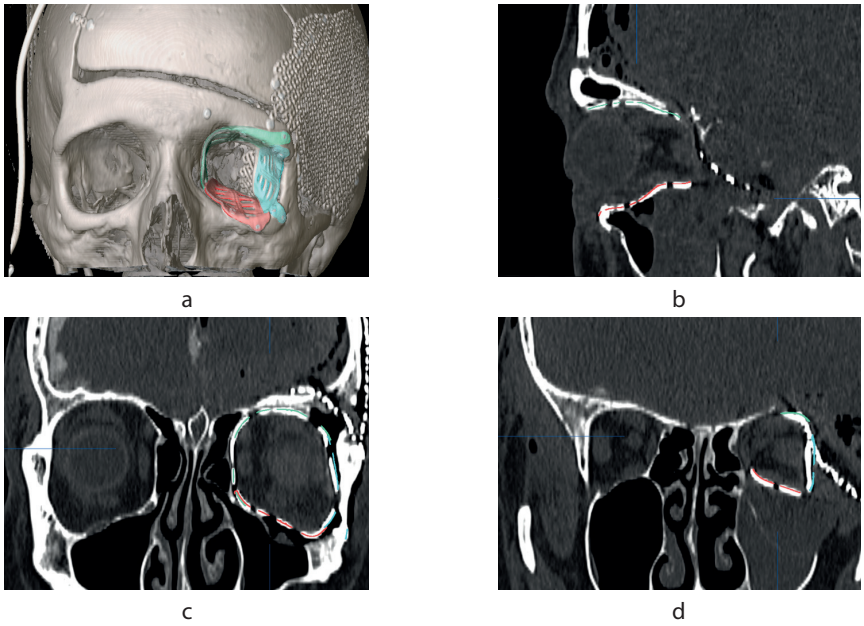


Figure 8. *Implant position verification with postoperative imaging. (a) 3D model with the planned PSIs; the roof implant (green), the floor implant (red), and the lateral implant (blue). (b) Sagittal view. (c) Coronal view at anterior 1/3 of the orbit. (d) coronal view at posterior 2/3 of the orbit. PSI, patient-specific implant.*

Two weeks postoperatively, an ophthalmic examination could be performed. An elevated position of the left eye with significant more scleral show compared to the right eye was noticeable. The eye-tracking movements seemed reasonably intact with insignificant motility differences between the left and right eye (*Figure 9*). The patient experienced constant diplopia in primary position (Bahn- Gorman diplopia score 4). Three weeks postoperatively, the vision of the left eye was 85%, with adequate depth perception. After 6 weeks, the position of the globe was comparable to the preoperative position with equal scleral show comparing the left and right globe and diplopia decreased and finally became insignificant (Bahn- Gorman diplopia score 2). Four months postoperatively, the eye-tracking movements were smooth and the diplopia disappeared (Bahn-Gorman diplopia score 1).



Figure 9. *Eye tracking movements at 2 weeks (first column), 6 weeks (second column), and 4 months postoperatively (third column).*

Discussion

This technical note evaluates the available options for orbital reconstruction of extensive defects (3–4 walls). It is essential to evaluate from the start whether there is an indication for the reconstruction of affected facial buttresses surrounding the orbit. If these are affected, sequencing the reconstruction may provide the opportunity to reduce the orbital defect or create bony support. The reduction of the defect or creation of bony support can simplify the second phase in the sequence, which could implicate that fewer walls need to be reconstructed and only one implant may be required. In a solitary three-wall or four-wall orbital defect, the application of multiple PSIs is recommended for reconstruction; the advantages of multiple implants are that the size of the incision may be minimized and the implants can be connected.[22] In addition, the use of multiple PSIs may facilitate creation of artificial support for the floor implant in case the OPPB is affected.

Different designs for the connections were illustrated in this technical note; patrix-matrix connection, ridges on the implant, and the hook and bar mechanism. The choice for the connection is dependent on its location and the necessity of artificial support of the floor implant. As demonstrated in the case of *Figure 3*, the patrix-matrix connection may not be compelling enough when the OPPB is affected. Due to gravitational forces the final implant position deviated from the planned position. Artificial support is desired in such cases, implicating a more rigid connection. In the demonstrated case, one compelling (hook and bar) and one less compelling (ridges) connection were embed-

ded. Although it is possible to interlock all implants at overlapping locations, this may complicate positioning. A balance between a compelling fit and the limited freedom of movement is important. The surgeon must be able to establish the connections between the PSIs within the confined space of the orbit.

Accurate implant positioning is essential for the adequate reconstruction of three- and four-wall orbital defects. The position of the second implant is dependent on the predictability of the positioning of the first implant.[19] The compelling design of PSIs have shown to lead to accurate implant positioning, especially if combined with other feedback techniques such as intraoperative navigation.[26] The use of existing fixation screw holes (either from previous reconstructions or artificially created as in the demonstration case) also provides feedback on implant positioning and prevents rotation and translation of the implant. All the above mentioned feedback mechanisms provide feedback on the position of individual PSIs; interlocking implant mechanisms add the possibility to obtain feedback on the relative implant positions as well.

The demonstration case is relatively rare due to the benign spheno-orbital meningioma etiology that does not grow invasively but expands surrounding structures and tissues, which led to extensive bone erosion with preserved periorbital structures. This explains the relatively unharmed motility of the affected eye and the quick recovery of the motility after reconstruction, even without adequate implementation of eye muscle exercises in the first 2 weeks due to the patient's deteriorated neurological state. The limited eye muscle movement led to a slighter decrease of postoperative intraorbital swelling but did not seem to have any detrimental effect on the diplopia recovery.

The debate on material for orbital reconstruction is ongoing. Whereas autologous bone is praised for its long-term efficacy, reliability, and revascularization potential, it is also known to have unpredictable resorption rates, suboptimal volume correction, and donor site morbidity.[10, 27] The inability to anatomically shape the bony parts is a disadvantage, especially for complex orbital defects. Titanium implants can be designed to restore the anatomical shape either intraoperatively (manual bending) or preoperatively (preformed implants or patient-specific). The high biocompatibility and the rigidity of titanium are ideal for the reconstruction of large orbital defects.[12] Well-known limitations of PSIs are the requirement of the state-of-the-art technology and the relatively high costs. The delay caused by manufacturing may be an additional disadvantage in primary reconstruction cases. For complex secondary cases, a PSI is still preferred due to the possibility of a true-to-original orbital reconstruction with predictable clinical outcome.[15]

Multiple (patient-specific) titanium implants have been recommended for the reconstruction of extensive orbital defects in literature.[4, 16] Mommaerts et al[22] described the application of a jigsaw puzzle-like interlocking system for 2 3D-printed titanium implants to reconstruct two-wall defects. Kim et al[21] described a jigsaw puzzle-like titanium implant coated with porous polyethylene, which was molded preoperatively using a 3D-printed patient model. Positioning through a limited transconjunctival incision enabled by the small size of the individual PSIs. In contrast to the presented hook and bar connection, these jigsaw puzzle-like connections were not designed to provide artificial support to the floor implant. This may be crucial in cases when the OPPB is affected. Both studies reported a near complete restoration of the orbital volume and ocular motility. No other studies have described the application of the jigsaw puzzle-like implants for three-wall or four-wall orbital defects. The study of Holmes et al described the application of multiple PSIs for the reconstruction of Jaquiery class III, IV, and V orbital

defects.[28] The jigsaw puzzle-like connection between the 2 plates was designed in an S-shape, to enable more precise co-localization. The third wall was reconstructed with a third, separate plate. No additional support between the implants was described.

Conclusion

The purpose of this article was to provide an overview of technical options with their advantages and disadvantages for complex three and four-wall orbital reconstructions. For these complex orbital defects, titanium PSIs has favorable material characteristics. This is due to its rigidity, biocompatibility, and the ability to perform true to- original reconstructions. Application of multiple PSIs, which may be interconnected using different connections, is possible for the extreme cases. Correct positioning was ensured due to different feedback mechanisms; interlocking of implants, preoperatively inserted screws, and intraoperative navigation. The presented clinical case was a demonstration of the possible techniques for complex three- and four-wall orbital reconstructions.

References

1. Grob S, Yonkers M, Tao J. Orbital Fracture Repair. Semin Plast Surg. 2017;31(1):31–9.
2. Dubois L, Jansen J, Schreurs R, Saeed P, Beenen L, Maal TJ, et al. Predictability in orbital reconstruction: A human cadaver study. Part I: Endoscopic-assisted orbital reconstruction. J Craniomaxillofac Surg. 2015;43(10):2034–41.
3. Gooris PJJ, Muller BS, Dubois L, Bergsma JE, Mensink G, van den Ham MFE, et al. Finding the Ledge: Sagittal Analysis of Bony Landmarks of the Orbit. J Oral Maxillofac Surg. 2017;75(12):2613–27.
4. Hur SW, Kim SE, Chung KJ, Lee JH, Kim TG, Kim YH. Combined Orbital Fractures: Surgical Strategy of Sequential Repair. Arch Plast Surg. 2015;42(4):424–30.
5. Jaquiéry C, Aeppli C, Cornelius P, Palmowsky A, Kunz C, Hammer B. Reconstruction of orbital wall defects: critical review of 72 patients. International Journal of Oral and Maxillofacial Surgery. 2007;36(3):193–9.
6. Zimmerer RM, Gellrich NC, von Bülow S, Strong EB, Ellis E, 3rd, Wagner MEH, et al. Is there more to the clinical outcome in posttraumatic reconstruction of the inferior and medial orbital walls than accuracy of implant placement and implant surface contouring? A prospective multicenter study to identify predictors of clinical outcome. J Craniomaxillofac Surg. 2018;46(4):578–87.
7. Dubois L, Schreurs R, Jansen J, Maal TJ, Essig H, Gooris PJ, et al. Predictability in orbital reconstruction: A human cadaver study. Part II: Navigation-assisted orbital reconstruction. J Craniomaxillofac Surg. 2015;43(10):2042–9.
8. Su GW, Harris GJ. Combined inferior and medial surgical approaches and overlapping thin implants for orbital floor and medial wall fractures. Ophthalmic Plast Reconstr Surg. 2006;22(6):420–3.
9. Eppley BL, Sadove AM, Havlik RJ. Resorbable plate fixation in pediatric craniofacial surgery. Plast Reconstr Surg. 1997;100(1):1–7; discussion 8–13.
10. Dubois L, Steenen SA, Gooris PJ, Bos RR, Becking AG. Controversies in orbital reconstruction-III. Biomaterials for orbital reconstruction: a review with clinical recommendations. Int J Oral Maxillofac Surg. 2016;45(1):41–50.
11. Shin J, Park SI, Hwang Y, Kwon H, Shim HS. Reconstruction of Medial Wall Blowout Fracture Defect with a Combination of Resorbable Meshed Plate and Cancellous Bone Allograft. Biomed Res Int. 2019;2019:2656503.
12. Bittermann G, Metzger MC, Schlager S, Lagrèze WA, Gross N, Cornelius CP, et al. Orbital reconstruction: prefabricated implants, data transfer, and revision surgery. Facial Plast Surg. 2014;30(5):554–60.
13. Choi JC, Fleming JC, Aitken PA, Shore JW. Porous polyethylene channel implants: a modified porous polyethylene sheet implant designed for repairs of large and complex orbital wall fractures. Ophthalmic Plast Reconstr Surg. 1999;15(1):56–66.
14. Dubois L, Jansen J, Schreurs R, Habets PE, Reinartz SM, Gooris PJ, et al. How reliable is the visual appraisal of a surgeon for diagnosing orbital fractures? J Craniomaxillofac Surg. 2016;44(8):1015–24.
15. Rana M, Chui CHK, Wagner M, Zimmerer R, Rana M, Gellrich N-C. Increasing the Accuracy of Orbital Reconstruction With Selective Laser-Melted Patient-Specific Implants Combined With Intraoperative Navigation. Journal of Oral and Maxillofacial Surgery. 2015;73(6):1113–8.
16. Schlittler F, Vig N, Burkhard JP, Lieger O, Michel C, Holmes S. What are the limitations of the non-patient-specific implant in titanium reconstruction of the orbit? Br J Oral Maxillofac Surg. 2020;58(9):e80–e5.
17. Schreurs R, Klop C, Maal TJJ. Advanced Diagnostics and Three-dimensional Virtual Surgical Planning in Orbital Reconstruction. Atlas Oral Maxillofac Surg Clin North Am. 2021;29(1):79–96.

18. Ali K, Lettieri SC. Management of Panfacial Fracture. Semin Plast Surg. 2017;31(2):108–17.
19. Schreurs R, Dubois L, Becking AG, Maal TJJ. The orbit first! A novel surgical treatment protocol for secondary orbitozygomatic reconstruction. J Craniomaxillofac Surg. 2017;45(7):1043–50.
20. Wang L, Lee TS, Wang W, Yi DI, Sokoya M, Ducic Y. Surgical Management of Panfacial Fractures. Facial Plast Surg. 2019;35(6):565–77.
21. Kim YC, Min KH, Choi JW, Koh KS, Oh TS, Jeong WS. Patient-specific puzzle implant preformed with 3D-printed rapid prototype model for combined orbital floor and medial wall fracture. J Plast Reconstr Aesthet Surg. 2018;71(4):496–503.
22. Mommaerts MY, Büttner M, Vercruysse H, Jr., Wauters L, Beerens M. Orbital Wall Reconstruction with Two-Piece Puzzle 3D Printed Implants: Technical Note. Craniomaxillofac Trauma Reconstr. 2016;9(1):55–61.
23. Metzger MC, Schön R, Zizelmann C, Weyer N, Gutwald R, Schmelzeisen R. Semiautomatic procedure for individual preforming of titanium meshes for orbital fractures. Plast Reconstr Surg. 2007;119(3):969–76.
24. Scolozzi P, Momjian A, Heuberger J. Computer-aided volumetric comparison of reconstructed orbits for blow-out fractures with nonpreformed versus 3-dimensionally preformed titanium mesh plates: a preliminary study. J Comput Assist Tomogr. 2010;34(1):98–104.
25. Kärkkäinen M, Wilkman T, Mesimäki K, Snäll J. Primary reconstruction of orbital fractures using patient-specific titanium milled implants: the Helsinki protocol. Br J Oral Maxillofac Surg. 2018;56(9):791–6.
26. Zimmerer RM, Ellis E, 3rd, Aniceto GS, Schramm A, Wagner ME, Grant MP, et al. A prospective multicenter study to compare the precision of posttraumatic internal orbital reconstruction with standard preformed and individualized orbital implants. J Craniomaxillofac Surg. 2016;44(9):1485–97.
27. Chowdhury K, Krause GE. Selection of materials for orbital floor reconstruction. Arch Otolaryngol Head Neck Surg. 1998;124(12):1398–401.
28. Holmes S, Schlittler FL. Going beyond the limitations of the non-patient-specific implant in titanium reconstruction of the orbit. Br J Oral Maxillofac Surg. 2021.

Chapter 4

Patient-specific implant design

This chapter is based on the following publication:

Sabelis J.F., Shaheen E., Willaert R., Becking A.G., Dubois L., Schreurs R. PSI: Planner-specific, physician-specific, or patient-specific implant for orbital reconstruction? J Craniomaxillofac Surg. 2024 Nov;52(11):1376-1382.

Abstract

This study aimed to identify and quantify the variations in PSI designs intended for an identical patient. Records from 10 patients with an orbital fracture involving two walls, for which a primary orbital reconstruction was indicated, were retrospectively included. Clinical engineers from two centers independently generated proposal designs for all patients. Following web meeting(s) with the surgeon from the same institute, the PSI designs were finalized by the engineer. A cross-over of the engineer with the surgeon of the other center created two new design teams. In total, 20 proposal and 40 final PSI designs were produced. A three-dimensional comparison between different PSI designs for the same patient was performed by computing a difference score. Initially, the design proposals of the two engineers showed a median difference score of 37%, which was significantly reduced to a median difference score of 26% for the final designs with different engineers. The median difference score of 22% between surgeons demonstrated that both parties introduced notable user variations to the final designs. Evidence supporting the advantages of an experienced design team was found, with significantly fewer modifications, fewer meetings, and less time required to complete the design (up to 40% time reduction). The findings of the study underline the dependency of PSI design on the surgeon and engineer, and support the need for a more evidence-based protocol for PSI design.

Introduction

The bony walls of the orbit are relatively thin, delicate, and prone to fracture upon traumatic impact to the periorbital region. The direction and intensity of the impact introduce varying fracture patterns, ranging from single-wall defects to extensive defects affecting multiple walls.[1-3] In turn, the presentation of clinical sequelae may be diverse. An orbital reconstruction may be indicated to restore the contours of the internal orbit and relieve clinical symptoms.[4, 5]

There are different implant possibilities available for orbital reconstruction. If more than one orbital wall is affected, titanium mesh implants are the preferred reconstruction material due to their biocompatibility and stability.[6-9] There are preformed titanium mesh implants, with a 3D shape based on an average orbit. The benefits of these mass-produced implants are the cost-effectiveness and availability.[10] In contrast to this 'one-size-fits-all' strategy is the patient-specific implant (PSI). Development of these implants is rooted in computer-assisted surgery (CAS) and computer-aided manufacturing (CAM). The PSI is individually designed to fit the patient's anatomy and pathology exactly. It is described as the most accurate option to reconstruct the pretraumatized anatomy and restore the orbital volume.[10, 11]

The PSI design workflow requires close collaboration between a surgeon and a clinical engineer.[12] A design proposal is generated by the engineer, which is based on the available information and case-specific preferences the surgeon might have. The design proposal is discussed with the surgeon, who may desire adjustments to the design. In this case, an adjusted design proposal is generated and re-evaluated by the surgeon. The PSI is taken into production only after the design meets all clinical and technical considerations. Previous experience in designing an orbital PSI by the engineer (in house or industry based) with the same surgeon may contribute to a more time-efficient workflow.[12, 13]

A PSI is considered to be the most 'patient'-specific implant option, but the design workflow entails manual and therefore subjective steps that result in numerous degrees of freedom. Although some studies have described potential design characteristics of a PSI,[14, 15] design options are implemented according to the preferences of the surgeon.[16, 17] Little is known about the variation in PSIs designed by different design teams. The primary goal of this study was to identify and quantify design variations between PSIs. The secondary aim was to assess whether differences between experienced and inexperienced design teams can be found in terms of PSI design, time required, and number of modifications.

Materials and Methods

Study Population

The study was approved by the local ethics committees of Amsterdam UMC, location AMC (W22_057) and of UZ Leuven hospital (S66491). The records of 10 patients (six from Amsterdam UMC and four from UZ Leuven) with an orbital fracture involving the medial wall, orbital floor, and medial strut, for which a primary orbital reconstruction was indicated, were retrospectively enrolled in the study. The exclusion criteria were insufficient quality of CT scan (i.e. slice thickness greater than 1 mm), involvement of surrounding bony structures (such as the zygomatic complex), and bilateral trauma.

Primary reconstruction was defined as a reconstruction within 6 weeks after trauma. Since there is no clear consensus in the literature on the indication for an orbital reconstruction with a PSI or a preformed implant, the expert opinion of the surgeons was the deciding factor in this study. Both surgeons evaluated the patient cases individually and agreed that a reconstruction with PSI was justified.

Design Workflow

The PSIs were virtually designed for all the cases. (The clinical workflow of both centers is based on in-house PSI design.) From each center, one clinical engineer (planner) with experience in PSI design and one surgeon (physician) experienced in orbital reconstruction, who previously worked with the clinical engineer on clinical PSI cases, participated in the study. The two engineers independently designed initial proposals (proposals A and B) for all patients, based on the CT scan and design experience. The engineers first discussed these proposals in a web meeting with the surgeon from the same institute — together considered an experienced team (A1 and B2 in *Figure 1*) — to prevent engineer or surgeon bias in subsequent designs. If necessary, the designs were adjusted based on the surgeon's remarks and re-evaluated in another web meeting; the design was considered final if the surgeon had no more desired design adjustments.

After the experienced teams had completed all cases, a cross-over was created in which the engineers discussed their initial proposals with the surgeon of the other center (A2 and B1 in *Figure 1*). Remarks and adjustments were again indicated by the surgeon and implemented in the design; the criteria for design finalization were the same. This study outline resulted in two proposal and four final PSI designs per patient. The durations of the web meetings and design sessions were recorded and the total time spent per case was calculated. The modifications indicated by the surgeon were also documented and categorized.

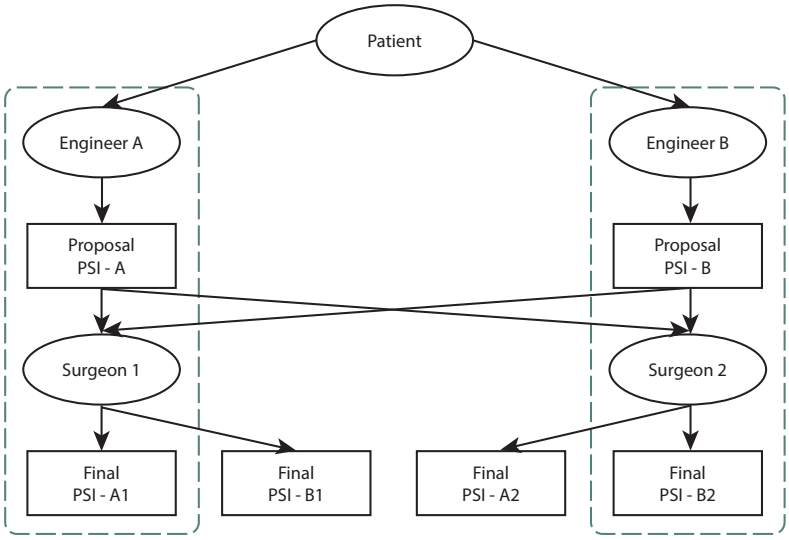


Figure 1. *Study workflow. The dotted boxes indicate the experienced design teams (A1 and B2).*

Comparison of the PSI Designs

The plane describing the floor of the implant was used for comparison of the designs. A difference score was defined to quantify the difference in PSI design between two PSI surfaces. Calculation of this score consisted of three steps: (1) Remeshing each plane in Meshmixer (version 3.5.474; Autodesk Inc., San Rafael, CA, USA) with a target edge length of 0.2 mm to ensure an even distribution of vertices while not affecting the shape of the plane. (2) Computation of the distance between each vertex and the other plane in Blender (version 3.2.2; Blender Foundation, Amsterdam, Netherlands). (3) Calculation of the percentage of vertices with a distance >1 mm for each plane and averaging the percentages from both planes to obtain one difference score between the two planes (*Figure 2*). The surface area of each design and the maximum length, width, and medial wall height were measured. The PSI reference frame described by Schreurs et al. was utilized to enable standardized length, width, and height measurements.[17]

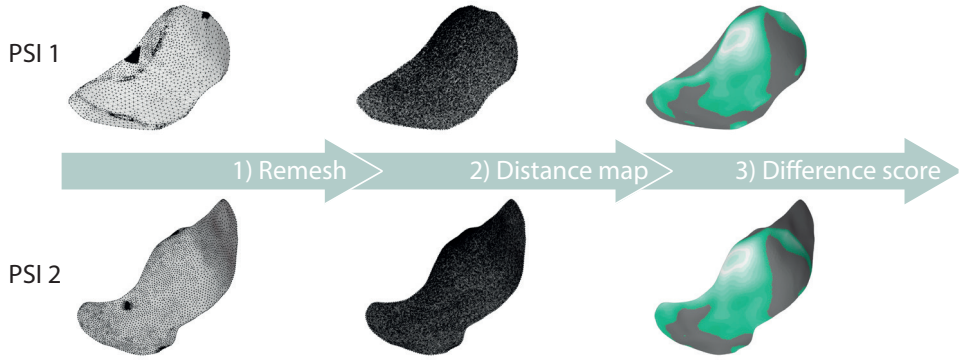


Figure 2. *Computation of difference scores. Both PSI planes are remeshed (1) and the distances from every vertex to the other plane are calculated (2). The difference score between two planes is calculated by averaging the extent of vertices outside the 1 mm range for both planes (3).*

Isolation of the Different Effects

Multiple difference scores could be computed between the two proposals and four final designs for one patient to isolate the effects of the engineer and surgeon on workflow and final design. *Figure 3* illustrates the comparisons that were made and the effect that was deduced from each comparison. The first comparison was made between the two PSI design proposals of the engineers. The difference between these two planes was indicative of the engineer's effect on the design process (1). After consultation with the surgeon, a final PSI design was made. By comparing all proposals with the final designs yielded from these proposals, the effect of the surgeon on the design process was measured (2). The difference score between the designs of the same surgeon and different engineers reflected the engineer effect on the final design (3). In contrast, the difference between the PSIs designed by the same engineer with different surgeons reflected the surgeon effect on the final design (4). Finally, the effect of experience was evaluated by grouping the experienced (A1 and B2) and inexperienced (A2 and B1) design teams' final designs and comparing them with the design proposals.

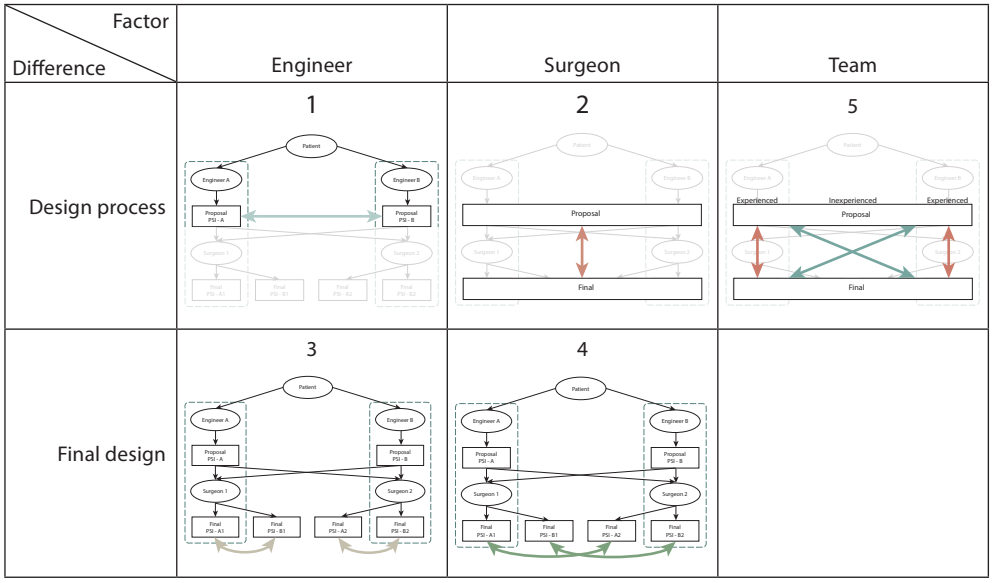


Figure 3. *Different comparisons made to isolate the effects of surgeon, engineer, and experience on the design process and final design. The numbers (1-5) are referred to in the results section.*

Statistical Analysis

The data were imported into R studio (version 4.2.1; RStudio, Inc., Boston, MA, USA) for statistical analysis. A paired sample t-test or Wilcoxon signed-rank test was used for statistical comparison, depending on the outcome of the Shapiro-Wilk test for normality. The four surgeon-engineer combinations were grouped into experienced and inexperienced teams for analyses of meeting times and numbers of design modifications.

Results

Effect of Engineer on Design Process

In total, 20 design proposals were generated. The median difference score between the proposals of the two engineers was 37% (interquartile range (ICR) 29–45%). A boxplot of the difference scores is provided in *Figure 4*. The overall median surface area of the proposal designs was 875 mm2, with a median relative difference of 19% between the engineers. The median length, width, and height were 36 mm, 33 mm, and 12 mm, respectively. The relative median difference was lowest for length (median 8%, ICR 4–12 %) and highest for height (median 22%, ICR 18–32%).

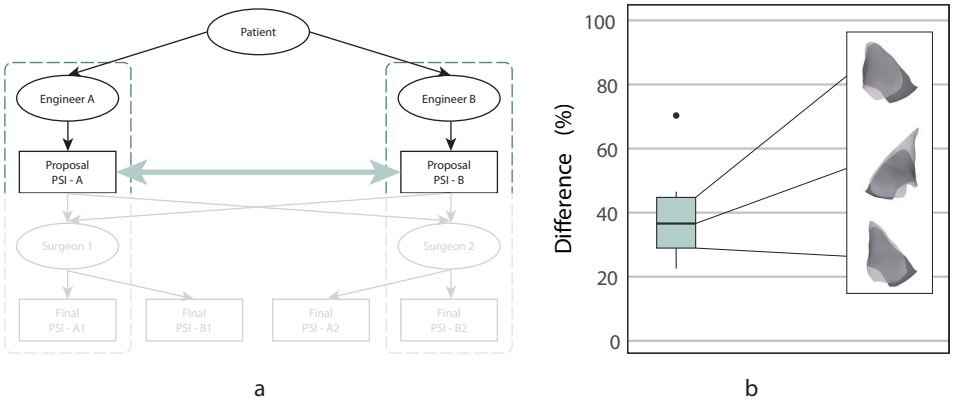


Figure 4. *(a) Illustration of the compared planes used to compute the difference score depicted in the boxplot in (b). The PSI combinations of the boxplot's 25th, 50th, and 75th quartile range are visualized.*

Effect of Surgeon on Design Process

This resulted in 40 final PSI designs. A median difference score of 15% (ICR 13–19%) between initial design proposal and final design was found, meaning that, on average, the surgeon induced design modifications of >1 mm in 15% of the PSIs (*Figure 5*). This difference was reflected in the implant parameters: a median change of 6% in surface area, 6% in length, 8% in width, and 11% in height was found. During the consultations, the surgeons commonly requested changes to screw positions (78%), overall shape (63%), medial wall support (58%), and rim extension (55%) (*Table 1*).

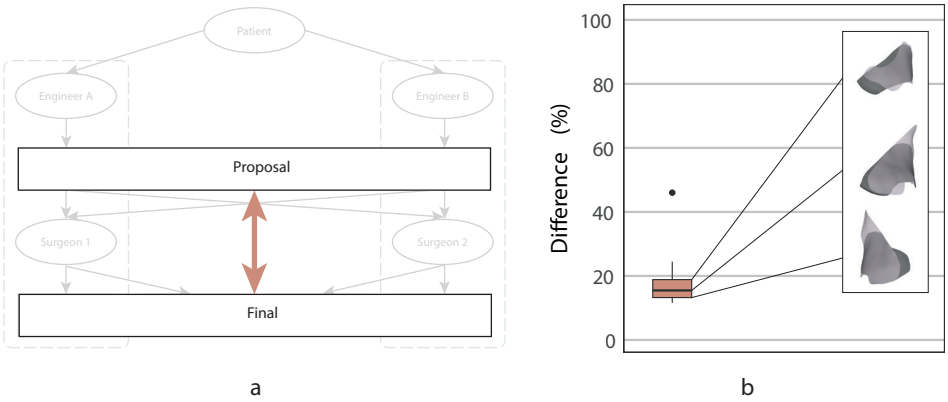


Figure 5. *(a) Illustration of the compared planes used to compute the difference score depicted in the boxplot in (b). The PSI combinations of the boxplot's 25th, 50th, and 75th quartile range are visualized.*

Table 1. *Modifications indicated per design team; the team codes correspond to Figure 1.*

Team	*Screw position*	*Overcorrection*	*Rim extension*	*Ledge*	*Medial Wall*	*Shape*	*Anatomy*
A1	0.3	0.0	0.1	0.1	0.3	0.1	0.3
A2	0.9	1.0	1.0	0.3	0.7	0.7	0.7
B1	0.9	0.0	1.0	1.0	1.0	0.8	0.8
B2	1.0	0.0	0.1	0.5	0.3	0.9	0.2
Total	0.78	0.25	0.55	0.48	0.58	0.63	0.50

Effect of Engineer on Final Design

The median difference between final PSIs designed by different engineers (grouped per surgeon) was 26% (ICR 20–34%) (*Figure 6*). This difference quantified the difference an engineer induces in the final design. The score was significantly lower ($p = 0.005$) than the difference score between the two initial design proposals, which was due to the adjustments indicated by the surgeon. The relative differences for the surface area, length, and width were slightly decreased to medians of 12%, 7%, and 6%, respectively, whereas the height difference increased to a median of 31%.

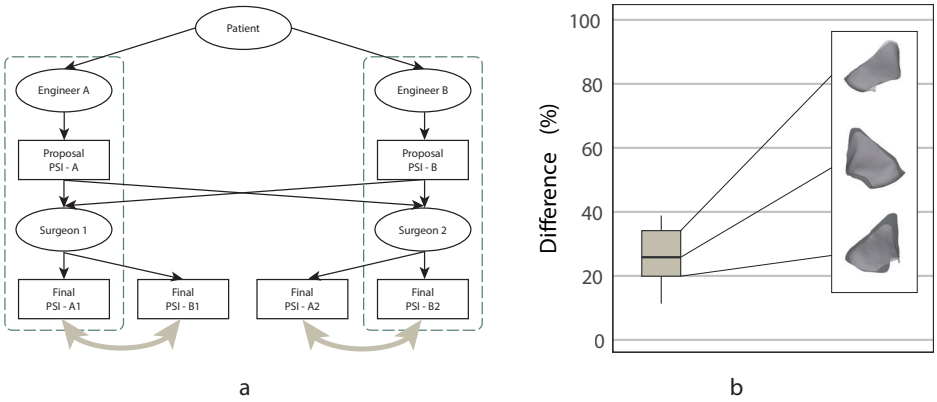


Figure 6. *(a) Illustration of the compared planes used to compute the difference score depicted in the boxplot in (b). The PSI combinations of the boxplot's 25th, 50th and 75th quartile range are visualized.*

Effect of Surgeon on Final Design

Each engineer discussed the same proposal design with two different surgeons. Comparisons of the resulting two final PSI designs (same engineer, different surgeons) yielded a median difference score of 22% (ICR 20–27%) (*Figure 7*). Differences were also seen in surface area, length, width, and height of the two final designs the same surgeon would approve, with relative difference values of 7%, 6%, 7%, and 20%.

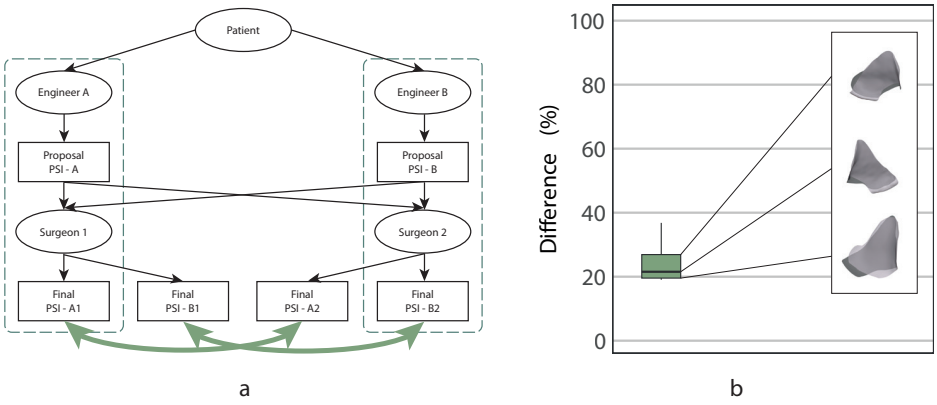


Figure 7. *(a) Illustration of the compared planes used to compute the difference score depicted in the boxplot in (b). The PSI combinations of the 25th, 50th and 75th quartile range of the boxplot are visualized.*

Effect of Experience on the Design Process

The difference scores between the proposal and final PSI designs of the experienced (A1 and B2) and inexperienced (A2 and B1) design teams were grouped, and a median difference score of 3% was found for the experienced team (ICR 2–8%) compared with 26% for the inexperienced team (ICR 23–30%) (*Figure 8*). This difference yielded through experience was statistically significant (Wilcoxon signed rank test, $p = 0.002$).

Median differences for the implant characteristics for the experienced teams ranged from 1 to 2%, while for the inexperienced teams they ranged from 8 to 15%. Overall, the experienced teams required significantly fewer changes to the PSI design than the inexperienced teams.

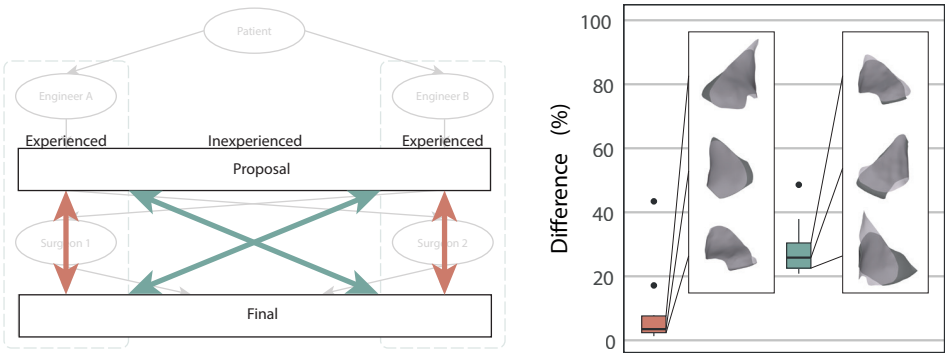


Figure 8. *(a) Illustration of the compared planes used to compute the difference score depicted in the boxplot in (b). Red = experienced, green = inexperienced. The PSI combinations of the boxplot's 25th, 50th and 75th quartile range are visualized.*

Analysis of the meeting characteristics also revealed other benefits of the experienced design teams: less time, as well as fewer meetings and modifications, were required per case. As detailed in *Table 2,* the experienced design teams required a median of 63.5 min (ICR 59–68 min) in total per case, whereas the inexperienced design teams required a median of 100 min (ICR 98–104 min) in total per case. This difference was statistically significant (p = 0.002). The experienced design teams also required significantly fewer meetings and modifications per case, on average, two meetings and two modifications, compared with three meetings and seven modifications.

Table 2. *Summary of meeting characteristics. Median (interquartile range).*

Outcome		*Experienced*	*Inexperienced*	*P-value*
Time	Total	63.5 (59 - 68)	100 (98 – 104)	0.002
	Design	56 (54 - 60)	83.5 (77 - 89)	0.004
	Meeting	7.5 (7 - 11)	17 (15 - 18)	0.008
Number	Meetings	2 (1-2)	3 (2-3)	0.003
	Modifications	2 (0-4)	7 (6-8)	<0.001

Discussion

The purpose of this study was to identify and quantify the variation in PSI design caused by factors other than the patient. A three-dimensional comparison between different PSI designs for the same patient was performed by computing a difference score. Significant differences between the PSI designs of four design teams for the same patient were found, with the initial design proposal of the two engineers showing a me-

dian difference score of 37%. Consultation with the surgeons led to alterations in 15% of the design and a significant reduction of the difference to a median score of 26% between final designs with different engineers. The final PSI designs produced by the same engineer and approved by a different surgeon demonstrated a median difference of 22%. All difference scores were strikingly different from the 0% difference score that would be obtained if only patient characteristics played a role in PSI design.

Significant user dependency of virtual surgical planning in orbital reconstruction has been demonstrated for the use of preformed orbital implants. In a study by Hierl et al.,[18] consensus about implant choice was found in only 30% of the cases, and significant differences in positioning were observed between the users even if the same implant was selected. The PSI design process is also known to suffer from a lack of standardization.[19] Although a one-to-one comparison between the results in preformed implants and the current study is unfeasible, the high degree of user input required in the design process will make virtual surgical planning for PSI cases even more susceptible to user variation. Personal design preferences based on previous experience, a multitude of design options that may be embedded, and the involvement of both an engineer and a surgeon are extra factors that may introduce possible variations in PSI design.

The cross-over design of our study allowed separation of the effects of the surgeon and the engineer on final PSI design. The median difference scores (26% between engineers and 22% between surgeons) demonstrated that both parties introduced notable user variation in the final design. In this study, the effects of engineer and surgeon were found to be roughly equal, but a larger sample of surgeons and engineers would be needed to verify this result. Clear personal preferences of the individual surgeons were observed in this study — for example, the locations of the screw positions (one medial and two lateral versus three lateral), the presence or absence of a rim extension, support location on the medial wall, and differences regarding specific anatomical landmarks (wider margin for the insertion of the obliquus inferior muscle versus support on the lacrimal extension). Differences seen in the final designs of the different engineers involved the amount of support and defect coverage (and thus the size of the implant).

It is difficult to truly isolate the differences in final design yielded by the surgeon and engineer because they have separate and successive roles in the design workflow. The engineer establishes the shape and curvature of the initial proposal, based on technical knowledge and previous experience. Subsequently, the surgeon indicates the required modifications to the proposal to suit clinical needs and surgical considerations; the exact execution of these preferences are, in turn, engineer-dependent and might result in small variations.

The magnitudes of the variations originating in the workflow through the surgeon or engineer were also investigated in this study. Large differences were found between the initial proposals, which was considered to be the effect of the engineer in the design process. Although the initial difference was identified as the engineer's effect in the workflow, since the surgeon was not involved in the process at this point, it could be argued that the experience an engineer uses in the process is built on cooperation with specific surgeons, and that specific design features that are preferred in their hospital are embedded. The surgeon's effect in the design process was assessed by comparing the alterations between initial proposal and final design. The alterations desired by the surgeons were found to be consistent for each surgeon; the surgeon's effect on the workflow was the significant reduction in differences from proposals to finals.

The cross-over design of the study also provided insights into the effect of team experience level on the design process. The difference score comparing the proposal and the final design of the experienced teams was significantly lower compared with the score for the inexperienced teams. This verified that the experienced engineers had already tailored the initial proposal to the surgeon's preference, which reduced the amount of change required from the proposal to the final design (and thus the direct effect of the surgeon on the design workflow). Teams well attuned to each other also required significantly fewer meetings and less time to complete the design (up to 40% time reduction). These findings emphasized the advantages of having engineers in the hospital to collaborate closely with the surgeons and build team experience, but this is not common practice in every hospital, since PSI design is frequently outsourced to commercial partners. A previous study by Korn et al. demonstrated that previous in-house training of the engineer provided the same time-saving advantages in the commercial setting.[19]

Ideally, patient characteristics would be the only factors contributing to PSI design. The results of this study demonstrate that there are several human factors that play a role in the design process, and which affect the patient specificity of the resulting final implant design. While many possible PSI design options have been suggested,[11, 14-16] there has yet to be a consensus on what constitutes the optimal design. It remains to be determined whether different designs lead to differences in surgery or patient outcome, and this could also not be deduced in the current study setup. Objective evidence as to which design leads to the most optimal clinical outcome might only be gathered by comparing large cohorts of patients from multiple centers treated with different PSI designs.

Collecting a large amount of data on PSI design and knowing which design features influence clinical outcome might also pave the way for implementation of artificial intelligence (AI) in the orbital reconstruction workflow. Potentially, AI can enable automatic segmentation, mirroring, and even design of the PSI itself. This might help to reduce design variation, improve clinical predictability, and truly achieve the full benefits of PSI construction.

Conclusion

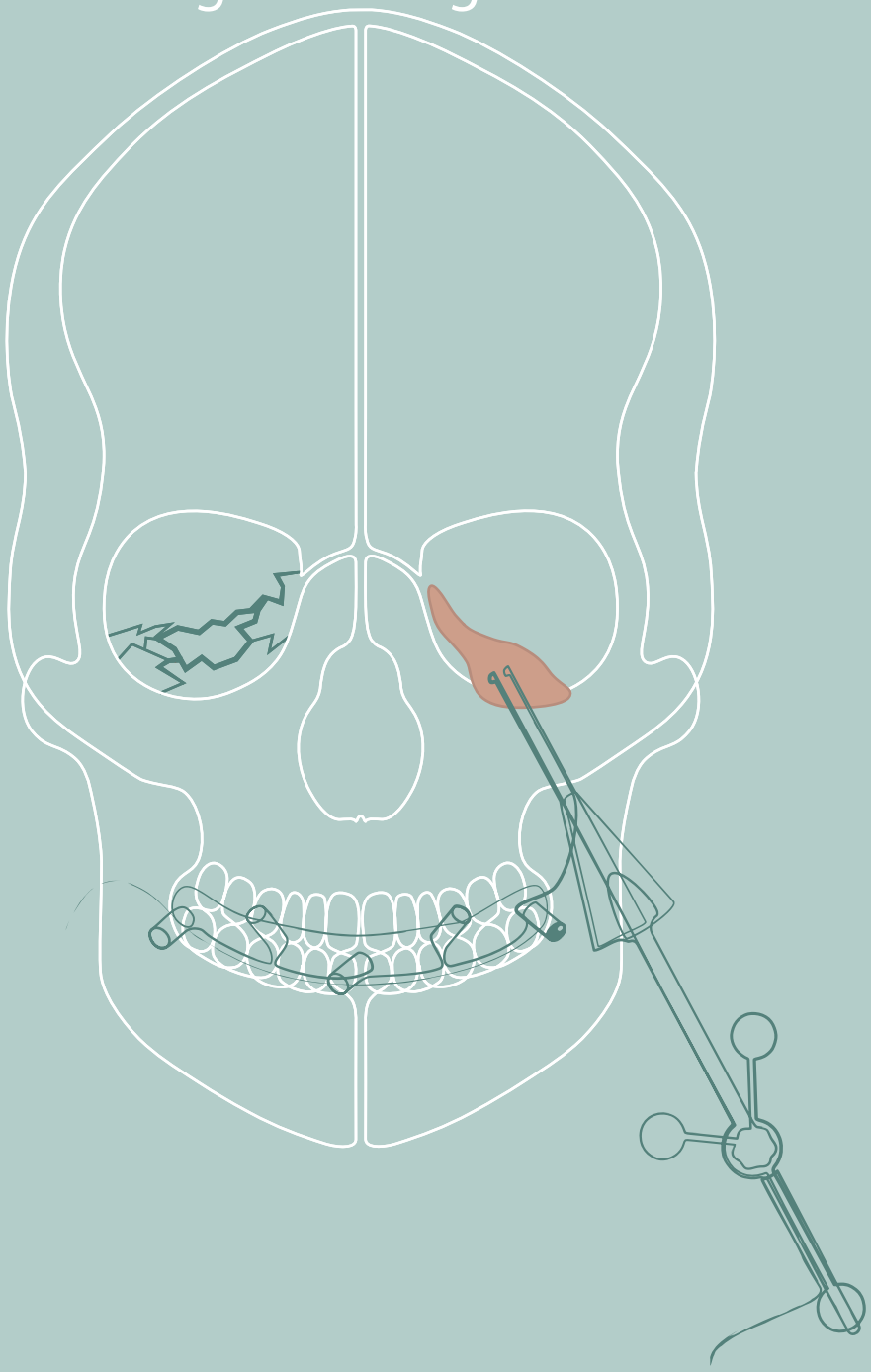
Our study compared the different PSI designs for a cohort of 10 post- traumatic orbital reconstruction patients. The results demonstrated a large variation in PSI designs for the same patient. The surgeon and the engineer played crucial roles in the PSI design process. The experience of the design team resulted in fewer modifications to the PSI design, fewer meetings, and a decrease in total time. The findings of this study support the need for a more evidence-based protocol for PSI design that is genuinely tailored to the patient, in order to minimize variations in PSI designs and improve the predictability of the clinical outcome.

References

1. Foletti JM, Martinez V, Haen P, Godio-Raboutet Y, Guyot L, Thollon L. Finite element analysis of the human orbit. Behavior of titanium mesh for orbital floor reconstruction in case of trauma recurrence. J Stomatol Oral Maxillofac Surg. 2019;120(2):91–4.
2. Grob S, Yonkers M, Tao J. Orbital Fracture Repair. Semin Plast Surg. 2017;31(1):31–9.
3. Raflo GT. Blow-in and blow-out fractures of the orbit: clinical correlations and proposed mechanisms. Ophthalmic Surg. 1984;15(2):114–9.
4. Ellis E, 3rd, Tan Y. Assessment of internal orbital reconstructions for pure blowout fractures: cranial bone grafts versus titanium mesh. J Oral Maxillofac Surg. 2003;61(4):442–53.
5. Shyu VB, Chen HH, Chen CH, Chen CT. Clinical outcome following intraoperative computed tomography-assisted secondary orbital reconstruction. J Plast Reconstr Aesthet Surg. 2021;74(2):341–9.
6. Dubois L, Dillon J, Jansen J, Becking AG. Ongoing Debate in Clinical Decision Making in Orbital Fractures: Indications, Timing, and Biomaterials. Atlas of the Oral and Maxillofacial Surgery Clinics of North America. 2021;29(1):29–39.
7. Ellis E, 3rd, Messo E. Use of nonresorbable alloplastic implants for internal orbital reconstruction. J Oral Maxillofac Surg. 2004;62(7):873–81.
8. Holmes S. Primary Orbital Fracture Repair. Atlas Oral Maxillofac Surg Clin North Am. 2021;29(1):51–77.
9. Dubois L, Steenen SA, Gooris PJ, Bos RR, Becking AG. Controversies in orbital reconstruction-III. Biomaterials for orbital reconstruction: a review with clinical recommendations. Int J Oral Maxillofac Surg. 2016;45(1):41–50.
10. Kotecha S, Ferro A, Harrison P, Fan K. Orbital reconstruction: a systematic review and meta-analysis evaluating the role of patient-specific implants. Oral Maxillofac Surg. 2023;27(2):213–26.
11. Gander T, Essig H, Metzler P, Lindhorst D, Dubois L, Rücker M, et al. Patient specific implants (PSI) in reconstruction of orbital floor and wall fractures. J Craniomaxillofac Surg. 2015;43(1):126–30.
12. Gellrich NC, Dittmann J, Spalthoff S, Jehn P, Tavassol F, Zimmerer R. Current Strategies in Post-traumatic Orbital Reconstruction. J Maxillofac Oral Surg. 2019;18(4):483–9.
13. Goodson AMC, Parmar S, Ganesh S, Zakai D, Shafi A, Wicks C, et al. Printed titanium implants in UK craniomaxillofacial surgery. Part II: perceived performance (outcomes, logistics, and costs). Br J Oral Maxillofac Surg. 2021;59(3):320–8.
14. Kärkkäinen M, Wilkman T, Mesimäki K, Snäll J. Primary reconstruction of orbital fractures using patient-specific titanium milled implants: the Helsinki protocol. Br J Oral Maxillofac Surg. 2018;56(9):791–6.
15. Rana M, Chui CHK, Wagner M, Zimmerer R, Rana M, Gellrich N-C. Increasing the Accuracy of Orbital Reconstruction With Selective Laser-Melted Patient-Specific Implants Combined With Intraoperative Navigation. Journal of Oral and Maxillofacial Surgery. 2015;73(6):1113–8.
16. Sabelis JF, Schreurs R, Essig H, Becking AG, Dubois L. Personalized Medicine Workflow in Post-Traumatic Orbital Reconstruction. Journal of Personalized Medicine. 2022;12(9):1366.
17. Schreurs R, Klop C, Gooris PJJ, Maal TJJ, Becking AG, Dubois L. Critical appraisal of patient-specific implants for secondary post-traumatic orbital reconstruction. Int J Oral Maxillofac Surg. 2021.
18. Hierl T, Kruber D, Doerfler HM, Huempfner-Hierl H, Krause M. Computer-Aided Versus Conventional Planning in Orbital Traumatology Using Preformed Meshes: Development of a New Workflow. J Oral Maxillofac Surg. 2019;77(8):1663–72.
19. Korn P, Jehn P, Nejati-Rad N, Winterboer J, Gellrich NC, Spalthoff S. Pitfalls of Surgeon-Engineer Communication and the Effect of In-House Engineer Training During Digital Planning of Patient-Specific Implants for Orbital Reconstruction. J Oral Maxillofac Surg. 2022;80(4):676–81.

Part II

Surgical navigation



Chapter 5

Clinical validation of virtual splint registration

This chapter is based on the following publication:

Sabelis J.F., Schreurs R., Dubois L., & Becking A.G. Clinical validation of the virtual splint registration workflow for craniomaxillofacial surgery. Int J Oral and Maxillofac Surg. 2025;54(8):741–6.

Abstract

Accurate registration is vital to transfer the virtual surgical plan during surgery. This study's goal was to present and clinically validate a virtual splint registration workflow. Ten dentate patients requiring revision surgery were included. Specific inclusion criterion for this study was the presence of at least two osteosynthesis screws on the orbital rim from a previous surgery. Dedicated orthognathic surgery software was used to fuse the maxillary dental scan with the computed tomography and generate a dental splint, which was imported into the navigation software and augmented with fiducial markers. Registration points were indicated virtually and the augmented splint was three-dimensionally printed. Intraoperatively, the splint was fitted on the maxillary dentition and the fiducial markers were used for registration. Accuracy of the registration procedure was quantified by calculating the difference between the landmarks acquired by indicating the pre-existing osteosynthesis material with the navigation pointer and in the virtual planning software. After acquisition of the landmarks, the screws were removed and surgery proceeded according to plan. A median target registration error of 1.53 mm was found. The advantages of the virtual splint registration workflow are that it does not require extensive computer-aided design skills or repeated preoperative imaging, and is noninvasive.

Introduction

Technological advancements have led to the application of novel techniques in oral and maxillofacial surgery, such as virtual surgical planning and surgical navigation. These techniques are commonly summarized under the term 'computer-assisted surgery'.[1-4] The virtual surgical plan can be transferred to the operating room with the use of surgical navigation. An essential prerequisite for navigation is an accurate registration procedure. During this process, the preoperative computed tomography (CT) scan is linked to the actual position of the patient in the operating room.5 The accuracy of the registration directly affects the accuracy of the navigational feedback and, thus, the effectiveness and reliability of its use during surgery.[5-7]

Several different registration techniques are currently available. The selection of a particular method may be based on technical and clinical considerations, including accuracy requirements, invasiveness of fiducial placement in relation to the invasiveness of surgery, the (expected) soft tissue deformation, and preoperative and intraoperative logistics. The different techniques can generally be categorized into the following methods of registration: surface-based registration, paired-point registration, and automatic registration. In automatic registration, the dynamic reference frame is fixed to the patient and an intraoperative CT scan is acquired and automatically aligned.[8] Application of this workflow is limited due to availability and the additional radiation exposure. In surface-based registration, the surface of the patient, often the soft tissue, is traced and aligned to the surface representation of the soft tissue in the preoperative CT scan.[9] While this is often used in neurosurgery,[10] its application is limited in facial trauma patients due to soft tissue alterations such as oedema. In the paired-point registration techniques, several recognizable landmarks are used for the registration. The landmarks are often artificially created (fiducial landmarks). The fiducial landmarks can be placed invasively; for example, bone screws may be placed in the maxilla, which has been identified as a practical location because of the vicinity to the midface and prevention of visible scars.[5, 11] Alternatively, non-invasive fiducials can be introduced by creating a dental splint bearing the fiducials that is positioned on the maxillary dentition.[11-13] With both paired-point registration techniques, a second CT scan or a cone beam computed tomography scan (CBCT) scan is necessary to identify the fiducials in the preoperative image volume, because these were not present in the diagnostic image volume. This places a burden on preoperative logistics and leads to additional radiation exposure for the patient.

With the virtual splint registration method reported here, a dental splint bearing fiducials is virtually designed, automatically aligned to the patient in the virtual surgical planning, and three-dimensionally (3D) printed to enable intraoperative use.[14] This workflow would thus resolve the previously mentioned issues, as it is non-invasive and eliminates the need for repeated preoperative (or intraoperative) CT scanning. Since its preclinical validation, the logistics surrounding the workflow have been improved and implemented within the clinical workflow at Amsterdam UMC, for dentate patients requiring oral and maxillofacial surgery with intraoperative navigation. The goal of this study was to present this easily applicable virtual splint workflow and to study the accuracy in a clinical setting.

Materials and Methods

Patient population

Eleven patients were enrolled in this prospective study. Inclusion criteria were dentate patients requiring revision surgery after previous facial trauma reconstruction; osteosynthesis material on the orbital rim that would be removed during the revision surgery, fixated with at least two osteosynthesis screws; preoperative CT scan with a slice thickness ≤1 mm and field of view including the maxillary dentition and the osteosynthesis material on the orbital rim. Exclusion criteria were mobility of the maxillary complex; inability to obtain dental models preoperatively (e.g., due to limited mouth opening); inadequate fixation of the osteosynthesis material (e.g., infection due to osteosynthesis material, visible screw loosening on the CT scan or intraoperatively); insufficient scan quality. Age, sex, and the Decayed, Missing and Filled Teeth (DMFT) score were recorded for each patient.

Preparation for Data Collection

The workflow for this study was based on the virtual splint workflow as described by Schreurs et al.14. The previous workflow was modified, obviating the need for manual creation of the splint and the required transformation of the splint to the reference frame of the virtual planning software. In brief, the new workflow consists of four steps: (1) creation of the virtual patient model by fusion of the dental scans with the CT in IPS CaseDesigner software (v2.5.7.1; KLS Martin, Tuttlingen, Germany); (2) creation of the dental splint in IPS CaseDesigner; (3) import of the dental splint into the virtual planning software, Brainlab Elements 'Craniomaxillofacial' module (Brainlab AG, Munich, Germany), preparation for intraoperative use, and 3D printing of the splint; (4) use of the 3D-printed splint for the registration.

A 3D model of the patient was acquired from a CT scan. As the dental information in a CT scan is of low quality, a separate dental scan of high quality is required.[15] Where possible, an intraoral scanner was used to acquire a high-definition dental scan (TRIOS 3 intraoral scanner; 3Shape, Copenhagen, Denmark). Otherwise, impressions were taken and the cast models were digitized through CBCT imaging (KaVo OP 3D Vision V17; Henry Schein Inc., Melville, NY, USA). The fusion of the dental scan with the patient model was performed using IPS CaseDesigner.

In IPS CaseDesigner, a splint for the 'preoperative position' covering the dentition from the first molar to the contralateral first molar (if present) was designed (*Figure 1a*). Four design characteristics were implemented: (1) autorotation of the mandible was performed to acquire a thicker and therefore robust splint design. As the splint is fitted on the maxillary dentition only, autorotation of the mandible does not affect the intraoperative position of the splint and thus the accuracy of the registration. (2) Splint thickness was maximized, deepening the dental impression and ensuring a stable fit during surgery. (3) A buccal extension was added, allowing attachment of the registration cylinders without risking interference with the dentition. (4) A name tag was added for patient identification.



a b c

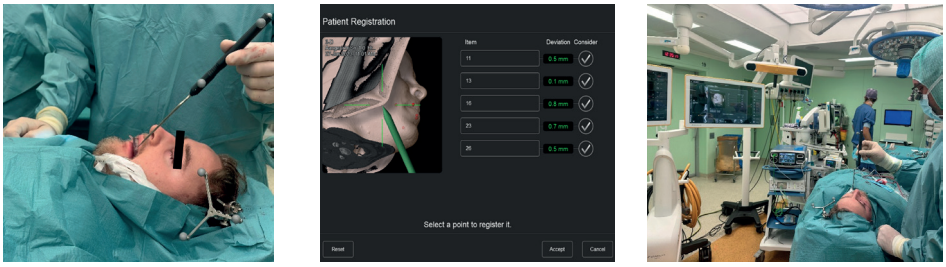
Figure 1. *Preparation required for virtual splint registration. (a) After fusion of the dental models to the CT scan, a dental splint was created using IPS CaseDesigner. (b) The created splint was imported into Brainlab Elements software, and cylinders bearing a fiducial marker were positioned and indicated as registration landmarks (red dots). (c) The splint was 3D-printed in transparent material; the name tag was removed for positioning.*

The splint was exported in stereolithography (STL) format and imported into Brainlab Elements software using the 'STL import' function, for the virtual surgical planning. The lower dentition impression was eliminated using the 'split' function, resulting in a slim yet robust splint, and preventing confusion on splint positioning intraoperatively. Additionally, a 3D model of a cylinder (1.5 mm radius, 10 mm length) with a hemisphere indentation at the end (0.5 mm radius) was imported. This spherical indentation became the fiducial landmark. In the Elements environment, five of these cylinders were optimally distributed to ensure fiducials in all planes, with two extending bilaterally from the molar regions, two cranially from the canine regions, and one extending caudally from the central incisors. In the iPlan Brainlab environment, registration landmarks were indicated in each of the spherical indentations on the cylinders (*Figure 1b*).

The cylinders have to be digitally fused to the splint to enable 3D printing. This can be performed in the Elements software or in any computer-aided design (CAD) software. For this study, the fusion was performed in Blender (version 2.81; Blender Foundation, Amsterdam, the Netherlands) to prevent resolution loss. The fused splint was 3D-printed using an in-house PolyJet printer (Objet30 Prime; Stratasys Ltd, Eden Prairie, MN, USA) in transparent material (VeroClear; Stratasys Ltd) (*Figure 1c*).

Data Collection

All surgeries and measurements were performed by one experienced surgeon. The surgical approach was performed to expose the infraorbital osteosynthesis material. The Reference Base Skull was fixated to the patient's cranium, and the Skull Reference Array was attached (Brainlab AG). The registration procedure was initiated in the Curve navigation system (Brainlab AG). The 3D-printed splint fitted tightly on the maxillary dentition and was held in place by the surgeon if necessary while the surgeon indicated the five indentations with the navigation pointer (*Figure 2a*). Registration was checked quantitatively and qualitatively. Quantitatively, the fiducial registration error (FRE) in the 'Details' was assessed; individual landmarks were re-registered if the FRE was higher than 1.0 mm, ensuring all were < 1.0 mm (*Figure 2b*). Screenshots captured the final FRE values. Qualitatively, the pointer was positioned on anatomical landmarks (nasion and pronasale) to verify the accuracy of its position on the navigation screen (*Figure 2c*). If this verification showed insufficient accuracy, the registration procedure was repeated from the start.



a b c

Figure 2. *Registration procedure using the virtual splint. (a) After positioning the splint on the dentition, the indentations on the cylinders are indicated by the surgeon using the navigation pointer. (b) Quantitative accuracy check of the fiducial registration error. (c) Qualitative accuracy check.*

For the accuracy measurements, the surgeon selected the most medial and most lateral of the pre-existing screws at the infraorbital rim that were accessible without enlarging the incision. The surgeon indicated the indentations in the screw heads with the tip of the pointer (*Figure 3*), and the 'Acquire' function of the Brainlab system was used to store the coordinate positions (acquired coordinates). The positions of the medial and lateral screws were acquired in three series. After acquisition, the surgery continued according to the clinical protocol, which also involved the removal of the screws.

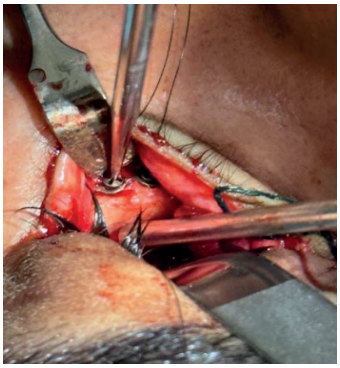


Figure 3. *Intraoperative acquisition of the acquired landmarks by the surgeon to assess the accuracy of the registration.*

Postoperatively, the selected medial and lateral screw heads were indicated in the iPlan Cranial software as navigation markers (target coordinates). This indicating in the image volumes was performed twice by one clinical engineer (J.S.) and once by another clinical engineer (R.S.), to reduce user-dependency and enable the assessment of intra- and inter-rater variability. The acquired coordinates were not visualized since this could affect the measurement, leading to bias in the results. The imaging volume was aligned to the axis of the individual screws, and the window level was set from –400 to 1600 Hounsfield units, to precisely identify the screw head in multiplanar views (*Figure 4*).

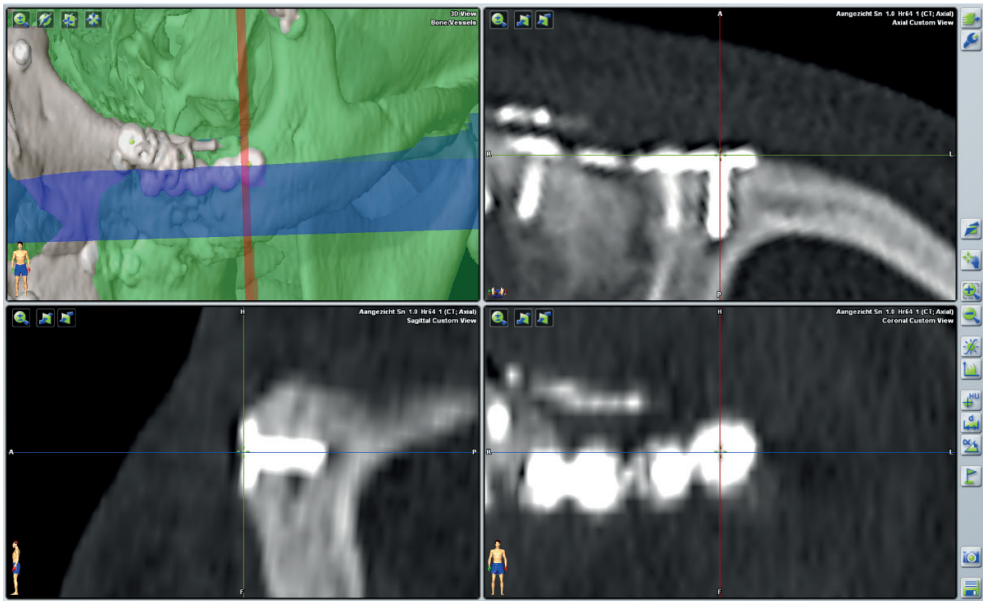


Figure 4. *Virtual acquisition of the target landmarks by the clinical engineers in the iPlan Cranial software.*

Data analysis

The x, y, and z coordinates of the landmarks were extracted from the Brainlab environment with the 'copy to clipboard' function, saved in a local database, and imported into RStudio (v4.3.3; RStudio Inc., Boston, MA, USA). The median and range values of the FRE, distance between the medial and lateral target screw positions, and distances between the individual acquired and target coordinates were calculated. The latter describes the spread of the acquired and target coordinates. The primary outcome parameter was the target registration error (TRE), calculated by computing the Euclidean distance between the average target coordinates and the individual acquired coordinates. An important factor influencing the TRE is the distance between the acquired landmark and the centre of gravity of the registration area, which was also calculated.

Results

Eleven patients were included in this study. One patient was excluded because after removal of the pre-existing screws it was discovered that the Skull Reference Array was not rigidly fixated to the skull, rendering the acquired coordinates unreliable. The baseline characteristics of the remaining 10 patients are described in *Table 1*. The mean age was 35 years (range 18–63 years). Eight patients were male and two were female. Apart from one patient with an orbital implant (10%), all measurements were performed using an infra-orbital rim plate (90%). The minimum dental span was from 16 (right side upper first molar) to 26 (left side upper first molar). The average number of fillings was 3 (metal and composite combined), with a range of 0–9.

Table 1. *Patient Characteristics, n = 10.*

Characteristics	
Age (years), mean ± SD	35 ± 16
Sex	2 female, 8 male
Osteosynthesis material used for measurement	
Infra-orbital rim plate	90%
Orbital implant	10%

SD, standard deviation

All splints were fitted on the maxillary dentition and used for intraoperative registration. A total of 59 acquired points, 60 target points, and 45 FRE measurements were collected. For one patient, the FRE measurements were not recorded, while for another patient, one medial screw measurement was missing.

Table 2. *Errors and calculated distances.*

Measurement		***Median (range)***
Error (mm)		
FRE		0.52 (0.30-9.74)
TRE	Total	1.53 (0.29-4.40)
	X	0.52 (0.04-1.87)
	Y	0.82 (0.02-2.10)
	Z	0.86 (0.17-1.71)
Distance between (mm)		
Acquired point to registration center		56.5 (46.5-76.5)
Acquired coordinates		0.54 (0.17-3.41)
Target medial and lateral screw		18.3 (4.1-30.8)
Target coordinates	Intra	0.08 (0.00-0.37)
	Inter	0.10 (0.01-0.52)

FRE, fiducial registration error; TRE, target registration error.

Table 2 summarizes the calculated distances and errors. A median TRE of 1.53 mm (range 0.29–4.40 mm) was found . The scatter plot in *Figure 5* visualizes the distribution of the TRE with respect to the distance to the registration area. Eighty percent of the measured TREs were below 2.0 mm. For one patient, a maximum TRE of 4.4 mm and mean of 3.1 mm was reported. The median FRE was 0.52 mm (range 0.30–9.74 mm). The medial and lateral acquired positions were a median 18.3 mm (range 4.1–30.8 mm) apart and these were located at a median distance of 56.5 mm (range 46.5–76.5 mm) from the centre of gravity of the registration area . The median intra- and inter-rater distances were 0.08 mm (range 0.00 –0.37 mm) and 0.10 mm (range 0.01–0.52 mm), respectively. Overall, a median distance of 0.54 mm (range 0.17–3.41 mm) between the acquired coordinates was measured.

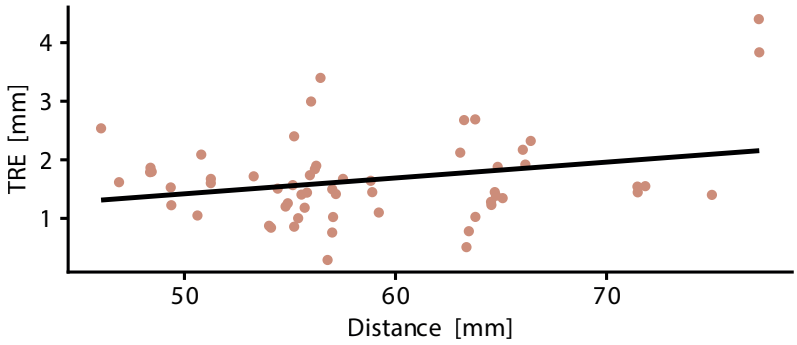


Figure 5. *Plot of target distance against target registration error (TRE) for each individual acquired landmark.*

Discussion

The purpose of this study was to clinically validate the virtual splint workflow, a non-invasive registration method for intraoperative navigation. Advantages of this workflow when compared to existing registration techniques relying on fiducial screws or splints that need to be in place during scan acquisition, are its non-invasiveness, improvements to preoperative logistics, and prevention of additional radiation exposure for the patient14. Compared to the previous workflow, improvements made the current workflow less reliant on CAD software, making it more accessible for hospitals without in-house engineers. Pre-existing osteosynthesis screws were chosen as target points for measuring registration accuracy, because these were easily identifiable in the image volume and during surgery. For 10 patients, the median registration accuracy was found to be 1.53 mm at the level of the infraorbital rim, at a mean 58.5 mm distance from the registration centre. The results for one patient (mean TRE 3.1 mm) negatively affected the mean accuracy, which could not be explained from the collected data. Possible explanations include suboptimal registration, unnoticed loosening of the reference array, or inaccurate pointer positioning during acquisition.

The accuracy of paired-point registration methods can be analysed using three errors: fiducial localization error (FLE), fiducial registration error (FRE), and the target registration error (TRE).[5] The FLE is the error in locating the fiducial landmarks, either in image space or physical space. The FRE is the resulting root-mean-square distance between the fiducial points after registration and is closely correlated to the FLE.[16] The accuracy of the registration is best described by the TRE, which is calculated by computing the distance between the target landmarks not used for the registration in both the scan and patient.[6]

Measurement of the TRE in vivo is challenging; in primary trauma patients, only anatomical landmarks (and occasional foreign bodies) are available as targets. In the clinical setting, Sun et al.[17] verified that the TRE for dental splints was below the 'clinically acceptable' 1.5 mm in the maxillary region using landmarks on the teeth. Since this measurement is performed near the registration centre, it may not be a good indication for the registration accuracy near the orbit. TRE measurement using anatomical landmarks is reported to yield inaccurate results due to the large difference in localization

in imaging and physical space.[5, 18] Eggers et al.[8] performed in vivo measurements of the TRE using screws embedded in a dental splint after automated registration, reporting a mean TRE of 1.20 mm near the dental region, with surgical regions ranging from the tongue base to the orbit. The current study uniquely performed in vivo TRE measurements in the surgical field using pre-existing screws at the infra-orbital rim.

Previous studies performed ex vivo measurements to evaluate dental splint-based registration techniques, reporting accuracies from 0.6 mm to 1.5 mm in the periorbital region, generally positively associated with the distance from the target registration centre.[11, 13, 14, 19-22] In comparison, the currently reported median TRE of 1.53 mm is at the higher end of the spectrum observed in these studies. A key difference is that the current study was performed in vivo, introducing more dynamic variables and sources of error (such as soft tissue interference or time pressure during surgery), while the other studies were ex vivo, conducted in controlled and stable conditions. Consequently, the ex vivo measurements may not be directly applicable to clinical practice.

Potential sources of error in the clinical TRE measurement were the identification of the acquired and target landmarks. In this study, repeated measurements of both the acquired and target landmarks were performed to minimize user variability. The locations of the pre-existing medial and lateral screw heads at the infra-orbital rim were captured by the surgeon three times, resulting in a median distance between the acquired coordinates of 0.54 mm. The medial and lateral screw heads were subsequently indicated in the virtual planning software by two clinical engineers, which resulted in median intra- and inter-rater distances between the target coordinates of 0.08 mm and 0.10 mm, respectively. These distances are in the same order of magnitude as the scan resolution, indicating that the identification of pre-existing screws can be reliably performed in both the image and physical space, making them suitable as additional registration landmarks.

Crucial factors affecting the accuracy of the virtual splint workflow include precise identification of the fiducial landmarks and the correct design and fit of the dental splint. The fiducial landmarks are identified manually in both the image and physical space. The pointer exactly fits in the spherical indentation on the splints, minimizing the FLE in physical space. In the image space, spherical indentations can be identified easily, although manual identification might introduce some variability. The low FRE of 0.52 mm in this study suggests that FLE is also low. Automatic identification of the fiducial landmarks in the image volume could be a further optimization.

The correct design and fit of the splint depend on proper alignment of the dental scans with the CT scan.[5] Dental restorations and a narrow dental span may negatively affect the accuracy of registration.[14] Correct alignment is ensured using IPS CaseDesigner, a virtual surgical planning software application dedicated to orthognathic surgery, which also facilitates the easy creation of a well-fitting dental splint. Implementing cylinders with spherical indentations in the software would further simplify this workflow. The virtual design of the splint must subsequently be 3D-printed; the in-house printer used has a resolution of 0.1 mm, and the 3D-printed splints are commonly used for orthognathic surgeries. High accuracy of the 3D printer ensures a perfect fit on the maxillary dentition and accurate fiducial landmark indentations.

Studies comparing splint-based registration to invasive fiducial registration techniques have reported higher accuracy for the latter.[11, 23] Splint-based registration centres near the maxilla, decreasing the navigation accuracy for surgical target areas further away,

such as the orbit. In the workflow presented here, care was taken to distribute the cylinders on the splint in a non-planar configuration to achieve clinically acceptable accuracy.[7, 17, 24] Other perceived disadvantages of splint-based registration include the need for specialized skills for splint fabrication, an additional CT scan with the splint in place, and the time delay for splint fabrication.[23] The virtual splint workflow has unique advantages over established techniques: it obviates the need for an additional CT scan, limiting the radiation exposure to the patient. Also dedicated orthognathic surgery software (IPS CaseDesigner) reduces the need for specialized CAD skills, although some virtual planning software knowledge is still required for the navigation. Splint production can be finished within half a day with in-house printing facilities, or a few days if outsourced. These advantages have made the virtual splint workflow the registration method of choice for oral and maxillofacial surgery patients at Amsterdam UMC who have a stable maxilla and a sufficient dentate status.

References

1. Edwards SP. Computer-assisted craniomaxillofacial surgery. Oral Maxillofac Surg Clin North Am. 2010;22(1):117–34.
2. Azarmehr I, Stokbro K, Bell RB, Thygesen T. Surgical Navigation: A Systematic Review of Indications, Treatments, and Outcomes in Oral and Maxillofacial Surgery. J Oral Maxillofac Surg. 2017;75(9):1987–2005.
3. Schreurs R, Klop C, Maal TJJ. Advanced Diagnostics and Three-dimensional Virtual Surgical Planning in Orbital Reconstruction. Atlas Oral Maxillofac Surg Clin North Am. 2021;29(1):79–96.
4. Grunert P, Müller-Forell W, Darabi K, Reisch R, Busert C, Hopf N, et al. Basic principles and clinical applications of neuronavigation and intraoperative computed tomography. Comput Aided Surg. 1998;3(4):166–73.
5. Maurer CR, Jr., Fitzpatrick JM, Wang MY, Galloway RL, Jr., Maciunas RJ, Allen GS. Registration of head volume images using implantable fiducial markers. IEEE Trans Med Imaging. 1997;16(4):447–62.
6. Widmann G, Stoffner R, Bale R. Errors and error management in image-guided craniomaxillofacial surgery. Oral Surg Oral Med Oral Pathol Oral Radiol Endod. 2009;107(5):701–15.
7. Fitzpatrick JM. The role of registration in accurate surgical guidance. Proc Inst Mech Eng H. 2010;224(5):607–22.
8. Eggers G, Kress B, Rohde S, Muhling J. Intraoperative computed tomography and automated registration for image-guided cranial surgery. Dentomaxillofacial Radiology. 2009;38(1):28–33.
9. Eggers G, Mühling J, Marmulla R. Image-to-patient registration techniques in head surgery. Int J Oral Maxillofac Surg. 2006;35(12):1081–95.
10. Marmulla R, Mühling J, Wirtz CR, Hassfeld S. High-resolution laser surface scanning for patient registration in cranial computer-assisted surgery. Minim Invasive Neurosurg. 2004;47(2):72–8.
11. Luebbers HT, Messmer P, Obwegeser JA, Zwahlen RA, Kikinis R, Graetz KW, et al. Comparison of different registration methods for surgical navigation in cranio-maxillofacial surgery. J Craniomaxillofac Surg. 2008;36(2):109–16.
12. Opdenakker Y, Swennen G, Abeloos J. Application of a non-invasive reference headband and a surgical splint for intraoperative paediatric navigation. Int J Oral Maxillofac Surg. 2017;46(3):360–2.
13. Venosta D, Sun Y, Matthews F, Kruse AL, Lanzer M, Gander T, et al. Evaluation of two dental registration-splint techniques for surgical navigation in cranio-maxillofacial surgery. J Craniomaxillofac Surg. 2014;42(5):448–53.
14. Schreurs R, Baan F, Klop C, Dubois L, Beenen LFM, Habets P, et al. Virtual splint registration for electromagnetic and optical navigation in orbital and craniofacial surgery. Sci Rep. 2021;11(1):10406.
15. Swennen GR. 3D virtual treatment planning of orthognathic surgery. 3D virtual treatment planning of orthognathic surgery: a step-by-step approach for orthodontists and surgeons. 2017:217–77.
16. Fitzpatrick JM, editor Fiducial registration error and target registration error are uncorrelated. Medical Imaging 2009: Visualization, Image-Guided Procedures, and Modeling; 2009: SPIE.
17. Sun Y, Luebbers HT, Agbaje JO, Schepers S, Vrielinck L, Lambrichts I, et al. Evaluation of 3 different registration techniques in image-guided bimaxillary surgery. J Craniofac Surg. 2013;24(4):1095–9.
18. Fitzpatrick JM, West JB, Maurer CR, Jr. Predicting error in rigid-body point-based registration. IEEE Trans Med Imaging. 1998;17(5):694–702.
19. Boeckx P, Essig H, Kokemuller H, Tavassol F, Gellrich NC, Swennen GR. Presentation and

Evaluation of a Modified Wax-Bite Dental Splint for Surgical Navigation in Craniomaxillofacial Surgery. J Oral Maxillofac Surg. 2015;73(11):2189–95.
20. Bettschart C, Kruse A, Matthews F, Zemann W, Obwegeser JA, Grätz KW, et al. Point-to-point registration with mandibulo-maxillary splint in open and closed jaw position. Evaluation of registration accuracy for computer-aided surgery of the mandible. J Craniomaxillofac Surg. 2012;40(7):592–8.
21. Eggers G, Senoo H, Kane G, Mühling J. The accuracy of image guided surgery based on cone beam computer tomography image data. Oral Surg Oral Med Oral Pathol Oral Radiol Endod. 2009;107(3):e41–8.
22. Eggers G, Mühling J, Marmulla R. Template-based registration for image-guided maxillofacial surgery. J Oral Maxillofac Surg. 2005;63(9):1330–6.
23. Metzger MC, Rafii A, Holhweg-Majert B, Pham AM, Strong B. Comparison of 4 registration strategies for computer-aided maxillofacial surgery. Otolaryngol Head Neck Surg. 2007;137(1):93–9.
24. West JB, Fitzpatrick JM, Toms SA, Maurer CR, Jr., Maciunas RJ. Fiducial point placement and the accuracy of point-based, rigid body registration. Neurosurgery. 2001;48(4):810–6; discussion 6–7.

Chapter 6

Visualization of real-time navigation

This chapter is based on the following publication:

Sabelis J.F., Maal T.J.J., Bruggink R., van de Steeg G., Becking A.G., Dubois L., & Schreurs R. Optimizing visualization feedback of real-time navigation for orbital reconstructions: A preclinical study. Int j Oral and Maxillofac surg. 2026.

Abstract

Surgical navigation can improve orbital implant positioning, yet current commercial systems are limited by the feedback interpretation and its timing after implant positioning. This study evaluated how different visualization methods impact the efficiency and interpretability of real-time feedback during orbital reconstruction. A standardized in vitro setup was used to simulate orbital reconstructions by six surgeons of varying experience levels. Each surgeon performed implant positioning tasks using six different visualization modes, starting from three predefined misaligned positions. Interpretation accuracy and time to correct implant positioning were recorded. Visualization methods varied in the presence of CT slices, visualization of 3D models, and use of implant-to-target distance visualization (distance mapping). Across a total of 108 reconstructions, no statistically significant differences in positioning time or interpretation accuracy were found between visualization methods. However, surgeon feedback revealed strong preferences: anatomical CT data and additional coronal view at the ledge improved spatial understanding, while views relying solely on 3D models or instrument orientation were seen as less intuitive. Notably, surgeons reported a consistent two-step strategy: initially 3D views were used for initial spatial alignment, followed by 2D slices for precise adjustments. These findings suggest that while performance metrics may not differ across visualization modes, surgeon usability and interpretability are critical for clinical implementation. Future development of a clinically viable navigation workflow should include real-time feedback with both anatomical context and tailored visual support to promote more intuitive navigation in orbital surgery.

Introduction

Computer-assisted surgery (CAS) includes various techniques aimed at improving the workflow and outcomes in orbital reconstruction.[1, 2] Virtual Surgical Planning (VSP) allows simulation of the procedure by mirroring the unaffected orbit to recreate pre-trauma anatomy. A virtual model of a preformed implant can be imported into the planning software to determine the optimal implant and optimal position of the implant.[3] This target position can be transferred to the operating room using surgical navigation. Current commercial systems rely on a tracked navigation pointer to visualize its position in a 3D view and three multiplanar reconstruction (MPR) views. By comparing the pointer's tip movement with the planned implant contour, the surgeon can assess alignment and adjust the implant as needed. Enhancements such as marker-based position tracking or vector tracing have been proposed to improve feedback.[4] These allow the surgeon to define specific landmarks and receive quantitative feedback on the distance of the pointer to the virtual landmark.

Surgical navigation has been shown to improve implant positioning and reduce surgery time.[4-10] However, two major drawbacks remain: the timing of feedback and its interpretation.[11] Navigation feedback is only available after positioning, requiring surgeons to estimate implant movement without real-time guidance. Interpretation of navigation data is not always intuitive and often requires mental integration of 2D MPR view information into a 3D understanding of the implant's position. This increases cognitive load and necessitates repeated trial-and-error adjustments. The constant shift in attention between the surgical field and navigation monitor further complicates the process.[12]

To address these challenges, a real-time navigation workflow was developed and its proof of concept validated in preclinical studies.[11, 13] This approach used a dedicated instrument rigidly attached to the implant and carrying reflective sphere markers enabling continuous position tracking. Initial cadaver studies showed improvements in both positioning accuracy and procedure time. While this study confirmed the benefits of real-time navigation, it also highlighted opportunities to enhance feedback interpretation through alternative visualization methods, which could improve positioning accuracy and reduce procedure time. Real-time navigation feedback can be visualized in numerous ways. The previous approach reduced visual complexity by showing only simplified 3D contours of the target and implant, omitting CT-based anatomical information.[11] In contrast, the clinical standard displays full CT slices and object contours, which offer rich anatomical context but are cognitively demanding. This illustrates a key challenge in navigation feedback design: balancing the need to reduce visual overload with the need to provide clear information for safe and accurate navigation.

Previous research in other surgical and non-surgical contexts has shown that visualization design can significantly affect task accuracy and efficiency.[14] In general, 3D views help users form a quick understanding of spatial relationships, whereas 2D slices allow for more precise, quantitative control.[15] This dual-view approach has proven beneficial in targeting tasks such as iliosacral screw placement, where combining 3D and 2D views optimized performance.[16] Orbital reconstruction involves complex multi-axial adjustments, making precise 2D visualization across three orthogonal planes particularly valuable. To our knowledge, no prior study has systematically evaluated how different real-time visualization methods affect performance in orbital reconstruction. This study addresses that gap by comparing six visualization methods in a controlled in vitro setting. It was hypothesized that the choice of visualization method would significantly

impact both positioning time and interpretation accuracy.

Materials and Methods

Real-time navigation workflow

The technical background of the real-time navigation workflow was described in a previous study.[11] Since then, a preformed implant (KLS Martin, Tuttlingen, Germany) was developed for improved anatomical fit and retention holes were added to enable a connection with the instrument (*Figure 1a*, research prototype, not yet commercially available). The instrument was redesigned to meet clinical standards: it is made of surgical-grade stainless steel, features a more stable coupling mechanism for enhanced stability (*Figure 1b*) and a turning knob for secure fixation and easy release.

A custom sleeve was 3D-printed for the instrument (*Figure 1c*). It allowed attachment of reflective spheres that matched the geometry of the Softouch pointer® (Brainlab AG, Munich, Germany), enabling the system to identify it as such. The sleeve also aligned the instrument tip precisely, eliminating the need for calibration.

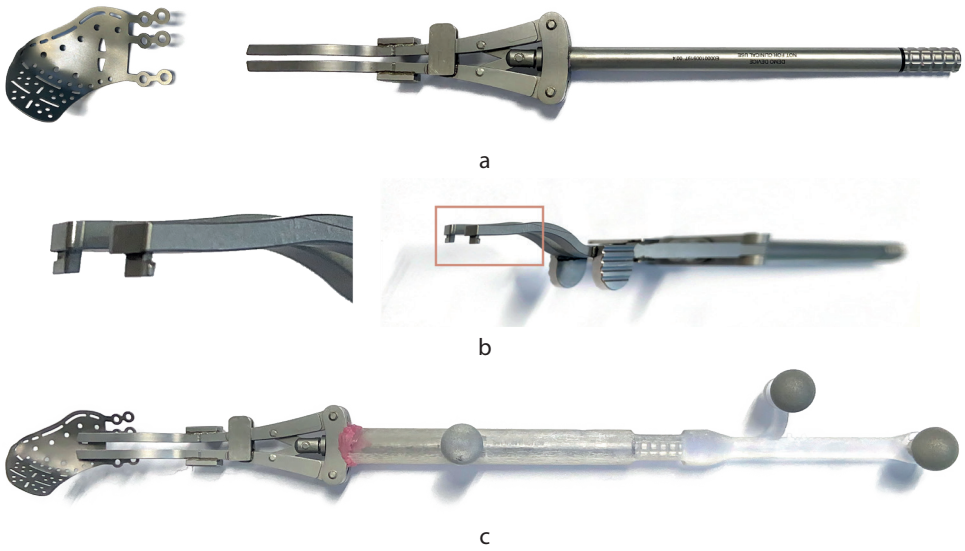


Figure 1. *Experimental instrumentation for navigation. (a) visualizes implant (research prototype) and instrument. (b) depicts a close-up of the connection part of the instrument. (c) illustrates the instrument connected to the implant and the custom-designed sleeve with reflective markers.*

The navigation software was integrated into the 3DMedX® platform (v1.2.34.0, 3D lab Radboudumc, Nijmegen, the Netherlands). Preoperative imaging data, the planned implant and a segmented skull were imported. The implant was aligned to its reference positions using the orbital implant positioning frame.[17] Through IGT Link, tracking data from Brainlab enabled real-time calculation of implant position and orientation.

Table 1. *List of visualization methods compared in this study.*

	3D overview	*Viewer 1-3*		*Figure*
		CT slices	*Objects*	
Method 1	Bone + Implants	Baseline		3a
Method 2	Bone + Implants	Instrument orientation		3b
Method 3	Bone + Implants	Axial -> coronal ledge		3c
Method 4	Bone + Implants		Implants	4a
Method 5	Bone + Implants		Implants + instrument	4b
Method 6	Bone + Implants + Distance map		Implants	5b

3D, three-dimensional; CT, computed tomography.

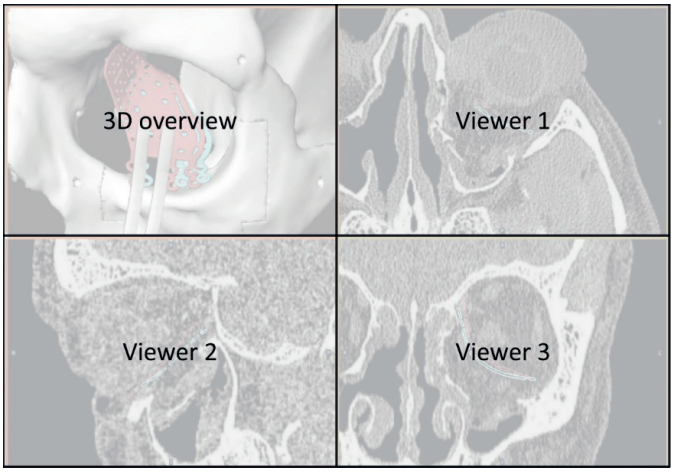
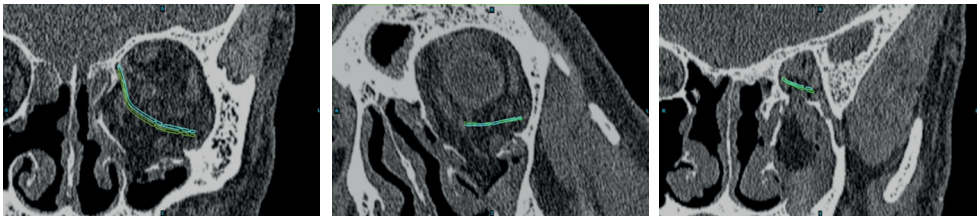


Figure 2. *Illustration of the standard lay-out of the navigation screen: 3D overview, Viewer 1 axial by default, Viewer 2 sagittal by default and Viewer 3 coronal by default.*

Figure 2 shows the navigation interface, based on the Brain commercial navigation system. It includes a 3D overview and three additional viewers (Viewer 1-3). Six visualization methods were created by adjusting display settings (*Table 1*). Methods 1-3 display CT slices. Method 1 replicates the standard coronal, axial and sagittal slices aligned with the patient reference frame (*Figure 3a*). Method 2 reorients these slices along the axis of the instrument (*Figure 3b*). Method 3, keeps patient orientation, but axial view is replaced with an additional coronal slice located at the posterior ledge, which is critical for accurate positioning (*Figure 3c*).



a b c

Figure 3. Visualization of the different options in the CT slice views in Viewer 1-3. (a) Baseline with slices aligned with the patient reference frame. (b) Slices aligned with the axis of the instrument. (c) Additional coronal slice at posterior ledge instead of the axial view.

Methods 4-6 display only 3D in Viewers 1-3. Method 4 shows only the planned and tracked implants (*Figure 4a*). Method 5 adds the instrument model to this setup (*Figure 4b*). Method 6 overlays a real-time, color-coded distance map on the tracked implant model, colors representing distance from the target: red (above), green (within 1 mm) and blue (below) (*Figure 5b*).



a b

Figure 4. *Visualization of the different options in the 3D model based views in Viewer 1-3. (a) Only planned and tracked implant models visible. (b) Instrument visible.*



a b

Figure 5. *Visualization of the different options in the 3D overview. (a) Bone model with planned and tracked implant. (b) Tracked implant is visualized with additional distance-map.*

All six methods include a quantification panel in the right bottom corner. The panel reported implant deviation relative to the plan, including translations (x, y, z) and rotations (roll, pitch, yaw).

Comparative study

The comparative study consisted of three steps; 1) Virtual preparation, 2) Experimental setup and 3) Data acquisition.

Virtual preparation

A 3D model of an orbital defect involving both the floor and medial wall was prepared. Virtual planning was done in the Elements environment (Brainlab AG, Munich, Germany) following clinical protocol.[3] A stereolithography (STL) file of the preformed implant (KLS Martin, Tuttlingen, Germany), was imported and positioned.

Three starting positions deviating from the planned position were defined (*Figure 6*). These simulated realistic surgical scenarios, where navigation feedback must guide correction. The predefined deviations served as ground truth for interpretation accuracy: the first had 6° yaw and 3 mm translation (smallest deviation), the second had 17° pitch and 8 mm translation (mimicking placement below the posterior ledge), and the third had 15° yaw and 19° pitch (largest deviation).

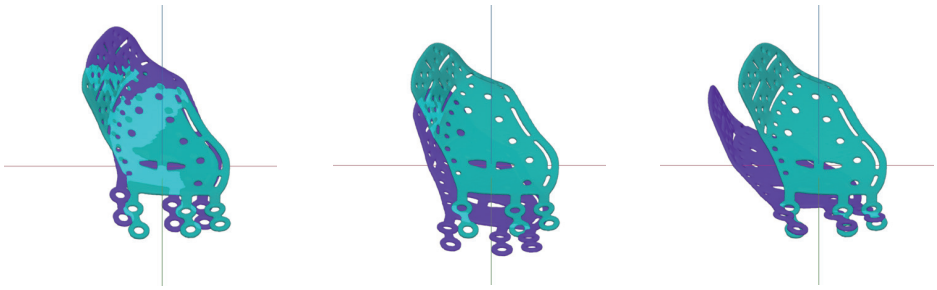


Figure 6. *Visualization of the planned implant (blue) and the three different starting positions (purple): position 1 in (a), position 2 in (b) and position 3 in (c).*

Experimental setup

A hard-tissue skull model was reconstructed from CT data and modified in Blender (version 4.0, Blender Foundation, Amsterdam, the Netherlands) with six indentations for registration. Three holding devices were designed to secure the implant in its starting position. Teeth were replaced with cones to enable fitting of the holding device on the skull (*Figure 7a and 7b*). To simulate in-vivo conditions, the orbit was filled with a sponge to restrict movement and visibility. A reference array was fixed to the skull. The plan was imported into the Kick navigation system (Brainlab AG, Munich, Germany) and registration was performed using the Cranial/ENT pointer. The full test setup is shown in *Figure 7c*.



a b c

Figure 7. *(a) Holding device defining the starting position of the implant. (b) Holding device fitted on the 3D-printed model with the implant on the intended starting position. (c) Test set-up with the instrument attached to the implant and sponge in the orbit. Computer screen visualizes the navigation feedback.*

Data acquisition

Six surgeons with varying experience (two trainees, two starting consultants and two with over 10 years of navigation experience) reconstructed the same orbital defect using six visualization methods, and three starting positions. A total of 108 reconstructions were performed. The order of both starting position and visualization method was randomized.

Before reconstruction, the quantification panel was hidden, and the implant was placed at the fixed starting position as defined by the holding device. Surgeons identified the most deviating degree of freedom (roll, pitch, yaw or translation) based on the screen. Their responses were scored against the known deviation: 0 (correct) or 1 (incorrect), forming the binary interpretation error variable (secondary outcome).

After this task, the quantification panel was revealed, the holding device removed, and the surgeons completed the reconstruction. The primary outcome was reconstruction time, measured from device removal until the implant position was within 1 mm and 2 degrees of the planned position. Surgeon perception of the visualization methods in the dynamic setting was assessed using a questionnaire completed after all reconstructions.

Sample size calculation

An a priori sample size calculation was performed for the primary outcome using a multilevel linear regression framework, accounting for clustering at surgeon level. The effective sample size was calculated using the 'liberal' procedure: $N_{effective}$= m *[1+(n-1)(1-ICC)], where m represents number of clusters (6 surgeons), n the number of observations for each cluster (3 positions * 6 methods = 18), and ICC denotes the intraclass correlation coefficient between the clusters.[18]. Because of the three-level hierarchical structure of the study, ICC was assumed to be 0.15. Based on this calculation, the required effective sample size was 93.

Statistical analysis

Statistical analyses were performed in R, using R studio (version 2023.12.1, RStudio, Inc., Boston, MA, USA).[19] Multilevel linear (primary outcome) and logistic regression (secondary outcomes) assessed the effect of visualization methods, using the 'lme4'-package.[20] The 'lmerTest' package provided approximate p-values.[21] The Model 0 (base) included only visualization methods as fixed effect. Surgeon (Model 1) and position (Model 2) were stepwise added as random effects, and surgeon experience as a fixed effect (Model 3). Models were compared using Aikake Information Criterion (AIC) and the likelihood ratio test (LRT).

Model assumptions were tested. For linear models, residuals were tested for normality (Shapiro-Wilk test), homoscedasticity (residuals vs. fitted plots), and autocorrelation (ACF plots). For the logistic model, residuals were assessed for uniformity and overdispersion using the DHARMa package.[22] If violated, data transformation was applied. Effect size was assessed using marginal and conditional R2 for mixed-effects models, quantifying variance explained by fixed effects alone and by the full model including random effects, respectively.

Results

Six surgeons reconstructed the orbital defect from three positions using the six visualization methods. Of the 108 data points, five were identified as outliers. In one case, the test setup restricted the surgeon, in four other the surgeons stated improvement within the allowed error margin was not possible. *Figure 8* presents a scatterplot of reconstruction time per method. Mean times ranges from 30 seconds (Methods 5) to 36 seconds (Method 4), with an overall mean of 33 seconds.

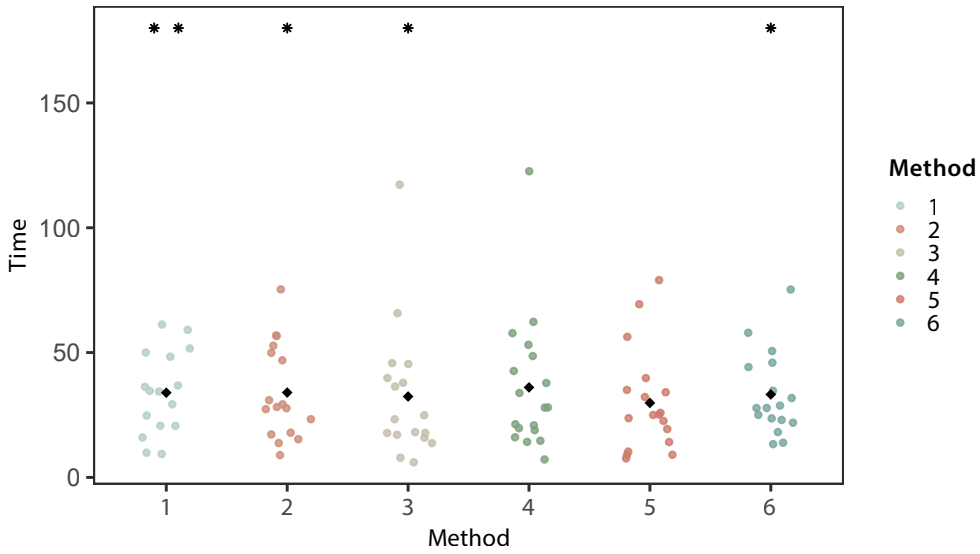


Figure 8. *Scatter plot of the individual reconstruction times, grouped per visualization method. The black diamonds signify the mean per visualization method, black asterisks are the outliers which were excluded from the statistical analysis.*

Time analysis

Diagnostic checks confirmed model validity. A log-transformation of the time variable, ensured normality of the residuals (Shapiro-Wilk test, W = 0.99, p = 0.75), and other model assumptions were met. Model 1, which included the surgeon as a random effect, showed the best fit (AIC: Model 0 = 207.5, Model 1= 203.8, Model 2 = 204.6 and Model 3 = 208.3) and significantly improved fit compared to the base model (p-value = 0.017).

The fixed effect of visualization method did not show statistically significant differences in time required to reach the correct implant position (all p-values>0.05; see *Table 2*). Thus, none of the methods consistently led to faster or slower performance.

Table 2. *Estimates of the effect of different visualization methods on positioning time*

Method	***Estimate (log-seconds)***	***Standard error***	***Confidence interval***	***P-value***
(Intercept)	3.4	0.18	3.1 – 3.8	<0.001
Method 1	Ref.			
Method2	-0.013	0.21	-0.42 – 0.39	0.95
Method 3	-0.17	0.21	-0.58 – 0.24	0.42
Method 4	-0.038	0.21	-0.44 – 0.36	0.85
Method 5	-0.22	0.21	-0.62 – 0.18	0.28
Method 6	0.01	0.21	-0.40 – 0.42	0.96

The random effect for surgeon indicated variability in reconstruction time between individuals, even after accounting for visualization method. The estimated random intercept was 0.061 (standard deviation = 0.25), with residual variance of 0.36. Effect-size analysis indicated that the full model explained 16% of the variance in reconstruction time (conditional R2 = 0.16), visualization method accounted for only 2% (marginal R2 = 0.02).

Interpretation error

A binary logistic mixed-effects model assessed how visualization method influenced interpretation error. There was no overdispersion, and a Kolmogorov-Smirnov test indicated no significant deviation from uniformity (p = 0.63). Model 2, which included surgeon and implant position as random effects, provided the best fit (AIC: Model 0 = 129, Model 1= 128.6, Model 2 = 74.7 and Model 3 = 77.2) and improved fit significantly (p <0.001).

While none of the methods reached statistical significance (all p-values > 0.05) (*Table 3*), Methods 2 and 5 were associated with lower odds of error compared to Method 1 (*Figure 9*). In contrast, Methods 3, 4 and 6 were linked to higher error likelihood (*Figure 9*). Effect-size analysis indicated that visualization method accounted for only a small proportion of variance in interpretation error (marginal R2 = 0.03), whereas the full model including surgeon and starting position explained 92% of the variance (conditional R2 = 0.92). Random effects showed that 23% of variability was attributable to individual surgeons, while 77% was explained by the implant starting position. *Figure 9* highlights Position 1 as the most error-prone.

Table 3. *Estimates of the effect of different visualization methods on interpretation error*

Method	*Estimate (log-odds)*	*Standard error*	*Confidence interval*	*Odds ratio*	*P-value*
(Intercept)	-5.4	4.3	1.1 *10^{-6} - 20	0.0047	0.21
Method 1	Ref.				
Method 2	-1.0	1.5	2.0 *10^{-2} – 6.3	0.35	0.48
Method 3	0.95	1.4	0.17 - 40	2.6	0.50
Method 4	0.95	1.4	0.17 - 40	2.6	0.50
Method 5	-1.0	1.5	2.0 *10^{-2} – 6.3	0.35	0.48
Method 6	1.9	1.5	0.38 - 1.2 *10^{2}	6.6	0.20

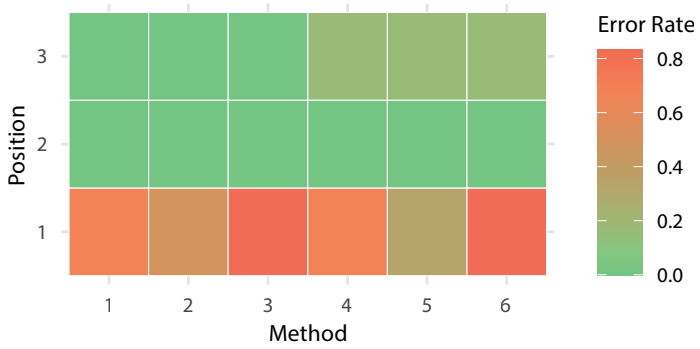


Figure 9. *Heatmap visualizing the error rate across different positions and methods. Green indicates a low error rate and red indicates high error rates.*

Surgeon perception

After completing all reconstructions, surgeons filled out a questionnaire assessing each visualization methods. All surgeons preferred CT slice-based views over 3D model-only views, as it provided anatomical information. Among the CT slice methods, Method 2, which aligned slices along the instrument axes, was perceived as confusing and overly dynamic during instrument movement. All but one surgeon preferred the additional coronal slice (Method 3), as it offered additional feedback on implant positioning at the posterior ledge.

Among the 3D models methods, Method 5, which displayed the instrument, received the lowest scores. Although it offered wider spatial context, the view was zoomed out, making small implant deviations harder to assess. Method 6, featuring the distance map, received mixed responses: some found it helpful for quantifying deviation, while others considered it visually distracting. Interestingly, most surgeons indicated implant positioning occurred in two stages; they relied on the 3D overview for global alignment and switched to the 2D viewers for finetuning.

Discussion

This study evaluated six visualization methods for real-time navigation in orbital implant positioning, focusing on timing, interpretation error, and surgeon perception. Real-time navigation, supported by custom software, provided continuous feedback and motion tracking. It was perceived as a fast and reliable technique to reach the planned implant position. No significant timing differences were found between methods. Surgeon- and position-related variability were modest, indicating similar performance across methods.

The simplified interpretation error parameter was intended as a proxy to assess how visualization methods influenced surgeons' perception of implant deviation in a controlled setting. This parameter captures only part of the dynamic implant positioning performance. Although Methods 2 and 5 showed slightly lower interpretation error values, no statistically significant differences between methods were observed, and results were strongly influenced by starting position. Notably, Position 1, which had the smallest deviation from the planned implant position and representing a clinically common scenario, was associated with higher interpretation errors. This finding likely reflects the perceptual difficulty of detecting subtle deviations.

Questionnaire-based assessments provided complimentary insights into the surgeon perception of the dynamic aspects of implant positioning. Surgeons favored anatomical information provided by CT multiplanar views over 3D model-only views, particularly when including an additional coronal slice at the ledge. Incorporation of a distance map on the tracked implant was polarizing. Some surgeons found it useful for interpreting deviation, while others considered it visually distracting. Most surgeons described a two-phase strategy: using 3D overview for general orientation and switching to CT slices for precise alignment. This supports including both view types in navigation design. These findings align with other surgical fields, where visualization modes significantly affect performance.[15, 16]

Importantly, the discrepancy between objective interpretation error and subjective preference highlights that quantitative performance metrics alone do not fully capture usability in dynamic implant positioning. Methods associated with slightly lower error rates were not necessarily received as advantageous. Together, these findings emphasize that both measures are necessary to comprehensively evaluate visualization methods in orbital reconstruction.

Alternative approaches to reduce cognitive load have been explored. Augmented reality (AR) can overlay navigation data directly in the surgeon's line of sight but faces challenges such as registration errors, depth perception issues, and visual obstruction risks.[23, 24] Tool-mounted displays or smart glasses offer a practical alternative by bringing navigation feedback closer to the surgical field, though current limitations in resolution and sterility hinder adoption.[25] Sonification, converting spatial data into auditory cues, shows promise for linear tasks like pedicle screw insertion, but may be less suited for complex multi-axial tasks like orbital reconstruction.[26] For now, the current separate monitor remains the most reliable and interpretable feedback modality during orbital reconstruction.

A strength of this study was the controlled and standardized in vitro setup. All surgeons reconstructed the same defect from predefined positions, enabling robust comparisons. The use of a real patient model and clinically relevant instruments, helped simulate the surgical procedure. The environment also reproduced common intraope-

rative challenges, such as limited access and obstructed views. Nonetheless, some limitations should be acknowledged. The instrument is a prototype with a 3D-printed sleeve to enable navigation. For clinical application the attachment of the navigation array should be implemented in the design. The test environment remains artificial. The material properties of the 3D-printed skull and sponge may not fully replicate biomechanical or tactile characteristics of in vivo tissue, possibly affecting cognitive and perceptual load. The sample size was modest, and the absence of accuracy data limits direct clinical translation. Randomization of starting positions and methods was used to minimize learning effects. Despite these limitations, the design enabled systematic and objective evaluation of the visualization strategies under controlled conditions.

To advance toward clinical translation, future studies should evaluate the real-time navigation workflow using the selected visualization method and assess its accuracy. Follow-up work could explore whether real-time navigation reduces attention shifts between the surgical field and the navigation screen, potentially improving surgeon focus and efficiency. Complementary research could assess whether phased use of navigation, with 3D views for spatial orientation and 2D slices for fine-tuning, can be objectively demonstrated. Eye-tracking could provide valuable insights into how surgeons interact with the navigation display and manage visual focus during surgery. Ultimately, clinical trials will be essential to determine whether improved visualization with real-time navigation translates into better clinical outcomes.

This study evaluated the impact of six distinct visualization methods for orbital implant positioning using real-time navigation, focusing on the time-efficiency, interpretation error, and surgeon perception. By including surgeons with different experience, the study provides insights into the generalizability and usability of each method. Questionnaire responses reflected surgeon perception, favoring a combination of the CT slice view including an additional coronal slice at the ledge, along with a distance map on the 3D implant overview. These findings support the development of a more intuitive navigation workflow.

References

1. Gellrich NC, Schramm A, Hammer B, Rojas S, Cufi D, Lagrèze W, Schmelzeisen R.. Computer-assisted secondary reconstruction of unilateral posttraumatic orbital deformity. Plast Reconstr Surg 2002;110:1417–29.
2. Scolozzi P. Applications of 3D orbital computer-assisted surgery (CAS). J Stomatol Oral Maxillofac Surg 2017;118:217–23.
3. Schreurs R, Klop C, Maal TJJ. Advanced diagnostics and three-dimensional virtual surgical planning in orbital reconstruction. Atlas Oral Maxillofac Surg Clin North Am 2021;29:79–96.
4. Dubois L, Essig H, Schreurs R, Jansen J, Maal TJ, Gooris PJ, Becking AG. Predictability in orbital reconstruction. A human cadaver study, part III: Implant-oriented navigation for optimized reconstruction. J Craniomaxillofac Surg 2015;43:2050–6.
5. Azarmehr I, Stokbro K, Bell RB, Thygesen T. Surgical navigation: a systematic review of indications, treatments, and outcomes in oral and maxillofacial surgery. J Oral Maxillofac Surg 2017;75:1987–2005.
6. Cai EZ, Koh YP, Hing EC, Low JR, Shen JY, Wong HC, Sundar G, Lim TC. Computer-assisted navigational surgery improves outcomes in orbital reconstructive surgery. J Craniofac Surg 2012;23:1567–73.
7. Parameswaran A, Pandey M, Panneerselvam E, Nisar SP, Bachiavathy V, Mukherjee B. Does intraoperative navigation improve implant position accuracy in orbital fracture repair? Fac Plast Surg Aesthet Med 2024;26:626–30.
8. Dubois L, Essig H, Schreurs R, Jansen J, Maal TJ, Gooris PJ, Becking AG. Predictability in orbital reconstruction. A human cadaver study, part III: Implant-oriented navigation for optimized reconstruction. J Cranio-Maxillofac Surg 2015;43:2050–6.
9. Schreurs R, Becking AG, Jansen J, Dubois L. Advanced concepts of orbital reconstruction: a unique attempt to scientifically evaluate individual techniques in reconstruction of large orbital defects. Atlas Oral Maxillofac Surg Clin North Am 2021;29:151–62.
10. Zimmerer RM, Ellis E, 3rd, Aniceto GS, Schramm A, Wagner ME, Grant MP, Cornelius CP, Stron EB, Rana M, Chye LT, Calle AR, Wilde F, Perez D, Tavassol F, Bittermann G, Mahoney NR, Alamillos MR, Bašić J, Dittmann J, Rasse M, Gellrich NC. A prospective multicenter study to compare the precision of posttraumatic internal orbital reconstruction with standard preformed and individualized orbital implants. J Craniomaxillofac Surg 2016;44:1485–97.
11. Schreurs R, Dubois L, Becking AG, Maal TJJ. Implant-oriented navigation in orbital reconstruction. Part 1: technique and accuracy study. Int J Oral Maxillofac Surg 2018;47:395–402.
12. Matinfar S, Salehi M, Suter D, Seibold M, Dehghani S, Navab N, Wanivenhaus F, Fürnstahl P, Farshad M, Navab N. Sonification as a reliable alternative to conventional visual surgical navigation. Sci Rep 2023;13:5930.
13. Schreurs R, Dubois L, Ho J, Klop C, Beenen LFM, Habets P, Becking AG, Maal TJJ. Implant-oriented navigation in orbital reconstruction part II: preclinical cadaver study. Int J Oral Maxillofac Surg 2020;49:678–85.
14. Tory M, Kirkpatrick AE, Atkins MS, Moller T. Visualization task performance with 2D, 3D, and combination displays. IEEE Trans Visualiz Comput Graphics 2005;12:2–13.
15. Springmeyer RR, Blattner MM, Max NL, editors. A characterization of the scientific data analysis process. IEEE Visualization; 1992.
16. Pandey PU, Guy P, Lefaivre KA, Hodgson AJ. What are the optimal targeting visualizations for performing surgical navigation of iliosacral screws? A user study. Archs Orthop Trauma Surg 2023;143:677–90.
17. Schreurs R, Dubois L, Becking AG, Maal TJ. Quantitative assessment of orbital implant position—a proof of concept. PLoS One 2016;11:e0150162.
18. Twisk JW. Applied multilevel analysis: a practical guide for medical researchers. Cambridge University Press; 2006.

19. R Core Team. R: a language and environment for statistical computing. Vienna, Austria: R Foundation for Statistical Computing; 2025. Available from: https://www.R-project.org/
20. Bates D, Mächler M, Bolker B, Walker S. Fitting linear mixed-effects models using lme4. J Stat Softw. 2015;67(1):1–48.
21. Kuznetsova A, Brockhoff PB, Christensen RHB. lmerTest package: tests in linear mixed effects models. J Stat Softw. 2017;82(13):1-26.
22. Hartig F. DHARMa: Residual diagnostics for hierarchical (multi-level/mixed) regression models. R package version 0.4.7. 2024. Available from: https://cran.r-project.org/web/packages/DHARMa.
23. Carbone M, Piazza R, Condino S. Commercially available head-mounted displays are unsuitable for augmented reality surgical guidance: a call for focused research for surgical applications. Los Angeles: Sage Publications, 2020: 254–5.
24. Choi H, Cho B, Masamune K, Hashizume M, Hong J. An effective visualization technique for depth perception in augmented reality-based surgical navigation. Int J Med Robot Comput Assist Surg 2016;12:62–72.
25. Schütz L, Brendle C, Esteban J, Krieg SM, Eck U, Navab N. Usability of graphical visualizations on a tool-mounted interface for spine surgery. J Imag 2021;7:159.
26. Ziemer T. Three-dimensional sonification as a surgical guidance tool. J Multimodal User Interfaces 2023;17:253–62.

Chapter 7

Preclinical validation of real-time navigation

This chapter is based on the following submmitted manuscript:

Sabelis J.F., Dubois L., Jansen J., Lobé N.H.J., Becking A.G., Maal T.JJ., Schreurs R. Toward Clinical Implementation of real-time navigation workflow for orbital reconstruction – A preclinical study with use of eye-tracking. Int J Oral Maxillofac Surg 2026.

Abstract

Surgical navigation is increasingly used in orbital reconstruction to improve implant positioning. Conventional marker-based navigation provides only feedback after implant positioning and requires surgeons to infer three-dimensional implant alignment from two-dimensional images, potentially increasing cognitive load. To address these limitations, a real-time navigation workflow was developed in which a tracked instrument is rigidly attached to the implant, enabling real-time feedback. This study compared real-time and conventional navigation in a cadaver model and evaluated surgeons' visual behavior using eye-tracking. Two surgeons reconstructed bilateral orbital defects in ten cadaver heads using both methods. Postoperative CT scans were used to quantify implant positioning accuracy in three dimensions (translation, roll, pitch, yaw). Secondary outcomes included total reconstruction time, time viewing the navigation screen, first screen region fixated by the surgeon, and number of focus switches. Linear mixed models were used for statistical analyses. Seventy-eight reconstructions were completed. Real-time navigation achieved positioning accuracy comparable to conventional navigation across all parameters (all $p > 0.05$) and significantly reduced total reconstruction time (4.2 vs. 9.5 minutes, $p < 0.001$), screen time (1.3 vs. 2.0 minutes, $p < 0.001$), and focus switches (15 vs. 29, $p < 0.001$). Eye-tracking revealed consistent first fixation on the 3D view with real-time navigation. Real-time navigation achieves accuracy equivalent to marker-based navigation, while improving time-efficiency and reduce focus switching. These findings support the hypothesis that this workflow improves efficiency and intuitiveness compared to conventional navigation for orbital reconstruction.

Introduction

Surgical navigation has become a viable and valuable tool in orbital reconstruction as it facilitates restoration of orbital volume, positioning of an implant, and reduces revision rates.[1-3] Conventional image-guided navigation systems track a navigation pointer in real time and display the pointer tip position on a navigation screen. The screen shows combined multiplanar views of three orthogonal Computed Tomography (CT) slices at the pointer tip, along with a reconstructed three-dimensional (3D) overview with the pointer tip in its actual position. When the surgeon moves the pointer over the positioned implant, the views update dynamically. This requires the surgeon to infer the implant's alignment based on the pointer's trajectory. To improve intraoperative assessment, object-oriented navigation was introduced, in which navigation rulers and markers are integrated into the implant design. Feedback is provided as the distance between planned and actual marker positions in all 3 dimensions within the reference frame, thereby improving positioning accuracy.[4]

Interpreting these dynamic two-dimensional (2D) images in a 3D context is challenging. Surgeons must be able to translate the visual feedback into corrective rotational and translational movements of the implant. Each adjustment requires retracing the implant with the pointer to reassess its position after each position change. This time-consuming, repetitive feedback loop, combined with the cognitive effort required to interpret the feedback while simultaneously managing the surgical field, may reduce procedural efficiency and positioning accuracy of this approach to surgical navigation.

To overcome these challenges, a real-time navigation workflow for orbital reconstruction was introduced.[5, 6] In this workflow, a dedicated instrument is rigidly attached to the implant and carries reflective sphere markers. It is continuously tracked, providing real-time feedback on the implant position during maneuvering. In a cadaver proof-of-concept study, positional feedback was presented using a simplified 3D visualization alongside the 2D contours of the planned and current implant. The underlying anatomical context of the orthogonal multiplanar reconstructed CT slices was not displayed. This approach demonstrated a promising reduction in positioning time and improved accuracy.

Building on these results, a subsequent in vitro study evaluated multiple visualization strategies to identify the most effective method for accurate and intuitive interpretation. No significant differences were observed between the methods in terms of positioning time or interpretation error. Qualitative feedback from the six participating surgeons highlighted the importance of anatomical context. Based on this input, a combined visualization method was recommended, incorporating multiplanar CT slices, with an additional coronal slice aligned to the posterior ledge and a color-coded distance map on the 3D implant model to indicate local deviations.[7]

The present study aims to compare the optimized real-time navigation workflow with the conventional marker-based navigation workflow in a cadaveric setting with positioning accuracy as the primary outcome. Secondary outcome parameters, including reconstruction time, screen time, focus switches, and first fixation, are acquired using surgeon eye-tracking. This will provide further insight into the interpretation process, enabling critical evaluation of the workflow's efficiency. This valorization study represents the final step toward clinical translation of a more intuitive and efficient navigation system for orbital reconstruction.

Materials and Methods

Technical background

The technical background of the real-time navigation workflow has been described previously.[5, 6] A preformed orbital implant design (L1 3D Plate Orbital Floor, 1.5, S, t=0.5, KLS Martin, Tuttlingen, Germany) incorporates attachment holes for a dedicated navigation instrument, which connects to a StarLink Instrument Adapter Array size M (Brainlab AG, Munich, Germany) via an extension (*Figure 1*).

Navigation was performed using a Kick navigation system (Brainlab AG, Munich, Germany), combined with a custom IGT Link containing a predefined transformation matrix. This enabled automatic tracking of the instrument tip without manual calibration.

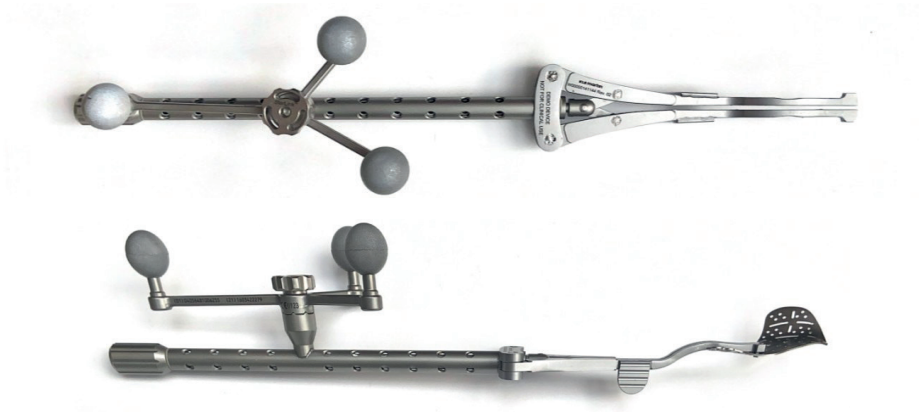


Figure 1. *A dedicated instrument designed to attach to the preformed orbital implant consistently. Built-in extension enables connection with Starlink Instrument Adapter Array size M (Brainlab AG, Munich).*

The navigation system was connected to a workstation running in-house-developed software, 3D MedX® (v1.2.41.1, Radboudumc, Nijmegen, the Netherlands). Based on prior in vitro results, the interface displayed a 3D overview with a color-coded distance map of the tracked implant and three CT slices: one sagittal and two coronal (central and posterior implant regions; *Figure 2*). Surgeons' visual attention during reconstruction was recorded using a mobile eye tracker (Ready Set Go, Pupil Labs, Berlin, Germany).[8]

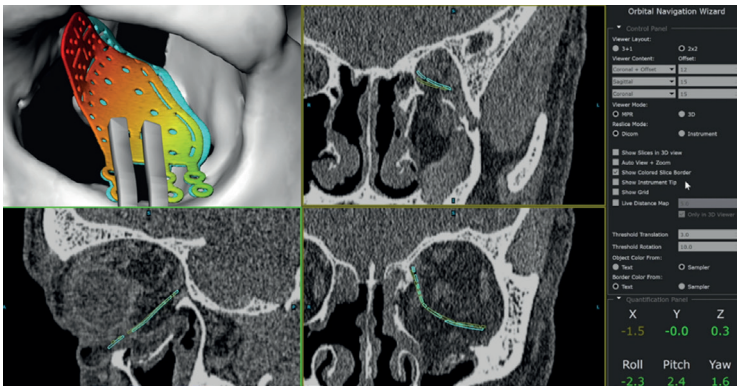


Figure 2. *Illustration of real-time navigation screen. On the right side is a control panel with quantification details. The top left depicts the 3D view with a distance map projected on the tracked implant model, the top right depicts the coronal view at the level of the ledge, the bottom left depicts the sagittal view, and the bottom right illustrates the coronal view at the midpoint of the implant.*

Preparations

Ten human cadaver specimens were obtained from the Department of Medical Biology, Section Clinical Anatomy and Embryology of the Amsterdam UMC. The specimens were fixated in a phenol (0.4% w/v), methanol (1.3% w/v), formaldehyde (4.8% w/v), glycerine (10.3% w/v), ethanol (24.8% w/v) solution in water and preserved in a phenol (0.21% w/v), ethanol (8.3% w/v), glycerol (16.7% w/v) solution in water. Preoperative computed tomography scans (CT_{pre}) were acquired from all specimens using a third-generation dual-source CT scanner (Somatom Force, Siemens Healthineers, Erlangen, Germany; collimation 0.6mm, 150 kV with selective photon shield Sn, scanmode ultra high resolution, 350 mAs, pitch 0.85, FOV diameter 25cm, matrix size 512 x 512, slice thickness 0.6mm bone kernel Ur77).

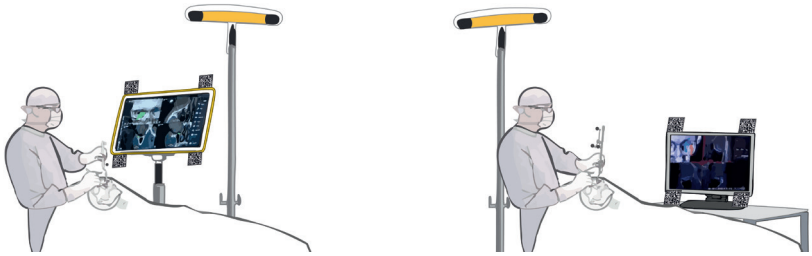
A transconjunctival incision with lateral canthotomy was made to expose the orbital floor and medial wall, after which complex orbital defects (Jaquiéry class III/IV) were created.[9] Five screws were placed for registration (nasion, bilateral maxilla, bilateral temporal bone). A second CT scan (CT_{defect}) was acquired using the same scan protocol as CT_{pre}.

CT_{pre} and CT_{defect} were imported and fused in Brainlab Elements software (Elements, Image Fusion, Brainlab AG, Munich, Germany). The stereolithography (stl) models of the preformed implants were imported and positioned to ensure optimal bony support, while covering the defect and closely following the contour of the unaffected orbit.[10] Virtual surgical plans were generated by a clinical engineer (J.S.), reviewed with both surgeons, and exported to the navigation system and in-house software.

Orbital reconstruction

Reconstructions were performed by two surgeons (L.D. and J.J., with more than 10 and more than 5 years, respectively, of high-volume experience in orbital reconstruction and the use of navigation in orbital reconstruction). They performed two reconstructions per specimen: one using the marker-based navigation workflow (conventional method) and one using the real-time navigation workflow (experimental method). Re-

gistration was performed using the five screw heads. During the conventional method, the infrared camera was positioned at the feet of the specimen, whereas for real-time navigation, it was placed at the head due to array orientation (*Figure 3*).



a b

Figure 3. *Schematic overview of the experimental setup for the (a) conventional workflow and the (a) real-time navigation workflow. Both screens were equipped with the QR codes for the eye-tracking analysis.*

After each reconstruction, a postoperative CT scan (CT_{post}) was acquired using the same scan protocol. Implants were removed afterwards, and screw holes were camouflaged with white PMMA. Surgeons were blinded to the CT reconstruction outcomes until all procedures were completed.

Data acquisition

CT_{post} scans were superimposed on the preoperative plan in Brainlab software. The implant was segmented using threshold-based segmentation (>1000 HU), and the anterior portion which was potentially bent during fixation was excluded. Volume matching on the segmented implant was used to determine the realized implant position. The planned and realized implant models were exported and analyzed using a predefined implant reference frame.[11] In Blender (v4.5.3; Blender Foundation, Amsterdam, the Netherlands), the planned implants were aligned to the reference implant, and the same transformation was applied to the realized implants. Subsequently, the planned implants were matched to the realized implants, and the transformation was used to calculate the positioning accuracy in Euclidean translation (mm) and rotations (roll around x-axis, pitch around y-axis, and yaw around z-axis; degrees).

Secondary outcome parameters were derived from eye-tracking data exported from the Pupil Cloud Environment. Reconstruction start and end times were manually annotated, excluding interruptions such as re-registration. Marker Mapper Analysis, using QR code-like markers on the navigation screen, enabled automatic gaze detection within predefined screen regions. Screen time was calculated by summing gaze durations per region. First fixated regions were identified from time-stamped data, and focus switches were counted manually.

Statistical analysis

Statistical analyses were performed in R (RStudio, version 2023.12.1, Boston, MA, USA).[12] Absolute translation and rotation values (roll, pitch, and yaw) served as dependent variables. Data were transformed when necessary to meet normality assumptions. Linear mixed-effects models were fitted using the 'lme4'-package,[13] with approximate p-values obtained via 'lmerTest'-package.[14] For each outcome, a null model (surgeon as a

fixed effect, orbit as a random intercept) was compared with a method model that included surgical method as an additional fixed effect. Models were estimated using restricted maximum likelihood (REML) with Satterthwaite degrees of freedom and compared using maximum likelihood refitting. Effect estimates with 95% confidence intervals were back-transformed for interpretation.

Results

Positioning accuracy

Due to iatrogenic damage in one orbit, two orbital reconstructions could not be completed, resulting in a total of 78 reconstructions. The distribution of translation, roll, pitch, and yaw is shown in *Figure 4*. The distributions of roll, pitch, and yaw deviated significantly from normality (Shapiro-Wilk: p = 4.8*10-5, 6.6*10-4, and 1.8*10-5, respectively) and were left-skewed as expected due to the use of absolute values. For consistency, a square-root transformation was applied to all parameters, after which the normality assumption was met for all outcomes (Shapiro-Wilk test: p = 0.79, 0.64, 0.079, 0.073, respectively). *Figure 5* shows the box plots of the square-root-transformed variables for each navigation method.

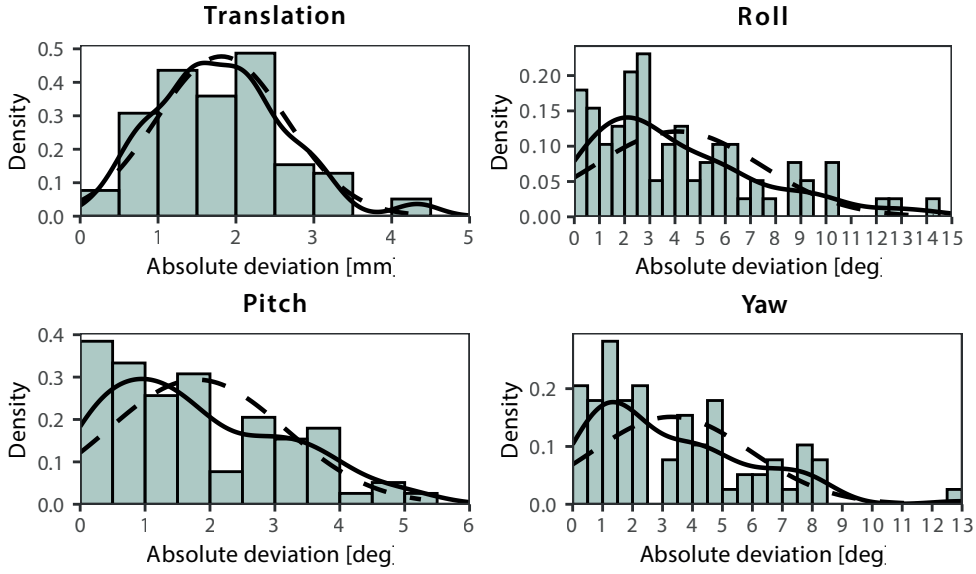


Figure 4. *Distribution of translation, roll, pitch, and yaw outcomes. Histograms are normalized. Density estimation is shown as a solid line. Normal distribution is visualized as a dashed line.*

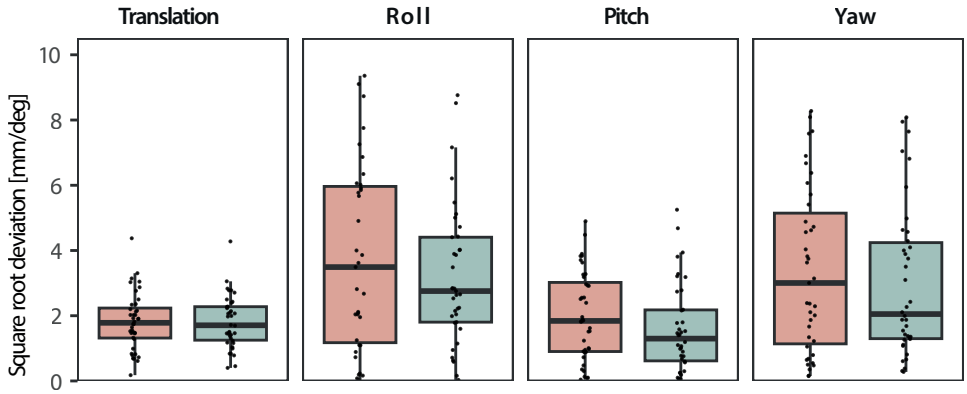


Figure 5. *Implant positioning accuracies by method across four parameters: translation, roll, pitch, and yaw. Boxplots display the distribution of accuracies for the conventional (pink) and real-time navigation (blue). Individual dots represent data points for each observation.*

Addition of the method as a fixed variable did not significantly improve the model, based on the p-values of the Likelihood Ratio Tests (translation: $\chi^2(1)=0.05$, p=0.82; roll: $\chi^2(1)=1.36$, p=0.24; pitch: $\chi^2(1)=1.94$, p=0.16; yaw: $\chi^2(1)=0.71$, p=0.40). The square-root-scale-estimates from the linear mixed model, along with the back-transformed intercept values, standard error, and 95% confidence intervals from both techniques, are provided in *Table 1*.

Table 1. *Linear mixed model estimates for the effect of navigation technique on the positioning accuracy (square root from model and back-transformed value). P-values of the Likelihood Ratio Tests comparing the null model to the method model are provided.*

	Model						*Back-transformation*						*P-value*
	Conventional (n=40)			Experimental (n=38)			Conventional (n=40)			Experimental (n=38)			
	Est.	SE	95% CI	Est.	SE	95% CI	Est.	SE	95% CI	Est.	SE	95% CI	
Trans.	1.3	0.067	1.2-1.4	1.3	0.058	1.2-1.4	1.6 mm	0.17	1.3-2.0	1.7 mm	0.15	1.4-2.0	0.82
Roll	2.0	0.17	1.6-2.3	1.8	0.17	1.5-2.1	4.0°	0.69	2.7-5.4	3.2°	0.60	2.1-4.4	0.24
Pitch	1.3	0.11	1.1-1.5	1.1	0.12	0.90-1.4	1.7°	0.28	1.2-2.3	1.3°	0.27	0.81-1.9	0.16
Yaw	1.5	0.14	1.2-1.8	1.4	0.16	1.0-1.7	2.3°	0.41	1.5-3.2	1.9°	0.44	1.1-2.9	0.40

Trans., translation; Est., estimate; SE, standard error; CI , Confidence Interval.

Timing analysis

Of 78 reconstructions, 77 time measurements were available; one recording failed. A log-transformation was applied to screen and total reconstruction time, meeting normality assumptions (Shapiro-Wilk 0.25, 0.37, respectively).

A linear mixed model indicated that real-time navigation significantly reduced total reconstruction time compared to the conventional method ($\beta = -0.80$, SE = 0.094, $t(74) = -8.55$, $p < 0.001$), with back-transformed means of 4.2 and 9.5 minutes, respectively. Screen time was also significantly decreased from 2.0 to 1.3 minutes ($\beta = -0.46$, SE = 0.13, $t(58) = -3.54$, $p < 0.001$).

Focus analysis

A linear model of log-transformed focus switches indicated that the real-time navigation workflow significantly reduced the number of switches compared to the conventional method ($\beta = -0.66$, $SE = 0.10$, $t(56) = -3.21$, $p < 0.001$). After back-transforming the estimates to the original scale, the mean number of switches was approximately 29 for the conventional and 15 for the real-time navigation workflow.

The surgeons' initial focus on the navigation screen was also recorded (*Figure 6*). Surgeons most frequently directed their initial focus to the 3D view, with overall notably higher counts in the real-time method compared to the conventional method. After the 3D view, surgeons focused on the MPR views of the CT scan for more detailed views. Heatmaps of the screen, per method and surgeon, are shown in *Figure 7*.

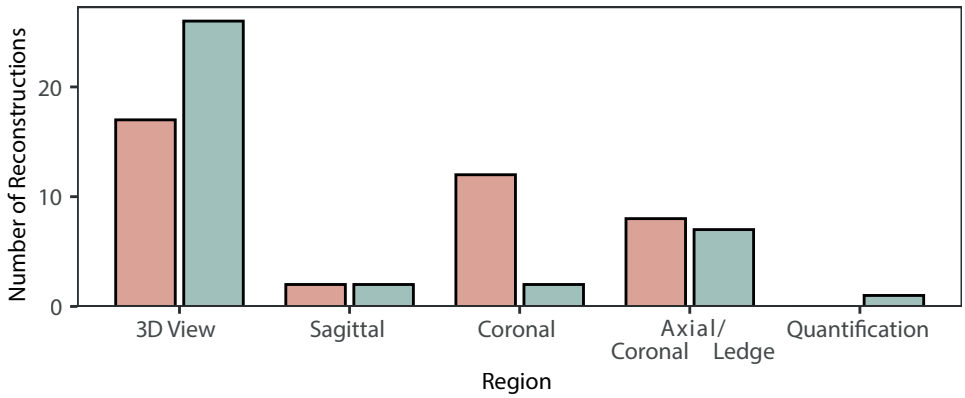


Figure 6. *Initial visual focus during reconstruction across navigation screen regions depicted in a bar chart. Pink bars indicate the conventional method, blue bars the real-time method.*

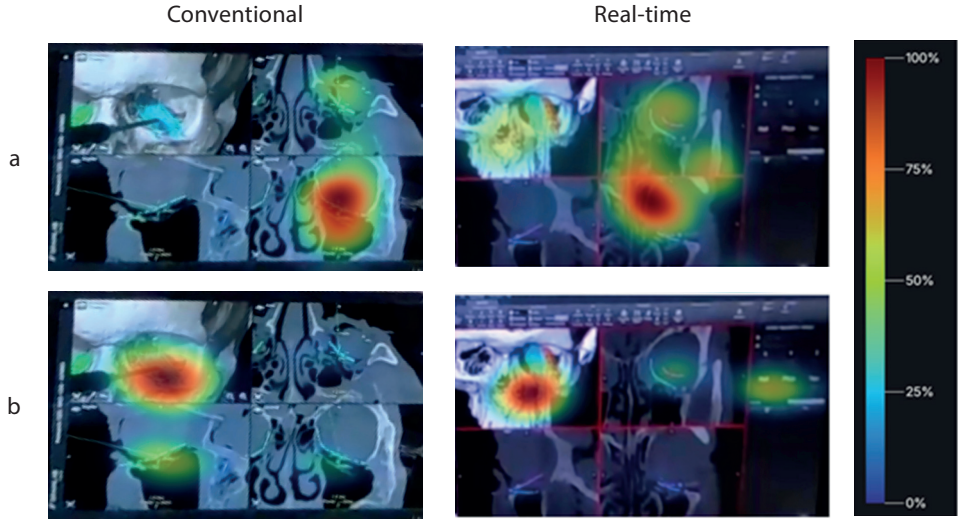


Figure 7. *Heatmap visualizing the surgeons' focus during the complete reconstruction. Heatmaps are created per surgeon (rows A and B) and per navigation method (Conventional and Real-time columns).*

Discussion

This study compared real-time navigation with conventional marker-based navigation for orbital reconstructions in a cadaver setting. Positioning accuracy with real-time navigation was comparable to the conventional method. Total reconstruction time was reduced, and fewer eye-tracking shifts between the surgical field and the navigation screen were recorded. This highlights that real-time navigation offers robust positioning accuracy while improving time-efficiency and reducing focus switches, which may reflect reduced cognitive demands.

The present preclinical validation study was designed to expand upon previous proof-of-concept studies on real-time navigation.[5, 6] Cadaver setup, registration workflow, and number of reconstructions were matched to allow direct comparison. Procedural updates included an advanced instrument prototype, a modified implant design, and updated visualization software. Contrary to previous studies, statistically significant differences in positioning accuracy were not observed. Differences between current and prior studies were minor (<1 mm or <1°), demonstrating consistency across iterations. The new implant geometry, optimized for average orbital anatomy, may have facilitated more consistent implant seating, reducing the relative benefit of real-time navigation. The absence of statistical significance could therefore reflect genuine convergence in performance, rather than a lack of technical improvement.

Overall, real-time navigation achieved 1.7 mm translational accuracy, with rotational deviations of 3.2° (roll), 1.3° (pitch), and 1.9° (yaw). This accuracy is comparable to previously reported object-oriented navigation techniques,4 and within the same order of magnitude as the reported bone-anchored registration accuracy (~1mm).[15, 16] Residual deviations may therefore reflect a combination of registration uncertainty and human factors during implant positioning, suggesting further improvements may increasingly be constrained by the registration method rather than the navigation workflow itself. Real-time navigation also significantly reduced total reconstruction time. Apart from the time and cost benefits, shorter reconstructions may require less manipulation of

orbital tissues, thereby potentially decreasing iatrogenic trauma and improving patient safety and postoperative outcomes.[17, 18] These findings highlight that real-time navigation offers meaningful workflow advantages while maintaining robust positioning accuracy.

The addition of eye-tracking provided unique insights into the surgeon's interaction with the navigation system. Previous studies reported initial reliance on the 3D view for implant positioning, with 2D slices for fine adjustments.[19, 20] The majority of reconstructions in the present study began with an initial focus on the 3D view, consistent with prior observations. Inter-surgeon differences were observed in screen coverage, but notably, the frequency of focus switches between the surgical field and the navigation screen was significantly reduced with real-time navigation. This suggests a more intuitive interface and lower cognitive load, further enhancing efficiency.

These results should be interpreted in the context of the cadaver setup, which enabled systematic evaluation but introduced inherent limitations. (Peri-) Orbital soft-tissue in a cadaver specimen is firmer than in vivo, requiring greater force to position the implant. Instrument handling could not be evaluated under realistic surgical conditions. Positioning accuracy represents only one aspect of surgical outcome.[18] Clinical parameters such as diplopia and hypoglobus can, off course, not be assessed pre- or postoperatively in a cadaver setting.

The results offer promising prospects for clinical translation. The real-time navigation workflow performed consistently with prior reports. Although minor instrument refinements remain necessary to improve handling and the software's integration into a certified surgical navigation environment, the workflow appears mature for clinical evaluation. Future studies should assess its effectiveness under surgical conditions and in larger patient cohorts, focusing on benefits beyond positioning accuracy, including efficiency and clinical outcomes.

The instrument is currently only compatible with one specific implant due to its connection mechanism and predefined transformation in the specific software. Extending real-time navigation to other implants will therefore require adaptations in (patient-specific) implant design, as well as in navigation software support to ensure that the correct transformation and implant contours are displayed.

Advanced visualization technologies may further enhance this workflow. Integration of extended reality (XR) means overlaying the implant position directly in the surgeon's field of view. This potentially reduces the number of switchovers in focus for surgeons. When XR glasses are used as a standalone navigation modality, the accuracy varies widely (1.3-6.0 mm for pedicle screw placement).[21] If XR was linked to conventional surgical navigation systems in a porcine model, more accuracy (~1 mm) was demonstrated.[22] XR use may be limited by potential occlusion of the surgical field and ergonomic constraints of head-mounted displays.[23] The added clinical value of such hybrid approaches should be carefully evaluated before clinical adoption.

The concept of tracking an instrument rigidly coupled to the object of interest provides a general-purpose solution for surgical tasks that require accurate, real-time knowledge of the object's pose relative to patient anatomy. The concept is applicable across multiple surgical domains, including orthopedic procedures such as joint arthroplasty and musculoskeletal tumor resections, where accurate spatial alignment of patient-specific cutting guides and/or implants is required to transfer the virtual plan to the OR table. In spine and neurosurgery, the same underlying requirement for precise pose control

governs tasks such as implant insertion and trajectory-controlled drilling. In addition, real-time direct tracking of the instrument-object system may provide a foundation for closed-loop guidance and control, facilitating future integration with robotic-assisted and semi-autonomous surgical platforms.

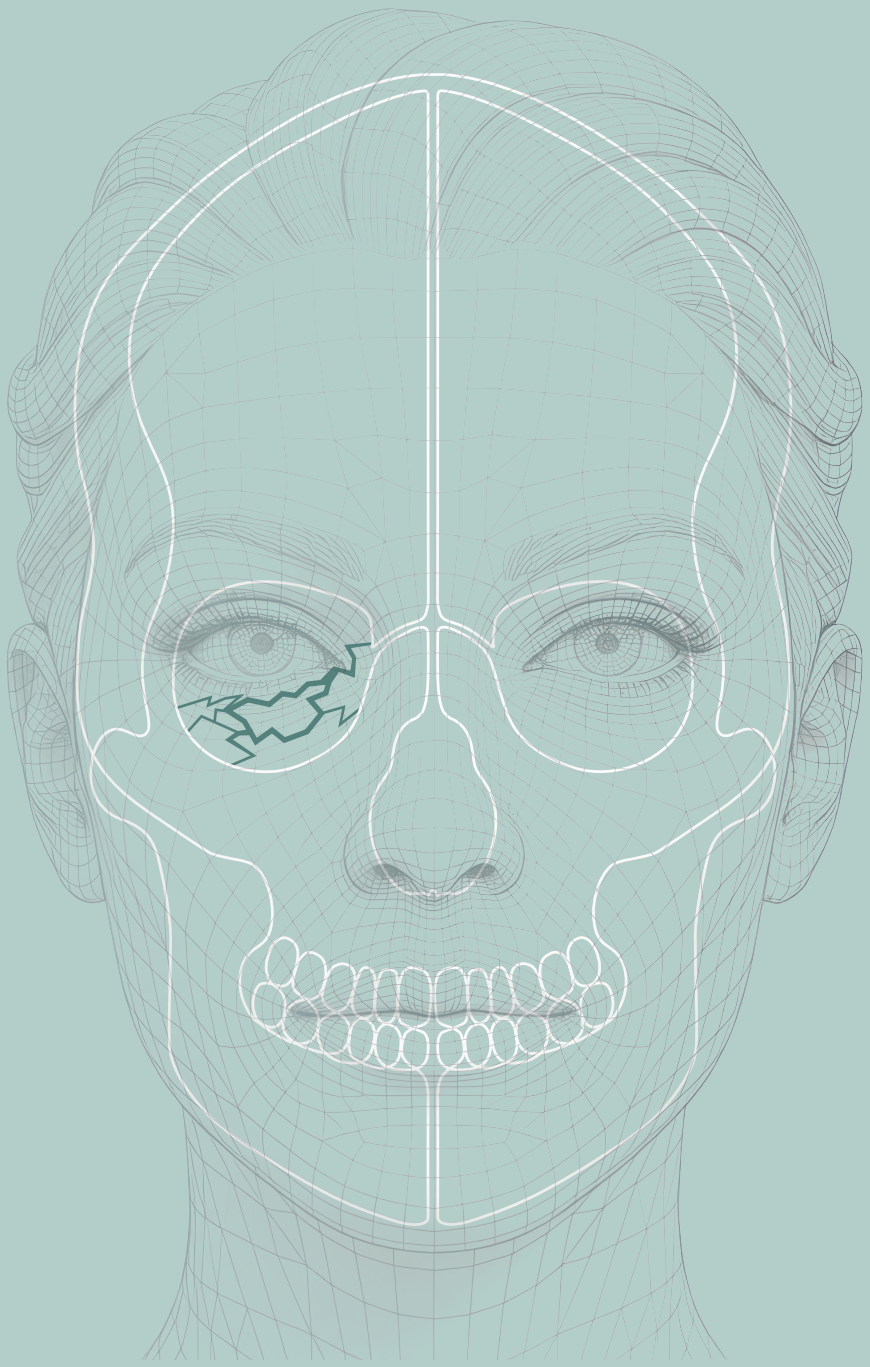
In conclusion, real-time navigation for orbital reconstruction achieves equal positioning accuracy to marker-based navigation while improving intraoperative efficiency, including reduced time and cognitive load. The consistent positioning accuracy observed across iterations indicates stable system performance. Minor instrument refinements and integration into a certified software environment are key steps toward clinical valorization. These findings provide a strong rationale for clinical studies to confirm that preclinical workflow improvements translate into real surgical practice.

References

1. Verbist M, Dubron K, Bila M, Jacobs R, Shaheen E, Willaert R. Accuracy of surgical navigation for patient-specific reconstructions of orbital fractures: A systematic review and meta-analysis. Journal of Stomatology, Oral and Maxillofacial Surgery. 2024;125(3):101683.
2. Cai EZ, Koh YP, Hing EC, Low JR, Shen JY, Wong HC, et al. Computer-assisted navigational surgery improves outcomes in orbital reconstructive surgery. J Craniofac Surg. 2012;23(5):1567–73.
3. De Cuyper B, Abeloos J, Swennen G, Pottel L. Intraoperative Navigation and Cone Beam Computed Tomography for Restoring Orbital Dimensions: A Single-Center Experience. Craniomaxillofacial Trauma & Reconstruction. 2020;13(2):84–92.
4. Dubois L, Essig H, Schreurs R, Jansen J, Maal TJ, Gooris PJ, et al. Predictability in orbital reconstruction. A human cadaver study, part III: Implant-oriented navigation for optimized reconstruction. J Craniomaxillofac Surg. 2015;43(10):2050–6.
5. Schreurs R, Dubois L, Becking AG, Maal TJJ. Implant-oriented navigation in orbital reconstruction. Part 1: technique and accuracy study. Int J Oral Maxillofac Surg. 2018;47(3):395–402.
6. Schreurs R, Dubois L, Ho J, Klop C, Beenen LFM, Habets P, et al. Implant-oriented navigation in orbital reconstruction part II: preclinical cadaver study. Int J Oral Maxillofac Surg. 2020;49(5):678–85.
7. Sabelis JF, Maal, T.J.J., Bruggink, R., van de Steeg, G., Becking, A.G., Dubois, L., Schreurs, R. Optimizing Visualization Feedback of Real-Time Navigation for Orbital Reconstructions - A Preclinical Study. Int J Oral Maxillofac Surg. 2026. [Accepted with minor revisions].
8. Baumann C, Dierkes K. Neon accuracy test report. Pupil Labs. 2023;10.
9. Jaquiéry C, Aeppli C, Cornelius P, Palmowsky A, Kunz C, Hammer B. Reconstruction of orbital wall defects: critical review of 72 patients. International Journal of Oral and Maxillofacial Surgery. 2007;36(3):193–9.
10. Schreurs R, Klop C, Maal TJJ. Advanced Diagnostics and Three-dimensional Virtual Surgical Planning in Orbital Reconstruction. Atlas Oral Maxillofac Surg Clin North Am. 2021;29(1):79–96.
11. Schreurs R, Dubois L, Becking AG, Maal TJ. Quantitative Assessment of Orbital Implant Position--A Proof of Concept. PLoS One. 2016;11(3):e0150162.
12. R Core Team. R: A language and environment for statistical computing. Vienna, Austria. R Foundation for Statistical Computing. 2025. Available from: https://www.R-project.org/.
13. Bates D, Mächler M, Bolker B, Walker S. Fitting linear mixed-effects models using lme4. J Stat Softw. 2015;67(1):1–48.
14. Kuznetsova A, Brockhoff PB, Christensen RH. lmerTest package: tests in linear mixed effects models. Journal of statistical software. 2017;82(13):1-26.
15. Schreurs R, Baan F, Klop C, Dubois L, Beenen LFM, Habets P, et al. Virtual splint registration for electromagnetic and optical navigation in orbital and craniofacial surgery. Sci Rep. 2021;11(1):10406.
16. Luebbers HT, Messmer P, Obwegeser JA, Zwahlen RA, Kikinis R, Graetz KW, et al. Comparison of different registration methods for surgical navigation in cranio-maxillofacial surgery. J Craniomaxillofac Surg. 2008;36(2):109–16.
17. Andrades P, Hernandez D, Falguera MI, Millan JM, Heredero S, Gutierrez R, et al. Degrees of Tolerance in Post-Traumatic Orbital Volume Correction: The Role of Prefabricated Mesh. Journal of Oral and Maxillofacial Surgery. 2009;67(11):2404–11.
18. Zimmerer RM, Gellrich NC, von Bülow S, Strong EB, Ellis E, 3rd, Wagner MEH, et al. Is there more to the clinical outcome in posttraumatic reconstruction of the inferior and medial orbital walls than accuracy of implant placement and implant surface contouring? A prospective multicenter study to identify predictors of clinical outcome. J Craniomaxillofac Surg. 2018;46(4):578–87.

19. Pandey PU, Guy P, Lefaivre KA, Hodgson AJ. What are the optimal targeting visualizations for performing surgical navigation of iliosacral screws? A user study. Archives of Orthopaedic and Trauma Surgery. 2023;143(2):677–90.
20. Tory M, Kirkpatrick AE, Atkins MS, Moller T. Visualization task performance with 2D, 3D, and combination displays. IEEE transactions on visualization and computer graphics. 2005;12(1):2–13.
21. Youssef S, McDonnell JM, Wilson KV, Turley L, Cunniffe G, Morris S, et al. Accuracy of augmented reality-assisted pedicle screw placement: a systematic review. Eur Spine J. 2024;33(3):974–84.
22. Frisk H, Burström G, Weinzierl J, Westernhagen L, Tranchant F, Edström E, et al. Pedicle Screw Placement Using an Augmented Reality Head-Mounted Display in a Porcine Model. J Vis Exp. 2024(207).
23. Barcali E, Iadanza E, Manetti L, Francia P, Nardi C, Bocchi L. Augmented Reality in Surgery: A Scoping Review. Applied Sciences. 2022;12(14):6890.

Discussion and future perspectives



Chapter 8

General discussion

The complex orbital anatomy and limited surgical access challenge accurate anatomical reconstruction, which has ignited the adoption of computer-assisted surgical (CAS) techniques.[1-3] The overall aim of this thesis was to optimize and clinically translate a personalized CAS workflow for orbital reconstruction. Two subgoals guided this aim. The first subgoal was to critically define and evaluate a personalized CAS workflow for orbital reconstruction. The personalized workflow introduces variability that extends beyond patient-specific factors, with both surgeons and engineers influencing workflow decisions and implant design. Ensuring that the treatment strategy is based on patient-specific anatomy and pathology requires critical selection criteria and careful outcome evaluation.

The second subgoal was to facilitate clinical translation of emerging technologies within the CAS workflow. The results underline that technological innovation alone is insufficient for clinical application. Careful methodological validation, combined with attention to usability, accuracy, and regulatory constraints, is essential to ensure effective translation. The virtual splint registration and real-time navigation workflows were validated in this thesis, supporting their broader clinical implementation.

Personalizing computer-assisted care

CAS can be conceptualized as a modular toolbox, in which various techniques can be selected and combined according to the specific requirements of each case (**Chapter 2**). Some components, such as implant selection during the virtual surgical planning (VSP), are indispensable to determine the course of treatment and achieve predictable outcomes in all cases.[4] The cumulative use of advanced CAS components increases training requirements, manpower demands, and procedural costs. Techniques with a high burden in these respects, such as surgical navigation and PSIs, are therefore most justified in complex cases requiring high precision.[5, 6] This modularity allows the workflow to be individually tailored to the complexity and requirements of the case, without compromising the overall procedural framework.

Personalization refers to the adaptation of the treatment strategy to the specific needs of the individual patient. It becomes relevant once a standardized approach is insufficient to meet these patient-specific requirements. CAS provides the technical toolbox that makes this adaptation achievable in practice. Anatomical variation and case complexity naturally determine which CAS tools are needed to achieve this. Beyond this, several practical factors determine whether this personalization can be realized. At the surgeon level, experience and familiarity with specific technologies influence workflow choices. At the institutional level, resources such as access to engineering support, research funding, software, and hardware infrastructure affect what is practically feasible. Healthcare system characteristics, including reimbursement policies, regulatory frameworks, and research grants, further shape the use of specific techniques across countries, with PSI adoption serving as an example of this.[7, 8] Institutional and healthcare system levels are relatively fixed constraints, leaving the surgeon as the most actionable target for improving workflow standardization. Exposure of trainees to CAS techniques during residency can help to standardize familiarity across centers and promote more uniform adoption nationally and internationally. This enables surgeons to make informed, case-specific decisions about the minimum set of CAS tools required for personalized care. When appropriate, complex cases can be referred to specialized centers capable of utilizing the full CAS toolbox.

Ultimately, personalization to the individual patient should remain the predominant determinant of workflow decisions, yet in practice, this remains difficult to achieve. Variation in CAS strategies makes it difficult to identify which components are truly required for a given patient. Most studies assess complete workflows rather than isolating the contribution of individual components, limiting the ability to determine the necessary tools for different case complexities systematically.[1, 9, 10] The Advanced Concepts of Orbital Reconstruction (ACOR) research program partially addressed this knowledge gap by evaluating the effect of specific workflow elements on implant positioning and surgical time in a cadaver setting.[11] This evaluation focused on class III and IV defects,[12] the most extensive orbital floor and wall defects, leaving the optimal workflow for less complex scenarios undefined. Building on these insights, the challenge is to establish evidence-based criteria that guide the selective application of CAS components. Such criteria should streamline the workflow, maximize clinical benefit, and reduce unnecessary complexity, while preserving the advantages of personalization.

Patient-Specific Implants: power, pitfalls, and performance

PSIs have expanded the technical possibilities of orbital reconstruction by offering exceptional design freedom. Advances in additive manufacturing enable the production of extremely thin (0.3 millimeters) yet rigid titanium implants that can be precisely tailored to fit the complex orbital anatomy.[13, 14] Design features such as support on the posterior ledge, infraorbital rim extension, and incorporation of pre-existing screw holes provide reliable positional guidance and ensure stable positioning.[15-18] In some cases, this precise positional guidance may reduce or even eliminate the need for surgical navigation.[19] Multiple PSIs with interlocking features may be designed to restore orbital shape, even when four walls require reconstruction.[20-22] As illustrated in **Chapter 3**, such complex defects cannot be addressed adequately with conventional implants, making PSIs the only feasible option for precise anatomical reconstruction.

Even years after clinical introduction, PSIs continue to be associated with the same practical limitations that hampered initial widespread adoption.[6, 9, 23, 24] Manufacturing costs are substantially higher than those of conventional implants, lead times are still long, and coordination between surgeon and manufacturer remains complex.[8, 25] Lead times and coordination demands can be partially mitigated through experienced collaboration among surgeon, engineer, and manufacturer (**Chapter 4**), although costs and logistical complexity remain significant considerations. These constraints partly affect the indications for PSI use and limit their routine application in primary trauma cases, while secondary cases provide the planning time required to fully exploit PSI capabilities.

Substantial variability exists in PSI design philosophies.[26, 27] While general principles such as adequate bony support and precise fit for positioning are widely accepted, there is no consensus regarding specific design features, and surgeon-specific preferences influence design decisions (**Chapter 2**). Volume overcorrection illustrates this well: some surgeons incorporate deliberate overcorrection to account for postoperative soft tissue fibrosis,[13, 15] others apply spacers intraoperatively to achieve volume compensation,[18, 28] and still others maintain anatomical volume as defined by the mirrored contralateral orbit as much as possible.[10, 29] Variability is further amplified by the iterative and manual nature of PSI design. Because a PSI is designed for a single patient, direct comparisons between alternative designs for the same defect had not been reported.

Chapter 4 addressed this gap by generating multiple PSI designs for identical virtual cases and quantitatively comparing them using a novel difference score based on preformed implant-fit comparisons.[30, 31] The results demonstrated that both the surgeon and the engineer significantly influence the final design, highlighting that a PSI is shaped by factors beyond the individual patient's anatomy and pathology. The impact of these design differences on clinical outcomes remains to be evaluated.

The performance of PSIs must therefore be interpreted within the context of this design variability. The same design freedom that enables precise personalization also challenges standardization and reproducibility. This flexibility complicates the generation of high-level evidence, as randomized controlled trials are difficult to conduct in the presence of confounding factors such as surgeon preference, indication, case selection, implant geometry, and surgical technique. This inability to systematically evaluate PSI design is reflected in the limited advancement of design recommendations, with a recent study largely reaffirming guidelines published almost ten years earlier.[14, 18] Within the personalized CAS workflow, PSIs exemplify how expanded technical possibilities must be balanced with critical selection and outcome evaluation to ensure that personalization remains patient-driven.

Accuracy versus usability: registration and navigation

Surgical navigation is a proven technique to dynamically guide the surgeon in executing the virtual surgical plan.[1, 2, 32-34] Its reliability critically depends on registration, which links the digital plan to the physical patient in the operating room. Any error at this stage propagates through the procedure, affecting subsequent guidance. Achieving accurate registration while maintaining clinical usability is a major challenge. Highly accurate registration methods, such as maxillary bone screws or automatic registration, increase invasiveness, hardware requirements, radiation dose, and logistical complexity.[35, 36] In contrast, simplified approaches such as soft-tissue registration may compromise accuracy and are often not feasible in trauma cases due to swelling.[37] Despite its importance, registration accuracy is not always measured clinically, and when assessed, is rarely evaluated at the surgical site itself. [36, 38-40] Reported accuracy estimations of 1 to 2 mm likely overestimate true surgical accuracy, as accuracy decreases with distance from the registration center.[38, 41] **Chapter 5** introduces a novel accuracy measurement methodology that utilizes pre-existing fixation screws within the area of interest to quantify clinically relevant registration accuracy.

To address the challenge of balancing accuracy with clinical usability, a virtual splint registration method was developed and evaluated in **Chapter 5**. Patient dental scans were fused with preoperative CT scans to generate virtual splints, which were equipped with registration landmarks, 3D-printed, and positioned onto the maxillary dentition during surgery to enable registration. This method avoids additional radiation exposure and the invasive placement of screws. Accuracy in the clinical setting was slightly lower than in preclinical cadaver studies, highlighting the influence of soft tissue, limited exposure, and intraoperative variability.[39] Future developments could further streamline this workflow: integrating registration landmarks directly into splint creation or enabling automatic landmark detection in navigation software could reduce human error and improve reproducibility. This study clinically validated a registration method that is accessible for centers with limited technical expertise, thereby providing a foundation for broader clinical adoption and further refinement of intraoperative registration stra-

tegies.

Surgical navigation bridges VSP and intraoperative execution, providing dynamic feedback on implant placement. Conventional surgical navigation provides intermittent feedback, requiring repeated verification with a tracked pointer and shifts in visual attention between the surgical field and a monitor.[42] While technically accurate, this approach may limit procedural efficiency. To address these limitations, a real-time navigation workflow was developed to provide continuous intraoperative feedback. Initial proof-of-concept work confirmed technical feasibility and laid the foundation for further workflow optimization.[42, 43] Collaboration with industrial partners, KLS Martin and Brainlab AG, enabled the production of a clinically viable instrument prototype, compatible implant, and foundation for feedback visualization.

Optimizing surgical navigation feedback requires a balance between usability and accuracy: reducing information can simplify interpretation, but may omit clinically relevant anatomical details. The proof-of-concept study confirmed technical feasibility but employed a visualization method that differed substantially from conventional navigation, as no CT imaging was displayed. This contrasted evidence highlighting the importance of anatomical information for fine-tuning implant positioning, underscoring the need for an evidence-based approach.[44, 45] **Chapter 6** uniquely addressed this gap by systematically evaluating multiple visualization methods and quantifying their effect on reconstruction time and interpretation accuracy. These methods included: image orientation alignment, supplementary image planes, distance maps, and a reduction in displayed imaging information. Interpretation accuracy was defined in this study as an objective measure of the surgeon's ability to correctly interpret navigation feedback. Although no single method demonstrated a clear objective advantage, surgeon preferences helped inform the final choice. The resulting visualization preserves critical anatomical information, supports intuitive implant positioning, and is grounded in both objective evidence and informed surgeon preference.

Building on the optimal visualization method, the preclinical validation in **Chapter 7** showed that real-time navigation achieved accurate implant positioning and reduced reconstruction time compared to conventional navigation. These results support its technical reliability and potential to improve intraoperative efficiency. A novel methodological aspect of this study was the use of eye-tracking to objectively evaluate surgeons' interaction with the navigation system. This revealed fewer visual attention shifts between the surgical field and navigation display, suggesting lower cognitive load. Eye-tracking provides a versatile tool for further analyses, such as comparing gaze patterns between expert and novice surgeons and temporally correlating visual attention with specific instrument actions. Together, accurate implant positioning and minimized visual attention shifts support clinical implementation of the real-time navigation workflow within certified platforms. Prospective clinical evaluation will enable a full assessment of workflow efficiency, surgeon usability, and patient outcomes.

Translation to clinical care

The development of the real-time navigation workflow illustrates that technical feasibility represents only the first step toward clinical implementation. Translation to clinical care requires objective methodological validation in both preclinical and clinical settings. In this thesis, dedicated study designs were developed to quantify relevant workflow parameters that are often assumed rather than measured: PSI design diffe-

rences (**Chapter 4**), clinically relevant registration accuracy (**Chapter 5**), interpretation of navigation feedback (**Chapter 6**), and visual attention shifts of the surgeon (**Chapter 7**). Each parameter was defined to quantify the clinical benefit or functional contribution of the corresponding technique within the workflow.

The parameters differ in their degrees of objectivity, measurability, and direct relationship to the intended function of the technique. Registration accuracy and visual attention shifts represent directly quantifiable, observer-independent metrics. Registration accuracy was measured using pre-existing fixation screws within the surgical field, thereby enabling a unique evaluation of the total registration accuracy under clinical conditions. Eye-tracking enabled objective quantification of surgeon visual behavior by quantifying visual attention shifts between the surgical field and the navigation display. This transformed a frequently described cognitive phenomenon into measurable parameters.[46] As cognitive load cannot be directly measured in a surgical setting, this metric served as an objective proxy, albeit indirect. Implant design variability required a different approach and was evaluated using a threshold-dependent surface deviation analysis. Although the selected threshold introduced some arbitrariness, this approach directly quantified geometric differences in implant fit and enabled a structured and reproducible comparison. Interpretation accuracy represented the most simplified metric, designed to assess whether surgeons correctly interpreted the visualization feedback without interfering with the experimental setup. Although simplified, it provided insight into perceptual comprehension and complemented subjective surgeon perception data. These measures reflect an attempt to balance methodological rigidity with practical feasibility, acknowledging that not all clinically relevant aspects of surgical workflow can be captured with equal precision.

Apart from methodological validation, clinical translation depends on regulatory and organizational constraints. The academic setting enables exploration of novel concepts through rapid iterations and flexible development. In contrast, industrial partners focus on economic viability, scalability, and regulatory compliance, which may result in de-prioritization of novel concepts that are not aligned with business strategy. Clinical application of novel medical devices requires ethical approval, compliance with the Medical Device Regulation,[47] comprehensive risk analysis, quality management procedures, and ultimately clinical evidence for certification. The real-time navigation workflow combines new hardware and software components developed in collaboration with two industrial partners. This combination substantially increased the complexity of documentation and coordination, thereby slowing the translation of the real-time navigation workflow relative to its technological development. This discrepancy is frequently underestimated in academic research settings, where the trajectory from concept to a certified clinical tool typically takes between three and seven years.[48] With this timeline in mind, study designs were developed to generate objective and reproducible outcome measures compatible with future regulatory and clinical evaluation. Collaboration with industrial partners ensured development within or in parallel with existing certified products, and the workflow was designed to integrate into established surgical practice. This thesis establishes a methodological foundation for clinical translation, although full clinical validation lies beyond its scope.

Future perspectives

Future developments in computer-assisted orbital reconstruction should pursue two complementary directions: ensuring that workflow decisions are guided by patient-specific anatomy and pathology, and translating emerging technologies into validated clinical tools.

Patient-driven computer-assisted workflow

Improving the diagnostic foundation of VSP represents a logical next step toward this goal. Reconstruction for unilateral defects relies on mirrored contralateral anatomy, derived from CT-based segmentation and manual mirroring. These processes may introduce operator-dependent variability. Artificial intelligence (AI)-based segmentation can reduce this variability by automating delineation of orbital anatomy and enabling a more precise definition of the defect outline. Statistical shape modelling can complement this by filling anatomical gaps where mirroring provides limited information, extending the applicability of these methods to bilateral defects.[49, 50] Together, these approaches enable the generation of patient-specific models, including quantification of orbital volume as an additional measure of defect severity. This bony characterization can be complemented by soft-tissue parameters, including extraocular muscle position and morphology, orbital fat distribution, and globe position, which are important determinants of functional outcomes.[51-53] Optimized CT and magnetic resonance imaging protocols could enable quantitative assessment of these characteristics, and provide the diagnostic foundation for soft-tissue-informed VSP.[54, 55] These advances in bony and soft tissue characterization could support a comprehensive, image-derived assessment that can inform all stages of the workflow.

PSI design is central to translating improved diagnostic information into patient-specific reconstruction. Yet, the evidence base guiding design decisions remains limited. Methodological heterogeneity across the literature, including substantial variation in patient populations, implant designs, outcome measures, and follow-up protocols, hampers development of evidence-based guidelines.[9] Future studies would therefore benefit from standardized reporting frameworks defining essential variables: fracture characteristics, implant design parameters, navigation and registration workflows, and structured reporting on accuracy and patient outcome parameters. Establishing multicenter registries with harmonized datasets is necessary for large-scale evaluation of treatment strategies. Such registries should also capture the soft tissue response to reconstruction, which ultimately shapes functional and aesthetic outcomes alongside bony reconstruction. Together this information can support evidence-based refinement of implant design principles. Partial automation of PSI design steps guided by these guidelines could reduce lead times, decrease dependence on engineering support, and minimize case-to-case variability. Experienced clinicians and engineers should always review automated PSI design outputs to ensure anatomical plausibility and optimize intraoperative handling.

Clinical promise of emerging technologies

Artificial intelligence (AI) may function as an enabling technology across multiple phases of the workflow, representing an additional tool within the CAS toolbox. In the diagnostic phase, AI-based segmentation has demonstrated accurate automated delineation of orbital anatomy.[56] In the planning phase, AI-based approaches have demonstrated potential for automated reconstruction of orbital defects.[29, 57, 58] For surgical guidance, AI-based soft-tissue surface registration has demonstrated submillimeter ac-

curacy in preclinical evaluation, outperforming conventional surface registration methods.[59] In trauma cases, however, soft tissue swelling limits facial surface registration, and intraoral scanning may provide a more stable alternative.

The phase-specific applications outlined above reflect a broader tendency to position AI as a solution across all aspects of CAS. This extends even to attempts at automating clinical decision-making, such as determining surgical indication for orbital fractures.[60, 61] Current performance of such applications remains limited, and clinical judgment extends beyond pattern recognition alone. A more realistic contribution lies in AI trained on historical cases and outcomes to support standardized, reproducible diagnostic assessment. Beyond fracture assessment, AI may also reveal patterns linking implant design parameters, surgical techniques, and patient outcomes, informing future refinements of treatment strategies. Realizing this potential requires more than technological development alone. Without a solid foundation of methodologically sound and consistently collected multicenter data, as proposed above, these developments risk remaining isolated advances rather than collectively unlocking the potential to transform the workflow as a whole. This represents a significant organizational and collaborative undertaking. In an ideal scenario, a patient's CT scan and clinical data would serve as input for an AI-driven system that supports standardized defect assessment and provides decision support, for example by proposing reconstruction techniques or flagging cases that deviate from typical patterns, leaving the final indication and treatment decision to the surgeon. Postoperative outcomes would feed back into the model across patients and centers, continuously refining its predictions. No matter how refined the underlying model becomes, it remains blind to what happens between planning and execution. Postoperative outcomes reflect execution accuracy as much as the plan itself, making this the critical link the feedback loop still needs to capture.

Augmented reality (AR) can contribute to accurate surgical execution by projecting the planned implant or instrument within or near the surgical field, potentially reducing attention shifts away from the surgical field. This may in turn reduce cognitive load and decrease the physical footprint and cost of navigation systems. Reported registration accuracies for stand-alone augmented reality systems vary markedly across studies, ranging from 2 to 10 mm,[46, 62, 63] reflecting methodological heterogeneity and a lack of standardized evaluation. Even at the lower end of this range, current systems remain insufficiently accurate for orbital reconstruction. Integration with established navigation platforms, where tracking is handled by the navigation system rather than the headset, may offer a pathway toward improved accuracy and clinical usability.[64, 65] Remaining challenges include overlay stability, co-visualization with patient anatomy, and ergonomic compatibility with surgical headlights or loupes. Consequently, clinical applications in oral and maxillofacial surgery remain limited and are often constrained by insufficiently validated registration techniques and small uncontrolled case series.[46]

Robotic assistance represents another potential extension of surgical guidance. Dental implant robots represent a relevant analogy to orbital reconstruction, ranging from active systems that autonomously execute a planned trajectory to passive haptic systems that constrain instrument movement while leaving execution to the surgeon.[66] Most current systems rely on optical tracking, which is subject to line-of-sight issues, and require patient registration to establish spatial correspondence with the surgical field. Passive haptic systems with mechanical tracking eliminate the line-of-sight issues, though accurate registration still relies on dental splint positioning and alignment of the dentition with the scan. Positioning deviations of approximately 1 mm have been reported for such systems.[67, 68] Translation to orbital reconstruction remains uncertain,

as the confined anatomical space and soft tissues demand considerably smaller instrumentation,[69] and the complex translation and rotation required for implant placement demands highly flexible multi-degree-of-freedom systems. Considering the relatively high positioning accuracy already achievable with navigation, the incremental benefit of robotic assistance may still be modest. At the same time, the associated system complexity, operative footprint, and financial investment may be substantial.[70]

In contrast to these emerging technologies, real-time navigation represents a development that is already preclinically validated, positioning it as the most immediate step toward clinical translation. Prospective clinical studies are needed to compare implant positioning accuracy between real-time navigation and conventional object-oriented navigation. Because both approaches rely on the same patient registration process, which is the principal determinant of navigation accuracy, large differences in absolute positioning between the two approaches are not expected. Nonetheless, clinical evaluation enables assessment of critical workflow metrics, including operative efficiency, surgical time, and surgeon interaction with the navigation system through eye tracking analysis. Fewer visual attention shifts may reflect reduced cognitive load, and continuous real-time feedback may reduce unnecessary implant manipulation, in theory limiting iatrogenic damage, although both hypotheses require prospective clinical evaluation. Most importantly, these future studies might allow correlation of technical performance with patient-relevant outcomes such as restoration of globe position, resolution of diplopia, and quality of life, which ultimately determine the clinical value.

Optimizing computer-assisted orbital reconstruction ultimately requires the iterative integration of comprehensive advanced diagnostics, structured surgical planning, accurate surgical execution, and thorough outcome evaluation. Emerging technologies discussed in this thesis hold promise across these stages. Their broader adoption will require regulatory frameworks and validation standards to evolve in parallel, ensuring that innovation is implemented responsibly and with appropriate clinical oversight. Quantifying the added value of individual techniques within a complex workflow presents distinct methodological challenges, requiring dedicated study designs that isolate and measure parameters that are often assumed rather than systematically evaluated. Even then, technical performance metrics provide important but incomplete reflections of the surgical outcome. The true measure of success lies in patient-relevant outcomes, including restoration of globe position, resolution of diplopia, and quality of life. These must be evaluated systematically and balanced against practical considerations of invasiveness, operative time, and cost. The work presented in this thesis demonstrates that realizing the full potential of computer-assisted orbital reconstruction requires both a workflow that is guided by the patient's anatomy and pathology, and a commitment to rigorous validation that bridges the gap between technical innovation and meaningful clinical benefit.

References

1. Azarmehr I, Stokbro K, Bell RB, Thygesen T. Surgical Navigation: A Systematic Review of Indications, Treatments, and Outcomes in Oral and Maxillofacial Surgery. J Oral Maxillofac Surg. 2017;75(9):1987–2005.
2. Bell RB, Markiewicz MR. Computer-Assisted Planning, Stereolithographic Modeling, and Intraoperative Navigation for Complex Orbital Reconstruction: A Descriptive Study in a Preliminary Cohort. Journal of Oral and Maxillofacial Surgery. 2009;67(12):2559–70.
3. Gellrich N-C, Schramm A, Hammer B, Rojas S, Cufi D, Lagrèze W, et al. Computer-Assisted Secondary Reconstruction of Unilateral Posttraumatic Orbital Deformity. Plastic and Reconstructive Surgery. 2002;110(6):1417–29.
4. Jansen J, Schreurs R, Dubois L, Maal TJJ, Gooris PJJ, Becking AG. The advantages of advanced computer-assisted diagnostics and three-dimensional preoperative planning on implant position in orbital reconstruction. J Craniomaxillofac Surg. 2018;46(4):715–21.
5. Verbist M, Dubron K, Bila M, Jacobs R, Shaheen E, Willaert R. Accuracy of surgical navigation for patient-specific reconstructions of orbital fractures: A systematic review and meta-analysis. Journal of Stomatology, Oral and Maxillofacial Surgery. 2024;125(3):101683.
6. Joachim MV, Farsio F, Markiewicz MR, Miloro M. Patient-Specific Implants in Post-traumatic Orbital Reconstruction: A Systematic Review. Journal of Oral and Maxillofacial Surgery. 2026;84(2):197–213.e4.
7. Allers S, Eijkenaar F, van Raaij EM, Schut FT. Patterns in the influence of funding and reimbursement on the development and implementation of healthcare innovation: A systematic review. Journal of Open Innovation: Technology, Market, and Complexity. 2025;11(1):100490.
8. Goodson AMC, Parmar S, Ganesh S, Zakai D, Shafi A, Wicks C, et al. Printed titanium implants in UK craniomaxillofacial surgery. Part I: access to digital planning and perceived scope for use in common procedures. Br J Oral Maxillofac Surg. 2021;59(3):312–9.
9. Kotecha S, Ferro A, Harrison P, Fan K. Orbital reconstruction: a systematic review and meta-analysis evaluating the role of patient-specific implants. Oral Maxillofac Surg. 2023;27(2):213–26.
10. Zimmerer RM, Ellis E, 3rd, Aniceto GS, Schramm A, Wagner ME, Grant MP, et al. A prospective multicenter study to compare the precision of posttraumatic internal orbital reconstruction with standard preformed and individualized orbital implants. J Craniomaxillofac Surg. 2016;44(9):1485–97.
11. Schreurs R, Becking AG, Jansen J, Dubois L. Advanced Concepts of Orbital Reconstruction: A Unique Attempt to Scientifically Evaluate Individual Techniques in Reconstruction of Large Orbital Defects. Atlas Oral Maxillofac Surg Clin North Am. 2021;29(1):151–62.
12. Jaquiéry C, Aeppli C, Cornelius P, Palmowsky A, Kunz C, Hammer B. Reconstruction of orbital wall defects: critical review of 72 patients. International Journal of Oral and Maxillofacial Surgery. 2007;36(3):193–9.
13. Kärkkäinen M, Wilkman T, Mesimäki K, Snäll J. Primary reconstruction of orbital fractures using patient-specific titanium milled implants: the Helsinki protocol. Br J Oral Maxillofac Surg. 2018;56(9):791–6.
14. Rana M, Chui CHK, Wagner M, Zimmerer R, Rana M, Gellrich N-C. Increasing the Accuracy of Orbital Reconstruction With Selective Laser-Melted Patient-Specific Implants Combined With Intraoperative Navigation. Journal of Oral and Maxillofacial Surgery. 2015;73(6):1113–8.
15. Schreurs R, Klop C, Gooris PJJ, Maal TJJ, Becking AG, Dubois L. Critical appraisal of patient-specific implants for secondary post-traumatic orbital reconstruction. Int J Oral Maxillofac Surg. 2021.
16. Gellrich NC, Dittmann J, Spalthoff S, Jehn P, Tavassol F, Zimmerer R. Current Strategies in Post-traumatic Orbital Reconstruction. J Maxillofac Oral Surg. 2019;18(4):483–9.

17. Zeller AN, Neuhaus MT, Gessler N, Skade S, Korn P, Jehn P, et al. Self-centering second-generation patient-specific functionalized implants for deep orbital reconstruction. J Stomatol Oral Maxillofac Surg. 2021;122(4):372–80.
18. Gellrich NC, Grant M, Matic D, Korn P. Guidelines for Orbital Defect Assessment and Patient-Specific Implant Design: Introducing OA(2) (Orbital Assessment Algorithm). Craniomaxillofac Trauma Reconstr. 2024;17(4):Np298–np318.
19. Probst FA, Cornelius CP, Otto S, Malenova Y, Probst M, Liokatis P, et al. Accuracy of freehand positioned patient specific implants (PSI) in primary reconstruction after inferior and/or medial orbital wall fractures. Comput Biol Med. 2021;137:104791.
20. Hajibandeh J, Be A, Lee C. Custom Interlocking Implants for Primary and Secondary Reconstruction of Large Orbital Floor Defects: Case Series and Description of Workflow. J Oral Maxillofac Surg. 2021;79(12):2539.e1–.e10.
21. Mommaerts MY, Büttner M, Vercruysse H, Jr., Wauters L, Beerens M. Orbital Wall Reconstruction with Two-Piece Puzzle 3D Printed Implants: Technical Note. Craniomaxillofac Trauma Reconstr. 2016;9(1):55–61.
22. Tikkanen J, Mesimäki K, Snäll J. Patient-specific two-piece screwless implant for the reconstruction of a large orbital fracture. Br J Oral Maxillofac Surg. 2020;58(1):112–3.
23. Gander T, Essig H, Metzler P, Lindhorst D, Dubois L, Rücker M, et al. Patient specific implants (PSI) in reconstruction of orbital floor and wall fractures. J Craniomaxillofac Surg. 2015;43(1):126–30.
24. Rana M, Chui CH, Wagner M, Zimmerer R, Rana M, Gellrich NC. Increasing the accuracy of orbital reconstruction with selective laser-melted patient-specific implants combined with intraoperative navigation. J Oral Maxillofac Surg. 2015;73(6):1113–8.
25. Goodson AMC, Parmar S, Ganesh S, Zakai D, Shafi A, Wicks C, et al. Printed titanium implants in UK craniomaxillofacial surgery. Part II: perceived performance (outcomes, logistics, and costs). Br J Oral Maxillofac Surg. 2021;59(3):320–8.
26. Yoon MK, Aakalu VK, Dagi Glass LR, Grob SR, McCulley TJ, Vagefi MR, et al. Orbital Patient-Specific (Customized) Implants: A Report by the American Academy of Ophthalmology. Ophthalmology. 2025;132(8):945–53.
27. Saptarshi VR, Natarajan S, Sudhakar Baviskar P, Arjun Ahuja S, Dinesh Dhirawani A. Does Integration of Technology and Customization of Implants Produce Better Outcomes in Post-Traumatic Orbital Reconstruction? A Systematic Review and Meta-Analysis. J Oral Maxillofac Surg. 2024;82(7):806–19.
28. Spalthoff S, Dittmann J, Zimmerer R, Jehn P, Tavassol F, Gellrich NC. Intraorbital volume augmentation with patient-specific titanium spacers. J Stomatol Oral Maxillofac Surg. 2020;121(2):133–9.
29. Chepurnyi Y, Zhukovtseva O, Kopchak A, Kanura O. Clinical application of automated virtual orbital reconstruction for orbital fracture management with patient-specific implants: A prospective comparative study. Journal of Cranio-Maxillofacial Surgery. 2022;50(9):686–91.
30. Hierl T, Kruber D, Doerfler HM, Huempfner-Hierl H, Krause M. Computer-Aided Versus Conventional Planning in Orbital Traumatology Using Preformed Meshes: Development of a New Workflow. J Oral Maxillofac Surg. 2019;77(8):1663–72.
31. Huempfner-Hierl H, Doerfler HM, Kruber D, Hierl T. Morphologic comparison of preformed orbital meshes. J Oral Maxillofac Surg. 2015;73(6):1119–23.
32. Cai EZ, Koh YP, Hing EC, Low JR, Shen JY, Wong HC, et al. Computer-assisted navigational surgery improves outcomes in orbital reconstructive surgery. J Craniofac Surg. 2012;23(5):1567–73.
33. Consorti G, Betti E, Catarzi L. Customized and Navigated Primary Orbital Fracture Reconstruction: Computerized Operation Neuronavigated Surgery Orbital Recent Trauma (CONSORT) Protocol. J Craniofac Surg. 2022.
34. Dubois L, Schreurs R, Jansen J, Maal TJ, Essig H, Gooris PJ, et al. Predictability in orbital

reconstruction: A human cadaver study. Part II: Navigation-assisted orbital reconstruction. J Craniomaxillofac Surg. 2015;43(10):2042–9.
35. Eggers G, Kress B, Rohde S, Muhling J. Intraoperative computed tomography and automated registration for image-guided cranial surgery. Dentomaxillofacial Radiology. 2009;38(1):28–33.
36. Luebbers HT, Messmer P, Obwegeser JA, Zwahlen RA, Kikinis R, Graetz KW, et al. Comparison of different registration methods for surgical navigation in cranio-maxillofacial surgery. J Craniomaxillofac Surg. 2008;36(2):109–16.
37. Eggers G, Mühling J, Marmulla R. Image-to-patient registration techniques in head surgery. Int J Oral Maxillofac Surg. 2006;35(12):1081–95.
38. Venosta D, Sun Y, Matthews F, Kruse AL, Lanzer M, Gander T, et al. Evaluation of two dental registration-splint techniques for surgical navigation in cranio-maxillofacial surgery. J Craniomaxillofac Surg. 2014;42(5):448–53.
39. Schreurs R, Baan F, Klop C, Dubois L, Beenen LFM, Habets P, et al. Virtual splint registration for electromagnetic and optical navigation in orbital and craniofacial surgery. Sci Rep. 2021;11(1):10406.
40. Boeckx P, Essig H, Kokemuller H, Tavassol F, Gellrich NC, Swennen GR. Presentation and Evaluation of a Modified Wax-Bite Dental Splint for Surgical Navigation in Craniomaxillofacial Surgery. J Oral Maxillofac Surg. 2015;73(11):2189–95.
41. Sun Y, Luebbers HT, Agbaje JO, Schepers S, Vrielinck L, Lambrichts I, et al. Evaluation of 3 different registration techniques in image-guided bimaxillary surgery. J Craniofac Surg. 2013;24(4):1095–9.
42. Schreurs R, Dubois L, Becking AG, Maal TJJ. Implant-oriented navigation in orbital reconstruction. Part 1: technique and accuracy study. Int J Oral Maxillofac Surg. 2018;47(3):395–402.
43. Schreurs R, Dubois L, Ho J, Klop C, Beenen LFM, Habets P, et al. Implant-oriented navigation in orbital reconstruction part II: preclinical cadaver study. Int J Oral Maxillofac Surg. 2020;49(5):678–85.
44. Springmeyer RR, Blattner MM, Max NL, editors. A characterization of the scientific data analysis process. IEEE Visualization; 1992.
45. Pandey PU, Guy P, Lefaivre KA, Hodgson AJ. What are the optimal targeting visualizations for performing surgical navigation of iliosacral screws? A user study. Archives of Orthopaedic and Trauma Surgery. 2023;143(2):677–90.
46. Strong EB, Patel A, Marston AP, Sadegh C, Potts J, Johnston D, et al. Augmented Reality Navigation in Craniomaxillofacial/Head and Neck Surgery. OTO Open. 2025;9(2):e70108.
47. Union EPaCotE. Regulation (EU) 2017/745 of the European Parliament and of the Council on medical devices. Official Journal of the European Union; 2017. p. 1–175.
48. Van Norman GA. Drugs, Devices, and the FDA: Part 2: An Overview of Approval Processes: FDA Approval of Medical Devices. JACC Basic Transl Sci. 2016;1(4):277–87.
49. Gass M, Füßinger MA, Metzger MC, Schwarz S, Bähr JD, Brandenburg L, et al. Virtual reconstruction of orbital floor defects using a statistical shape model. J Anat. 2022;240(2):323–9.
50. Vanslambrouck P, Van Dessel J, Politis C, Willaert R, Bila M, Sun Y, et al. Virtual reconstruction of orbital defects using Gaussian process morphable models. International Journal of Computer Assisted Radiology and Surgery. 2024;19(9):1909–17.
51. Frohwitter G, Wimmer S, Goetz C, Weitz J, Ulbig M, Kortuem KU, et al. Evaluation of a computed-tomography-based assessment scheme in treatment decision-making for isolated orbital floor fractures. Journal of Cranio-Maxillofacial Surgery. 2018;46(9):1550–4.
52. Shah HA, Shipchandler TZ, Sufyan AS, Nunery WR, Lee HBH. Use of fracture size and soft tissue herniation on computed tomography to predict diplopia in isolated orbital floor fractures. American Journal of Otolaryngology. 2013;34(6):695–8.
53. Matic DB, Tse R, Banerjee A, Moore CC. Rounding of the inferior rectus muscle as a predic-

tor of enophthalmos in orbital floor fractures. J Craniofac Surg. 2007;18(1):127–32.
54. Degraeve M, Ninclaus V, Deferm J, Brusselaers N, Jacobs R, Willaert R. A systematic review on volumetric analysis in orbital MRI. Neuroradiology. 2025;67(9):2533–49.
55. Willaert R, Degrieck B, Orhan K, Deferm J, Politis C, Shaheen E, et al. Semi-automatic magnetic resonance imaging based orbital fat volumetry: reliability and correlation with computed tomography. Int J Oral Maxillofac Surg. 2021;50(3):416–22.
56. Morita D, Kawarazaki A, Koimizu J, Tsujiko S, Soufi M, Otake Y, et al. Automatic orbital segmentation using deep learning-based 2D U-net and accuracy evaluation: A retrospective study. Journal of Cranio-Maxillofacial Surgery. 2023;51(10):609–13.
57. Yu F, Liu C, Zhong C, Zeng W, Chen J, Liu W, et al. 3D Deep Learning for Virtual Orbital Defect Reconstruction: A Precise and Automated Approach. Journal of Craniofacial Surgery. 2025;36(6).
58. Xu J, Wei Y, Jiang S, Zhou H, Li Y, Chen X. Intelligent surgical planning for automatic reconstruction of orbital blowout fracture using a prior adversarial generative network. Medical Image Analysis. 2025;99:103332.
59. Yoo H, Sim T. Automated machine learning (AutoML)-based surface registration methodology for image-guided surgical navigation system. Medical Physics. 2022;49(7):4845–60.
60. Gernandt S, Aymon R, Scolozzi P. Assessing the accuracy of artificial intelligence in the diagnosis and management of orbital fractures: Is this the future of surgical decision-making? JPRAS Open. 2024;42:275–83.
61. Czako L, Sufliarsky B, Simko K, Sovis M, Vidova I, Farska J, et al. Exploring the Practical Applications of Artificial Intelligence, Deep Learning, and Machine Learning in Maxillofacial Surgery: A Comprehensive Analysis of Published Works. Bioengineering (Basel). 2024;11(7).
62. Dubron K, Verbist M, Jacobs R, Olszewski R, Shaheen E, Willaert R. Augmented and Virtual Reality for Preoperative Trauma Planning, Focusing on Orbital Reconstructions: A Systematic Review. J Clin Med. 2023;12(16).
63. Benmahdjoub M, van Walsum T, van Twisk P, Wolvius EB. Augmented reality in craniomaxillofacial surgery: added value and proposed recommendations through a systematic review of the literature. International Journal of Oral and Maxillofacial Surgery. 2021;50(7):969–78.
64. Frisk H, Burström G, Weinzierl J, Westernhagen L, Tranchant F, Edström E, et al. Pedicle Screw Placement Using an Augmented Reality Head-Mounted Display in a Porcine Model. J Vis Exp. 2024(207).
65. Meulstee JW, Nijsink J, Schreurs R, Verhamme LM, Xi T, Delye HHK, et al. Toward Holographic-Guided Surgery. Surg Innov. 2019;26(1):86–94.
66. Bahrami R, Pourhajibagher M, Nikparto N, Bahador A. Robot-assisted dental implant surgery procedure: A literature review. J Dent Sci. 2024;19(3):1359–68.
67. Bolding SL, Reebye UN. Accuracy of haptic robotic guidance of dental implant surgery for completely edentulous arches. The Journal of Prosthetic Dentistry. 2022;128(4):639–47.
68. Neugarten JM. Accuracy and Precision of Haptic Robotic-Guided Implant Surgery in a Large Consecutive Series. Int J Oral Maxillofac Implants. 2024;39(1):99–106.
69. Dandoulakis E. Robotic surgery in craniofacial reconstruction: A systematic review of techniques, outcomes, and limitations. World Journal of Advanced Research and Reviews. 2025;27:1522–30.
70. Chatterjee S, Das S, Ganguly K, Mandal D. Advancements in robotic surgery: innovations, challenges and future prospects. J Robot Surg. 2024;18(1):28.
71. Zimmerer RM, Gellrich NC, von Bülow S, Strong EB, Ellis E, 3rd, Wagner MEH, et al. Is there more to the clinical outcome in posttraumatic reconstruction of the inferior and medial orbital walls than accuracy of implant placement and implant surface contouring? A prospective multicenter study to identify predictors of clinical outcome. J Craniomaxillofac Surg. 2018;46(4):578–87.

Appendices

Summaries

Summary

Optimizing computer-assisted orbital reconstruction – From digital design to clinical care

The orbit is a complex three-dimensional bony structure that is highly vulnerable to traumatic impact. Orbital fractures may cause clinically relevant sequelae, including enophthalmos, hypoglobus and diplopia. The primary goal of surgical reconstruction is to restore the pre-traumatized orbital anatomy and recover ocular function. Computer-assisted surgery (CAS) has been increasingly integrated into this workflow to improve the accuracy and predictability. CAS can be conceptualized as a modular toolbox of techniques spanning four phases: advanced diagnostics, virtual surgical planning (VSP), surgical guidance, and postoperative evaluation. The overall aim of this thesis was to optimize and translate a personalized computer-assisted workflow for orbital reconstruction. Two subgoals were defined: evaluating and refining key workflow components, and advancing the clinical translation of novel surgical navigation techniques. In practice, the approach to patient-specific implant (PSI) design can vary considerably, a challenge further explored in the following chapters. The thesis is therefore organized into two parts. Part I focuses on PSI design and part II on surgical navigation.

Chapter 2 provides the conceptual foundation of this thesis by presenting a comprehensive overview of the personalized CAS workflow for post-traumatic orbital reconstruction. Each phase is described in detail, with particular emphasis on PSI design as the pinnacle of both CAS and personalized medicine in this context. PSIs offer several advantages over other implant types, including improved ease of use, a precise and accurate fit, decreased surgery time, and reduced iatrogenic soft-tissue damage during positioning, contributing to a lower revision rate. These benefits come with drawbacks, including cost and manufacturing lead time. Although no strict design guidelines exist, PSI design offers considerable freedom to adapt the implant to a patient's specific anatomy.

Chapter 3 explores the range of possibilities available in PSI design for reconstructing extensive orbital defects involving three or four walls. A single implant is generally limited to a maximum of two walls. Beyond this size, incision access and implant positioning become increasingly difficult. Complete reconstruction of larger defects may therefore require multiple PSIs with interlocking connections. A framework of design strategies is described, including support areas, volume overcorrection, and interlocking connections. Three types of interlocking connections were illustrated: a patrix-matrix connection, implant ridges, and a hook and bar mechanism. All were successfully implemented in clinical practice, offering the designer and surgeon freedom in even the most challenging cases. The final choice can be based on factors such as location and the need for additional support. Their successful application is demonstrated in a four-wall reconstruction case, illustrating the possibilities of a multi-PSI approach with advanced design options.

The same design freedom highlighted in **Chapter 3** also exposes a fundamental limitation of PSI application: the absence of standardized design guidelines. Design variability may arise from factors other than patient anatomy alone, including individual preferences of the surgeon and the training background of the engineer. **Chapter 4** aims to quantify this variability. PSI designs generated by two engineers and two surgeons from different centers were compared for identical patient cases. The PSIs were compared using a novel difference score based on preformed implant-fit comparisons.

The initial design proposals generated by the engineers alone showed a median difference score of 37%, which was reduced to 26% after consultation with the surgeons. The final PSI designs approved by different surgeons showed a median difference of 22%. Specific differences between surgeons included the number and location of screw positions, the presence of a rim extension, and the location of support on the medial wall. Experienced design teams required significantly fewer modifications, fewer meetings, and up to 40% less time. These findings underline that PSI design is influenced by the surgeon and engineer to a degree that warrants development of evidence-based design protocols.

Part II of this thesis shifts to surgical navigation, for which an accurate registration procedure is a prerequisite. **Chapter 5** aims to present and clinically validate a virtual splint registration workflow in ten patients undergoing revision orbital surgery. To this end, a novel methodology is introduced to quantify clinically relevant registration accuracy. A distinguishing feature of this methodology is the use of pre-existing fixation screws within the area of interest as accuracy reference points. Dental scans were fused with preoperative CT data to generate a virtual dental splint, which was equipped with fiducial markers, three-dimensionally printed, and used for intraoperative registration. A median target registration error of 1.5 mm was found at the infraorbital rim. This non-invasive method eliminates the need for repeated preoperative imaging and requires limited computer-aided design expertise, making it accessible for broader clinical implementation. By enabling in-vivo accuracy assessment, this method helps to objectify claims about the accuracy of surgical navigation and registration procedures.

Conventional navigation provides only intermittent positional feedback, requiring the surgeon to repeatedly verify implant position with a tracked pointer and shift visual attention between the surgical field and an external monitor. The feedback itself can also be difficult to interpret. To address these limitations, a real-time navigation workflow was developed in which a dedicated instrument is rigidly attached to the implant, enabling continuous tracking of implant position. Collaboration with industrial partners KLS Martin and Brainlab AG enabled the production of a clinically viable instrument prototype and compatible implant. In **Chapter 6**, six surgeons evaluated six visualization approaches in a standardized in vitro setting, testing several image orientations and visualizations, 3D objects in the overviews, and color-coded distance representation. Position interpretation and positioning time were recorded for each visualization method. No statistically significant differences in positioning time or interpretation accuracy were found between methods. Surgeon feedback consistently favored a combination of CT slice views, including an additional coronal slice at the posterior ledge, with a distance map overlay on the three-dimensional implant model. Surgeons commonly described a two-phase strategy, using the three-dimensional overview for general orientation before switching to CT slices for precise alignment.

Chapter 7 validated the optimized real-time navigation workflow in a cadaveric setting, comparing it with the current clinical navigation standard. Real-time navigation achieved a translational accuracy of 1.7 mm and rotational deviations of 3.2 degrees (roll), 1.3 degrees (pitch), and 1.9 degrees (yaw), and reduced total reconstruction time compared to conventional navigation. Eye-tracking analysis demonstrated fewer visual attention shifts between the surgical field and the navigation display, suggesting reduced cognitive load for the surgeon. This also confirmed the two-phase strategy observed in Chapter 6, with surgeons relying on the three-dimensional view for initial orientation before switching to CT slices for fine adjustments.

The general discussion in **Chapter 8** reflects on the broader implications for personalized CAS in orbital reconstruction. The results demonstrate that personalization extends beyond patient anatomy: both surgeons and engineers shape workflow decisions and implant design. Anatomical variation and case complexity determine which CAS tools are needed, but whether this personalization can be realized in practice depends on additional factors, including surgeon experience, institutional resources such as engineering support and infrastructure, and healthcare system characteristics such as reimbursement policy. Since institutional and system-level factors are relatively fixed, the surgeon remains the most actionable target for improving workflow standardization, for example through structured exposure to CAS techniques during residency. Technical innovation alone is insufficient for clinical adoption. Methodological validation, usability, and compliance with the Medical Device Regulation are equally essential, and the pathway from concept to certified clinical tool typically takes several years. The virtual splint registration and real-time navigation workflows were clinically and preclinically validated respectively, establishing the scientific foundation for implementation.

Future developments should focus on patient-driven workflow decisions. Artificial intelligence-based defect assessment could reduce operator-dependent variability, while standardized reporting frameworks and multicenter registries could support evidence-based refinement of PSI design principles. Augmented reality and robotic assistance hold long-term promise for surgical guidance, though current registration accuracies and instrumentation constraints still limit their clinical application in orbital reconstruction. Real-time navigation, already preclinically validated, represents the most immediate step forward in orbital reconstruction, with prospective studies needed to evaluate operative efficiency and surgeon interaction through eye tracking. Patient-relevant outcomes, including restoration of globe position, resolution of diplopia, and quality of life, remain the ultimate measure of success.

Samenvatting

Optimaliseren van computer-geassisteerde orbitareconstructie – Van digitaal ontwerp naar klinische toepassing

De orbita is een complexe driedimensionale botstructuur die kwetsbaar is voor traumatisch letsel. Orbitafracturen kunnen klinisch relevante gevolgen hebben, waaronder enoftalmos, hypoglobus en diplopie. Het primaire doel van chirurgische reconstructie is het herstel van de pretraumatische orbita anatomie en het herstel van de oogfunctie. Computer-geassisteerde chirurgie (CAS, van het Engelse computer-assisted surgery) is in toenemende mate geïntegreerd in deze workflow om de nauwkeurigheid en voorspelbaarheid te verbeteren. CAS kan worden gezien als een modulaire gereedschapskist van technieken, verdeeld over vier fasen: advanced diagnostics, virtuele chirurgische planning (VSP, van het Engelse virtual surgical planning), chirurgische begeleiding en postoperatieve evaluatie. Het overkoepelende doel van dit proefschrift was het optimaliseren en klinisch vertalen van een gepersonaliseerde, computer-geassisteerde workflow voor orbitareconstructie. Twee subdoelen werden gedefinieerd: het evalueren en verfijnen van de belangrijkste workflow componenten, en het bevorderen van de klinische vertaling van nieuwe chirurgische navigatietechnieken. In de praktijk kan de aanpak van patiënt-specifieke implantaten (PSI)-ontwerp aanzienlijk variëren, een uitdaging die in de volgende hoofdstukken verder wordt uitgewerkt. Het proefschrift is daarom opgedeeld in twee delen: Deel I richt zich op het ontwerp van PSI's en Deel II op chirurgische navigatie.

Hoofdstuk 2 vormt de conceptuele basis van dit proefschrift door een uitgebreid overzicht te bieden van de gepersonaliseerde CAS-workflow voor posttraumatische orbitareconstructie. Elke fase wordt in detail beschreven, met bijzondere aandacht voor het ontwerp van PSI's als het hoogtepunt van zowel CAS als gepersonaliseerde geneeskunde. PSI's bieden verschillende voordelen ten opzichte van andere implantaattypen, waaronder eenvoudiger gebruik, een nauwkeurige en precieze pasvorm, kortere operatietijd en minder iatrogene weke delenschade tijdens plaatsing, wat bijdraagt aan een lager revisiepercentage. Hiertegenover staan de belangrijkste nadelen: hogere kosten en langere productietijd. Hoewel er geen strikte ontwerprichtlijnen bestaan, biedt PSI-ontwerp aanzienlijke vrijheid om het implantaat aan te passen aan de specifieke anatomie van de patiënt.

Hoofdstuk 3 verkent de mogelijkheden binnen het ontwerp van PSI's voor de reconstructie van uitgebreide orbita defecten waarbij drie of vier wanden betrokken zijn. Een enkel implant is doorgaans beperkt tot een maximum van twee wanden. Boven deze grootte worden incisietoegang en het positioneren van het implant steeds lastiger. Voor de reconstructie van grotere defecten zijn daarom vaak meerdere PSI's met onderlinge verbindingen nodig. Een raamwerk van ontwerpstrategieën wordt beschreven, waaronder afsteuning, volume-overcorrectie en verbindingen. Drie typen verbindingen worden geïllustreerd: een patrix-matrixverbinding, implantaatranden en een haak-en-balkmechanisme. Alle werden succesvol klinisch toegepast en bieden de ontwerper en chirurg vrijheid in zelfs de meest uitdagende gevallen. De uiteindelijke keuze kan worden gebaseerd op factoren zoals locatie en de noodzaak van aanvullende afsteuning. De succesvolle toepassing wordt geïllustreerd aan de hand van een reconstructiecasus met een vierwandsdefect, wat de mogelijkheden van een multi-PSI benadering met geavanceerde ontwerpopties laat zien.

Dezelfde ontwerpvrijheid die in **Hoofdstuk 3** naar voren komt, legt ook een fundamen-

tele beperking van de toepassing van PSI's bloot: het ontbreken van gestandaardiseerde ontwerprichtlijnen. Ontwerpvariabiliteit kan voortkomen uit andere factoren dan alleen de anatomie van de patiënt, waaronder individuele voorkeuren van de chirurg en de opleidingsachtergrond van de engineer. Het doel van **Hoofdstuk 4** was deze variabiliteit te kwantificeren. PSI ontwerpen van twee engineers en twee chirurgen uit verschillende centra werden vergeleken voor identieke patiëntcasussen. De PSI's werden vergeleken aan de hand van een nieuwe verschilscore, gebaseerd op een eerder beschreven maat voor vergelijkingen van de pasvorm van voorgevormde implantaten. De initiële ontwerpvoorstellen van de engineers alleen hadden een mediane verschilscore van 37%, die na overleg met de chirurgen daalde naar 26%. De uiteindelijke PSI-ontwerpen die door verschillende chirurgen werden goedgekeurd, verschilden mediaan 22%. Specifieke verschillen tussen chirurgen betroffen het aantal en de locatie van schroefposities, de aanwezigheid van een extensie over de infra orbitale rand en de locatie van ondersteuning op de mediale wand. Ervaren ontwerpteams hadden significant minder aanpassingen, minder overlegmomenten en tot 40% minder tijd nodig. Deze bevindingen onderstrepen dat PSI-ontwerp in zodanige mate wordt beïnvloed door de chirurg en engineer, dat de ontwikkeling van op bewijs gebaseerde ontwerpprotocollen gerechtvaardigd is.

Deel II van dit proefschrift richt zich op chirurgische navigatie, waarvoor een nauwkeurige registratieprocedure een vereiste is. **Hoofdstuk 5** introduceert een virtual splint registratie workflow en valideert deze klinisch bij tien patiënten die een revisieoperatie aan de orbita ondergingen. Hiertoe wordt een nieuwe methodologie geïntroduceerd om de klinisch relevante registratienauwkeurigheid te kwantificeren. Kenmerkend aan deze methodologie is het gebruik van reeds aanwezige fixatieschroeven binnen het interessegebied als referentiepunten voor de nauwkeurigheid. Intraorale scans van de dentitie werden gefuseerd met preoperatieve CT-data om een virtuele dentale splint te genereren, die werd voorzien van fiduciale markers, 3D geprint en intraoperatief gebruikt voor registratie. Een mediane target registration error van 1,5 mm werd gevonden ter hoogte van de infra orbitale rand. Deze niet-invasieve methode elimineert de noodzaak van herhaalde preoperatieve beeldvorming en vereist beperkte expertise in computer-aided design, waardoor bredere klinische implementatie mogelijk wordt. Door in-vivo nauwkeurigheidsmeting mogelijk te maken, helpt deze methode eerdere claims over de nauwkeurigheid van chirurgische navigatie- en registratieprocedures te objectiveren.

Huidige chirurgische navigatie biedt slechts intermitterende positioneringsfeedback, waarbij de chirurg herhaaldelijk de positie van het implantaat moet verifiëren met een getrackte pointer en de visuele aandacht moet verschuiven tussen het operatieveld en een extern scherm. Ook de interpretatie van deze feedback kan lastig zijn. Om deze beperkingen aan te pakken werd een real-time navigatie workflow ontwikkeld, waarbij een speciaal instrument rigide aan het implantaat wordt bevestigd, wat continue positiebepaling van het implantaat mogelijk maakt. Samenwerking met de industriële partners KLS Martin en Brainlab AG maakte de productie van een klinisch bruikbaar instrumentprototype en bijbehorend implantaat mogelijk. In **Hoofdstuk 6** evalueerden zes chirurgen zes visualisatiemethoden in een gestandaardiseerde in-vitro-opstelling, waarbij verschillende beeldoriëntaties en visualisaties, 3D-objecten in de overzichten, en kleur-gecodeerde afstandsweergave werden getest. Positie-interpretatie en positioneringstijd werden voor elke visualisatiemethode geregistreerd. Er werden geen statistisch significante verschillen in positioneringstijd of interpretatienauwkeurigheid gevonden tussen de methoden. Chirurgen gaven consistent de voorkeur aan een combinatie van CT-coupes, inclusief een aanvullend coronaal vlak ter hoogte van de

posterieure ledge, gecombineerd met een distance map-overlay op het driedimensionale implantaatmodel. Chirurgen beschreven veelal een twee-fasen-strategie, waarbij het driedimensionale overzicht werd gebruikt voor algemene oriëntatie, gevolgd door CT-coupes voor precieze uitlijning.

Hoofdstuk 7 valideerde de geoptimaliseerde real-time navigatie workflow in een kadaverstudie, waarbij deze werd vergeleken met de huidige klinische navigatiestandaard. Real-time navigatie behaalde een translatie nauwkeurigheid van 1,7 mm en rotatie afwijkingen van 3,2 graden (roll), 1,3 graden (pitch) en 1,9 graden (yaw), en verkortte de totale reconstructietijd ten opzichte van conventionele navigatie. Eye-trackinganalyse toonde minder verschuivingen van de visuele aandacht tussen het operatieveld en het navigatiescherm, wat duidt op een verminderde cognitieve belasting voor de chirurg. Dit bevestigde tevens de in Hoofdstuk 6 waargenomen twee-fasen-strategie, waarbij chirurgen het driedimensionale overzicht gebruikten voor initiële oriëntatie, gevolgd door CT-coupes voor precieze plaatsing.

De algemene discussie in **Hoofdstuk 8** reflecteert op de bredere implicaties voor gepersonaliseerde CAS bij orbitareconstructie. De resultaten tonen aan dat personalisatie verder reikt dan de anatomie van de patiënt: zowel chirurgen als engineers beïnvloeden workflow beslissingen en implantaatontwerp. Anatomische variatie en de complexiteit van de casus bepalen welke CAS-hulpmiddelen nodig zijn, maar of deze personalisatie in de praktijk kan worden gerealiseerd, hangt af van aanvullende factoren, waaronder de ervaring van de chirurg, institutionele middelen zoals engineeringondersteuning en infrastructuur, en kenmerken van het zorgstelsel zoals vergoedingsbeleid. Omdat institutionele en systeemfactoren relatief vaststaand zijn, blijft de chirurg het meest bruikbare aangrijpingspunt om workflow standaardisatie te verbeteren, bijvoorbeeld door gestructureerde blootstelling aan CAS-technieken tijdens de opleiding. Technologische innovatie alleen is onvoldoende voor klinische adoptie. Methodologische validatie, gebruiksvriendelijkheid en naleving van de Medical Device Regulation zijn eveneens essentieel, en het traject van concept tot gecertificeerd klinisch hulpmiddel duurt doorgaans meerdere jaren. De virtual splint registratie- en real-time navigatie workflows werden respectievelijk klinisch en preklinisch gevalideerd, waarmee de wetenschappelijke basis voor implementatie is gelegd.

Toekomstige ontwikkelingen dienen zich te richten op patiënt-gestuurde workflow beslissingen. Defectbeoordeling door kunstmatige intelligentie zou de operator-afhankelijke variabiliteit kunnen verminderen, terwijl gestandaardiseerde rapportage en multicenter-registers de evidence-based verfijning van PSI-ontwerpprincipes kunnen ondersteunen. Augmented reality en robotondersteuning bieden op lange termijn perspectief voor chirurgische begeleiding, hoewel de huidige registratienauwkeurigheid en instrumentatiebeperkingen de klinische toepassing ervan in orbitareconstructie nog beperken. Real-time navigatie, reeds preklinisch gevalideerd, vormt de meest directe volgende stap in orbitareconstructie, waarbij prospectieve studies nodig zijn om operatieve efficiëntie en de interactie van de chirurg te evalueren met behulp van eye tracking. Patiëntrelevante uitkomsten, waaronder herstel van de oogbolpositie, vermindering van diplopie en kwaliteit van leven, blijven de ultieme maatstaf voor succes.


A

Author list

A.G. Becking **AB**

Department of Oral and Maxillofacial Surgery
Amsterdam University Medical Centers
University of Amsterdam, The Netherlands

R. Bruggink **RB**

Department of Oral and Maxillofacial Surgery 3D Lab
Radboud University Medical Center Nijmegen
Radboud Institute for Health Sciences, The Netherlands

L. Dubois **LD**

Department of Oral and Maxillofacial Surgery
Amsterdam University Medical Centers
University of Amsterdam, The Netherlands

H. Essig **HE**

Department Oral & Maxillofacial Surgery,
University Hospital, Switzerland

J. Jansen **JJ**

Department of Oral and Maxillofacial Surgery
St. Antonius Hospital, Nieuwegein, The Netherlands

N.H.J. Lobé **NL**

Radiology and Nuclear Medicine,
Amsterdam University Medical Centers
University of Amsterdam, The Netherlands

T.J.J. Maal **TM**

Department of Oral and Maxillofacial Surgery 3D Lab
Radboud University Medical Center Nijmegen
Radboud Institute for Health Sciences, The Netherlands

Department of Oral and Maxillofacial Surgery
Amsterdam University Medical Centers
University of Amsterdam, The Netherlands

R. Schreurs **RS**

Department of Oral and Maxillofacial Surgery
Amsterdam University Medical Centers
University of Amsterdam, The Netherlands

E. Shaheen **ES**

OMFS-IMPATH Research Group, Department of Imaging and Pathology,
Catholic University Leuven, Leuven, Belgium

Department of Oral and Maxillofacial Surgery
University Hospitals Leuven, Belgium

G. van de Steeg **GS**

Department of Oral and Maxillofacial Surgery 3D Lab
Radboud University Medical Center Nijmegen
Radboud Institute for Health Sciences, The Netherlands

R. Willaerts **RW**

OMFS-IMPATH Research Group, Department of Imaging and Pathology,
Catholic University Leuven, Leuven, Belgium

Department of Oral and Maxillofacial Surgery
University Hospitals Leuven, Belgium

Chapter information

Chapter 2

Published as

Personalized Medicine Workflow in Post-Traumatic Orbital Reconstruction

Published in

Journal of Personalized Medicine**, 2022**

Authors

J.F. Sabelis, R. Schreurs, H. Essig, A.G. Becking, L. Dubois

Author contributions

Study conception and design	JS, RS, AB, LD
Data collection	JS, RS
Data analysis	JS, RS, LD
Manuscript writing and review	JS, RS, HE, AB, LD

Funding resources and in-kind contributions

KLS Martin and Brainlab AG	Funding

Conflict of interest

None of the funding parties had any involvement in the contents or decision to submit the manuscript.

Chapter 3

Published as

Technical Note on Three- and Four-Wall Orbital Reconstructions With Patient-Specific Implants

Published in

Journal of Craniofacial Surgery, 2021

Authors

J.F. Sabelis, S.A.L.Y. Youssef, F.W.A. Hoefnagels, A.G. Becking, R. Schreurs, L. Dubois

Author contributions

Study conception and design	JS, RS, LD
Data collection	JS, SY, FH, LD
Data analysis	JS, SY, LD
Manuscript writing and review	JS, SY, FH, AB, RS, LD

Funding resources and in-kind contributions

KLS Martin and Brainlab AG	Funding

Conflicts of interest

None of the funding parties had any involvement in the contents or decision to submit the manuscript.

Chapter 4

Published as

PSI: Planner-specific, physician-specific, or patient-specific implant for orbital reconstruction?

Published in

Journal of Cranio-Maxillo-Facial Surgery, 2024

Authors

J.F. Sabelis, E. Shaheen, R. Willaert, A.G. Becking, L. Dubois, R. Schreurs

Author contributions

Study conception and design	JS, LD, RS
Data collection	JS, ES, RW, LD, RS
Data analysis	JS, RS
Manuscript writing and review	JS, ES, RW, AB, LD, RS

Funding resources and in-kind contributions

KLS Martin and Brainlab AG	Funding

Conflicts of interest

None of the funding parties had any involvement in the contents or decision to submit the manuscript.

Chapter 5

Published as

Clinical validation of the virtual splint registration workflow for craniomaxillofacial surgery

Published in

International Journal of Oral and Maxillofacial Surgery, 2025

Authors

J.F. Sabelis, R. Schreurs, L. Dubois, A.G. Becking

Author contributions

Study conception and design	JS, RS
Data collection	JS, RS, LD
Data analysis	JS
Manuscript writing and review	JS, RS, LD, AB

Funding resources and in-kind contributions

KLS Martin and Brainlab AG	Funding

Conflicts of interest

None of the funding parties had any involvement in the contents or decision to submit the manuscript.

Chapter 6

Published as

Optimizing Visualization Feedback of Real-Time Navigation for Orbital Reconstructions – A Preclinical Study

Published in

International Journal of Oral and Maxillofacial Surgery, 2026

Authors

J.F. Sabelis, T.J.J. Maal, R. Bruggink, G. van de Steeg, A.G. Becking, L. Dubois, R. Schreurs

Author contributions

Study conception and design	JS, TM, RB, GS, RS
Data collection	JS, RS, LD
Data analysis	JS
Manuscript writing and review	JS, TM, RB, GS, AB, LD, RS

Funding resources and in-kind contributions

KLS Martin	Funding and in-kind: prototype instrument and implant
Brainlab AG	Funding and in-kind: navigation system, software, instruments, and IGT-link

Conflicts of interest

None of the funding parties had any involvement in the contents or decision to submit the manuscript.

Chapter 7

Submitted as

Toward clinical implementation of real-time navigation workflow for orbital reconstruction – A preclinical study with use of eye-tracking

Submitted in

International Journal of Oral and Maxillofacial Surgery, 2026

Authors

J.F. Sabelis, L. Dubois, J. Jansen, N.H.J. Lobé, A.G. Becking, T.J.J. Maal, R. Schreurs

Author contributions

Study conception and design	JS, NL, TM, RS
Data collection	JS, LD, JJ, NL, RS
Data analysis	JS, RS
Manuscript writing and review	JS, LD, JJ, NL, AB, TM, RS

Funding resources and in-kind contributions

KLS Martin:	Funding and in-kind: prototype instrument and impants.
Brainlab AG:	Funding and in-kind: navigation system, software instru ments, and IGT-link.

Conflicts of interest

None of the funding parties had any involvement in the contents or decision to submit the manuscript.


A

List of publications

List of publications

In this thesis

Published

1. Sabelis JF, Schreurs R, Essig H, Becking AG, Dubois L. Personalized Medicine Workflow in Post-Traumatic Orbital Reconstruction. Journal of Personalized Medicine. 2022;12(9):1366.
2. Sabelis JF, Youssef S, Hoefnagels FWA, Becking AG, Schreurs R, Dubois L. Technical Note on Three- and Four-Wall Orbital Reconstructions with Patient-Specific Implants. J Craniofac Surg. 2021.
3. Sabelis JF, Shaheen E, Willaert R, Becking AG, Dubois L, Schreurs R. PSI: Planner-specific, physician-specific, or patient-specific implant for orbital reconstruction? J Craniomaxillofac Surg. 2024;52(11):1376–82.
4. Sabelis JF, Schreurs R, Dubois L, Becking AG. Clinical validation of the virtual splint registration workflow for craniomaxillofacial surgery. Int J Oral Maxillofac Surg. 2025;54(8):741–6.
5. Sabelis JF, Maal, TJJ, Bruggink, R, van de Steeg, G, Becking, AG, Dubois, L, Schreurs, R. Optimizing Visualization Feedback of Real-Time Navigation for Orbital Reconstructions - A Preclinical Study. Int J Oral Maxillofac Surg. 2026.

Submitted

6. Sabelis JF, Dubois, L, Jansen, J, Lobé, NHJ, Becking, AG, Maal, TJJ, Schreurs, R. Toward Clinical Implementation of Real-Time Navigation Workflow for Orbital Reconstruciton - A preclinical study with use of eye-tracking. Int J Oral Maxillofac Surg. 2026.

Other publications

7. Baan F, Sabelis JF, Schreurs R, van de Steeg G, Xi T, van Riet TCT, et al. Validation of the OrthoGnathicAnalyser 2.0-3D accuracy assessment tool for bimaxillary surgery and genioplasty. PLoS One. 2021;16(1):e0246196.
8. Dubois L, Sabelis JF, Jansen J, Maal TJJ, Schreurs R. Surgical Treatment of Solitary Orbital Wall Fractures. In: Gooris PJJ, Mourits MP, Bergsma JE, editors. Surgery in and around the Orbit: CrossRoads. Cham: Springer International Publishing; 2023. p. 215–36.
9. Youssef S, Klop C, Sabelis JF, Schreurs R, Nolte JW, Helmers R, et al. Restoring Mandibular Anatomy After Complex Trauma: Clinical Applications of a Statistical Shape Model. J Clin Med. 2026;15(3).

Acknowledgements - Dankwoord

Dankwoord

Een proefschrift schrijf je niet alleen. De afgelopen zes jaar heb ik het geluk gehad omringd te zijn door mensen die elk op hun eigen manier hebben bijgedragen: met een scherpe blik op het onderzoek, met praktische hulp op momenten dat ik het nodig had, of simpelweg een luisterend oor voor mijn gezeur als het even tegenzat. Want ja, zoals bij ieder promotietraject, zijn er ups en downs geweest. Bij promoveren leer je naast de kunst van het onderzoeken ook die van het vooruitdenken, het geduldig zijn en het doorzetten. In dit dankwoord wil ik graag iedereen bedanken die mij de afgelopen jaren hiermee heeft geholpen.

Prof. Dr. A.G. Becking, hooggeleerde promotor, beste Eddy. Tijdens mijn eerste onderzoeksbespreking met 'de professor' die mijn promotor ging worden, was ik nogal zenuwachtig en kwam ik niet goed uit mijn woorden. Je precieze woorden weet ik niet meer, maar het was iets in de trant van "en nu graag in hele zinnen spreken alsjeblieft". Dit brak het ijs en was de start van een goede samenwerking. Ik heb jouw rol tijdens het gehele traject als prettig ervaren: de stille kracht op de achtergrond. Jij was er op de momenten dat het nodig was, en als ik ergens op vastliep kon ik altijd bij je aankloppen. De herhaaldelijke reminders om de balans tussen onderzoek en 3D planningen te bewaken hebben uiteindelijk vruchten afgeworpen. De zeiluitjes in Friesland, samen met je vrouw Loes, waren een welkome onderbreking van de academische strubbelingen. Ik kijk met veel plezier terug op die momenten.

Prof. Dr. T.J.J. Maal, hooggeleerde promotor, beste Thomas. Eigenlijk begint mijn hele PhD-traject bij jou. Je geeft orthodontieonderwijs, waarin de mogelijkheden van de 3D-technologie worden belicht. Toevallig had mijn zus, Aaltje, dit gevolgd en mij hierover getipt. Hierdoor heb ik contact met je opgenomen voor een afstudeerstage in Amsterdam. De afstand tussen Amsterdam en Nijmegen is niet altijd makkelijk te overbruggen, maar jij hebt altijd je best gedaan om betrokken te blijven. Niet alleen inhoudelijk, maar ook op persoonlijk vlak. Ik waardeer hoe benaderbaar en oprecht geïnteresseerd je bent. Het moment dat jij ging meehelpen met coderen in C++ voor de navigatiesoftware is me goed bijgebleven en heeft me geleerd hoe belangrijk (en leuk) het kan zijn om je in de details te blijven verdiepen.

Prof. Dr. L. Dubois, hooggeleerde copromotor, beste Leander, beste Leo. Samenwerken met jou heeft me veel geleerd. Termen als hakkeltjes, haakjes en botdiktes kan ik inmiddels dromen. Maar ook op ander vlak heb ik het nodige opgestoken: omgaan met overvolle agenda's, krappe deadlines en de kunst van het schakelen. Jij leerde me hoe belangrijk het is om verder te denken. Er is altijd een plan B nodig, en het liefst ook een plan C, zeker als blijkt dat het oorspronkelijke plan alweer aan verandering toe is. Ik vind het oprecht knap hoe jij alle balletjes hoog weet te houden. Dat heeft soms de nodige flexibiliteit gevraagd, van alle betrokken partijen, maar jouw gedrevenheid werkt aanstekelijk. Uiteindelijk streven we naar de optimale uitkomst voor de patiënt en dat doel hebben we altijd gedeeld.

Beste Ruud, hooggeleerde copromotor, prof. Dr. R. Schreurs. Bij jou wijk ik bewust af van de standaard adressering: toen ik op deze afdeling kwam voor mijn afstudeerstage was jij nog bezig met je PhD, welke je hebt afgerond en gelijk de stap naar professor hebt gezet tijdens mijn PhD. Het is dan ook niet gek dat we daar allemaal nog aan moeten wennen. Al vanaf het begin beschreef ik jou tegenover vrienden en familie als een verstrooide professor: geniaal vakinhoudelijk, maar wat warrig als het aankomt op agendamanagement, mail bijhouden of bestandsnamen die na een half jaar nog

te achterhalen zijn. Dit proefschrift was er simpelweg niet geweest zonder jou. Jij was de eerste die al mijn stukken las en ze vervolgens volledig rood terugstuurde. Ik put er enige hoop uit dat die hoeveelheid rood over de jaren wat is afgenomen. Van jou heb ik ook geleerd dat een congres altijd gecombineerd kan, of eigenlijk moet, worden met een avontuur. Zo hebben we na congressen in Enschede een biertje gedronken bij jouw oude studentenvereniging, in Rome de toerist uitgehangen bij het Colosseum, en zijn we vanuit Vancouver gaan toeren door de Canadian Rockies in een echt 'huisje op wielen'. Gelukkig heb je inmiddels je eigen kamer om dit nummer, en de rest van je geliefde muziekgenre, ongestoord af te spelen. Op naar nieuwe avonturen, binnen én buiten het ziekenhuis.

Prof. Dr. J. de Lange, hooggeleerde opponent, beste Jan. Toen ik hier begon liep je eerst altijd de 3D kamer binnen voor een voetbalpraatje met Ruud. Na de ontdekking van onze wederzijdse interesse in de Formule 1, hadden we er al snel een wekelijks onderonsje bij. Jouw voorliefde voor Ferrari en de motoren van vroeger steek je niet onder stoelen of banken. Dat botst wel eens met mijn voorkeur voor Max. Hier moet ik toch een parallel trekken. Op de racebaan houd jij van de gevestigde glorie, maar op de werkvloer gaf je juist alle ruimte aan ontwikkeling, met de groei van het 3D lab tot een vaste waarde binnen de afdeling. Misschien is het dan ook niet meer dan logisch dat je op een dag ook Max een kans geeft: zijn ontwikkeling en gedrevenheid zouden je toch moeten aanspreken.

Geachte overige leden van de promotiecommissie, **prof. dr. P. Saeed, prof. dr. B.J. van Royen, prof. dr. S.J. Bergé, dr. B van Minnen, dr. F. Baan, dr. R. Helmers**, wil ik hartelijk bedanken voor de tijd die u heeft genomen om mijn proefschrift grondig te lezen en ook alvast voor de kritische vragen hierover tijdens de plechtigheid. Het is een eer dit proefschrift tegenover u te mogen verdedigen.

Ook wil ik hier de mensen bedanken die het onderzoek mogelijk hebben gemaakt: de patiënten die mee hebben gedaan aan het onderzoek en de mensen die hun lichaam ter beschikking hebben gesteld aan de wetenschap. Daarnaast wil ik de mensen bedanken die hebben ondersteund in het ontwikkelen van de methodes en het uitvoeren van het onderzoek. **Mara Clerkx en alle technici** van de anatomieafdeling, zonder jullie flexibiliteit in de planning zouden de kadaverstudies nu nog steeds niet zijn afgerond. **Meindert Rijpkema en Marc Steenmetz**, dank voor het enthousiaste meedenken in de prints en het ontwikkelen van het instrument. **Gert van de Steeg en Robin Bruggink** van het 3D lab Nijmegen, bedankt voor het ontwikkelen van de software voor de real-time navigatie. Zonder jullie was ik nu nog bezig C++ te leren. **Sylvia Marks** van KLS Martin Nederland wil ik graag bedanken voor haar hulp om de implantaten voor de patiënten op tijd in Amsterdam te krijgen, waardoor ik weer met een gerust hart door kon gaan met het onderzoek. Ook **Rens Bouwmans** van Brainlab Nederland ben ik dankbaar voor de snelle ondersteuning tijdens het uitvoeren van de onderzoeken. This research relied on the support of and collaboration with KLS Martin and Brainlab. I would like to thank **Ismael Gonzalez Flores** from Brainlab for his contribution to this project. I would also like to extend special thanks to **Stefan Betzler and Timo Sprenger** from KLS Martin. When you joined this project, we were able to take significant steps in product development. The fact that we are now close to clinical application of real-time navigation is something we could not have achieved without you.

Ook mijn collega's van het 3D lab wil ik graag bedanken. **Beste Niels, beste paranimf,** wij zijn dit PhD-avontuur samen begonnen. Jij hebt me destijds geleerd om te gaan met zowel Blender als de chirurgen. Sindsdien weet jij als geen ander wat ervoor no-

dig is geweest om dit traject te doen slagen: het constante switchen tussen klinische planningen en onderzoek, en de discipline om daarbij ook nog je grenzen te bewaken. Ik kan altijd mijn ei kwijt bij jou, of het nou werk- of privé-gerelateerd is. Je klusadvies (en -hulp) wordt ook altijd zeer gewaardeerd. Toen ik begon met m'n PhD was ik het derde en nieuwste lid van het 3D lab, maar inmiddels is het team versterkt met **Lynn, Milou en Hugo**. Ik vind het erg leuk dat dit hechte team langzaam aan het groeien is. Ik koester de (vaste) koffiemomentjes, wandelingetjes voor frisse lucht, kroketjes op vrijdag (of welke dag dan ook) en ijsjes als er ook maar een hint van een zonnestraal is. Daarnaast wil ik ook **Iva** graag bedanken voor alles. Je zit in het traject om kaakchirurg te worden (alleen daar heb ik al veel respect voor), maar door de technische kant van je onderzoek ben je ook ons geadopteerde 3D lab-lid geworden. Door onze verwante onderzoeksonderwerpen en overlap in ons promotieteam hebben we vaak al genoeg aan één blik om te weten hoe de vlag ervoor staat. Los van hoe druk je zelf bent, sta je altijd klaar om me te helpen, of het nou gaat om meedenken over het ontwerp van de voorkant van dit proefschrift, het omgaan met familieperikelen of het kiezen van een congres-outfit. Niks is jou te gek, bedankt!

Beste **Amsterdam UMC (oud-)staf** en **(oud-)aios**. Jullie maken het succes van het 3D lab mogelijk. Zonder de klinische behoefte en het enthousiasme zou er voor ons geen plaats zijn in het ziekenhuis. Ook toen ik hier begon, midden in de coronaperiode, voelde ik me al snel onderdeel van dit mooie team. Van gezamenlijke lunches tot druivenplukken in Frankrijk en de jaarlijkse (après)ski-vakanties, de sfeer is goed ook buiten het werk om. Ik ben blij dat ik bij deze afdeling ben beland en de mogelijkheid kreeg om hier te groeien.

Naast alle collega's wil ik ook graag de belangrijke mensen buiten werk om bedanken. Ik prijs mij gelukkig met een hecht groepje vrienden en vriendinnen die met mij hebben meegeleefd. Lieve **Monica, Jorike, Jessica en Kevin**, we kennen elkaar al sinds de middelbare school en hebben sindsdien het nodige samen meegemaakt. Jullie eindeloze gesprekken over Pokémon vliegen volledig langs me heen, maar van de gezamenlijke etentjes geniet ik des te meer. Lieve **Moon**, jij in het bijzonder, je hebt een uitgesproken mening en bent zeker niet bang deze te ventileren. Ook kun je lekker overdrijven en heb je altijd een goed verhaal paraat. Eigenlijk lijken we dus totaal niet op elkaar. Maar toch begrijpen we elkaar heel goed en kunnen we samen lachen, ook tijdens het rennen: de Dam tot Damloop, de Prosecco run en de halve van Haarlem. Ik ben benieuwd wat de volgende gaat worden. Lieve **Gracia**, jou ken ik vanaf het eerste jaar van geneeskunde. Ik vond het destijds erg jammer dat je ervoor koos om niet mijn huisgenoot te worden in Leiden. Maar dat heb je dubbel en dwars goed gemaakt door (twee keer) bij mij in te trekken in Haarlem. Toen het leven weleens tegenzat, was jij er voor mij, en ik hoop dat ik de afgelopen tijd hetzelfde voor jou heb kunnen betekenen. Ik heb er alle vertrouwen in dat we er allebei sterker uit komen. Fancy uiteten, slechte romcoms kijken, sporten, ik hoop dat we dat samen blijven doen tot we nóg ouder en (hopelijk ook) wijzer zijn. Tot slot wil ik ook de toppers van tennis bedanken, met in het bijzonder **Jolanda, Lisette en Mick**. Op én naast de baan moedigen we elkaar aan. Ik geniet ervan dat jullie mijn werk nog spannender laten klinken dan wanneer ik er zelf over vertel, ook al is het dan wel iets minder waarheidsgetrouw.

Hiernaast heb ik ook een grote familie die ik dankbaar ben. Om te beginnen bij mijn ouders, **lieve pap en mam, Frans en Uschi**, jullie hebben me altijd gestimuleerd om overal het maximale uit te halen. Of dat nou vroeger op het hockeyveld was (vroeg opstaan in de zomervakantie voor dat trainingsschema, geen excuusjes mogelijk), of in de keuze voor een middelbare school (ja pap, tweetalig onderwijs bleek uiteindelijk erg

handig), of in de switch van geneeskunde naar technische geneeskunde ("Oh eindelijk ga je voor wat meer technisch"). Niet alles kon ik op dat moment waarderen, maar ik pluk er nu, met dit proefschrift, de vruchten van. Jullie hebben elkaar ontmoet op ACTA, en hoewel ik bewust een andere richting dan tandheelkunde heb gekozen, vind ik het mooi om symbolisch de cirkel weer rond te maken door hier nu zelf te promoveren. Dank voor alle mogelijkheden die jullie me hebben geboden.

Ook dank aan mijn broers en zussen: **Simon, Aaltje, Ursula, Catharina, Elisabeth en Sophie**, voor de altijd levendige en soms ietwat hectische thuisbasis. In een gezin van deze omvang loop je (gelukkig) niet allemaal dezelfde weg, maar we doen ons best om elkaar op te blijven zoeken. Want familie moet je koesteren. **Lieve Aaltje, beste paranimf**, aan jou wil ik nog een extra woord wijden. Jij bent niet alleen mijn tien jaar oudere zus en peettante, maar jij was in mijn jongere jaren een soort tweede moeder voor me. Gek genoeg voelt dat verschil niet als een afstand: in karakter lijken we juist erg op elkaar. Ook nu, als paranimf, sta je letterlijk en figuurlijk naast me tijdens de belangrijke momenten in mijn leven, en ik ben op mijn beurt trots dat ik peettante van Mats mag zijn. Het is altijd een feestje om jou en je gezin in Tilburg op te zoeken.

Lieve **Thomas**, halverwege dit traject ben ik jou tegengekomen, met een handje hulp van technologie. We zullen nooit weten hoe vaak we elkaar al voorbij zijn gelopen in de supermarkt bij ons om de hoek voordat het algoritme van Bumble ons aan elkaar voorstelde. Jij zei op onze eerste date dat je maar twee W's tegelijk goed kan doen: Wielrennen, Werk of Wederhelft. Ik ben blij dat jij stap voor stap ook hebt geleerd om de derde W 'best goed' erbij te doen. Allebei hadden we al ons eigen leventje opgebouwd met een huisje, hobby's en sporten. Toen we gingen samenwonen gingen we alles delen, inclusief de werkkamer. Jij noemt hem nog steeds koppig de fietskamer, met een naambordje van collega's als bewijs. Hierdoor heb ik dit proefschrift letterlijk voltooid tussen de fietsen. Rustig aan hebben we onze levens goed weten te verweven tot een thuisbasis voor elkaar, juist omdat we elkaar de ruimte gunnen om ook ons eigen ding te blijven doen. Jij straalt een rust uit die ik in stressvolle periodes hard nodig heb, en ik zorg op mijn beurt voor een gezellige chaos in de keuken. Van jou heb ik geleerd dat het juist goed is om voor jezelf, en elkaar, te zorgen en om ook onderweg te blijven genieten van de kleine dingen. Ik kijk uit naar onze komende ritten.


A

About the author

Juliana Sabelis was born in Haarlem on the 21st of December, 1993. She grew up with her parents Frans and Uschi and six siblings in Heemstede. She completed bilingual secondary education at the Haarlemmermeer Lyceum in Hoofddorp in 2012.

She subsequently pursued a Bachelor's degree in Medicine at Leiden University. After completing her first medical internship, she was drawn to the intersection of medicine and engineering. She transitioned into the field of Technical Medicine, completing a Master's degree in Technical Medicine at the universities of Delft, Rotterdam and Leiden. Her master's thesis was completed at the department of Oral and Maxillofacial Surgery in Amsterdam.

In November 2020, she commenced her PhD research at the same department, resulting in the present thesis. The research focused on development and evaluation of a computer-assisted workflow for orbital reconstruction. Alongside her PhD research, she was responsible for virtual surgical planning within the department, with a focus on trauma and gender-affirming surgeries. In this role, she contributed directly to patient care by designing and coordinating digital planning workflows for complex surgical cases.

She has presented her work at national and international conferences, including the annual meetings of the Dutch Association of Oral and Maxillofacial Surgery meeting (2022, 2023, 2025), the European Association of Cranio-Maxillo-Facial Surgery (EACMFS, 2024), and the International Conference on Oral and Maxillofacial Surgery (ICOMS, 2022, 2025).

She currently lives in Haarlem with her partner Thomas.